

**Tsunami Hazard Assessment of Portions of Island and Skagit
Counties, Washington**

Project Report

Draft of November 30, 2019 (updated)

**Randall J. LeVeque, Loyce M. Adams, and Frank I. González
University of Washington**

Study funded by Washington State Emergency Management Division

http://depts.washington.edu/ptha/IslandSkagitTHA_2019

Contents

1	Introduction	4
2	Earthquake Sources	6
2.1	Cascadia megathrust event CSZ-L1	6
2.2	Seattle Fault event SF-L	8
2.3	Aleutian Subduction Zone event AKmaxWA	8
3	Topography and Bathymetry	10
3.1	1/3 Arc-second DEMs	10
3.2	Coarser DEMs	10
4	Modeling uncertainties and limitations	12
4.1	Tide stage and sea level rise	12
4.2	Subsidence	12
4.3	Structures	12
4.4	Bottom friction	12
4.5	Tsunami modification of bathymetry and topography	12
5	Study regions	13
5.1	Issues with land below MHW	14
6	Results – Maximum flow depth and speeds	17
6.1	Region SW_Whidbey	18
6.2	Region W_Whidbey	21
6.3	Region NW_Whidbey	24
6.4	Region E_Whidbey	27
6.5	Region SE_Whidbey	30
6.6	Region Skagit	33
7	Results – Gauge output	36
	Appendices	68
A	Data format	68
A.1	fgmax values	68
A.2	Gauge time series	69
B	Modeling Details and GeoClaw Modifications	69
C	Gauge comparisons	70
C.1	Admiralty Inlet, Gauge 21	70
C.2	Polnell Point, Gauge 69	72

C.3 Deception Pass, Gauge 8	74
D Skagit River Delta	76
Acknowledgments	79
References	79

1 Introduction

This report documents the results of a study supported by the Washington State Emergency Management Division of the tsunami hazard along the coast of portions of Island and Skagit Counties, including the entire coast of Whidbey Island and the Skagit River Delta. Earthquake sources from the Seattle Fault, the Cascadia Subduction Zone, and the Aleutian Subduction Zone were considered. Results include inundation depths and times of arrival that will be useful to coastal communities, as well as tsunami current speeds and momentum flux. A pre-release version of GeoClaw Version 5.6.1 was used for the modeling [7], with some modifications as described in the appendices. The exact version of the code used in the simulations reported here [\[\[TODO: will be\]\]](#) archived at [13, 14].

Figure 1 shows the portion of Island and Skagit Counties studied, the union of the six polygons. These are the “fgmax regions” where GeoClaw results are provided for each considered earthquake. An fgmax grid is a fixed grid (fg) on which is saved the maximum (max) values of model variables attained during the duration of the simulation, including the fundamental variables water depth (h) and water speed (s) derived from the velocity components ($s = \sqrt{u^2 + v^2}$), as well as other quantities of interest derived from the depth (h) and horizontal momenta (hu and hv), the quantities modelled in the shallow water equations.

For each of these 18 sets of results (3 events on 6 regions), the quantities of interest have been provided as netCDF files on a set of points with $1/3$ arcsecond ($1/3''$) spacing in both longitude and latitude (approximately 7 m and 10 m respectively). The data format is discussed further in Appendix A.

All DEMs and project data utilize World Geodetic System 1984 (WGS84, EPSG:4326) as the standard coordinate system for this study.

Difficulties arose in accurately capturing the tsunami inundation in this region since much of the land is already below Mean High Water (MHW), which is both the vertical datum of the DEMs and the initial sea level assumed for the tsunami simulations. These areas are shown as pink in Figure 1. A new procedure to initialize GeoClaw was developed for an earlier project [1] and developed further for this project in order to insure that this land was initially dry in the simulations rather than being initialized with water, the usual default behavior for areas below MHW. This is discussed further in Section 5.1.

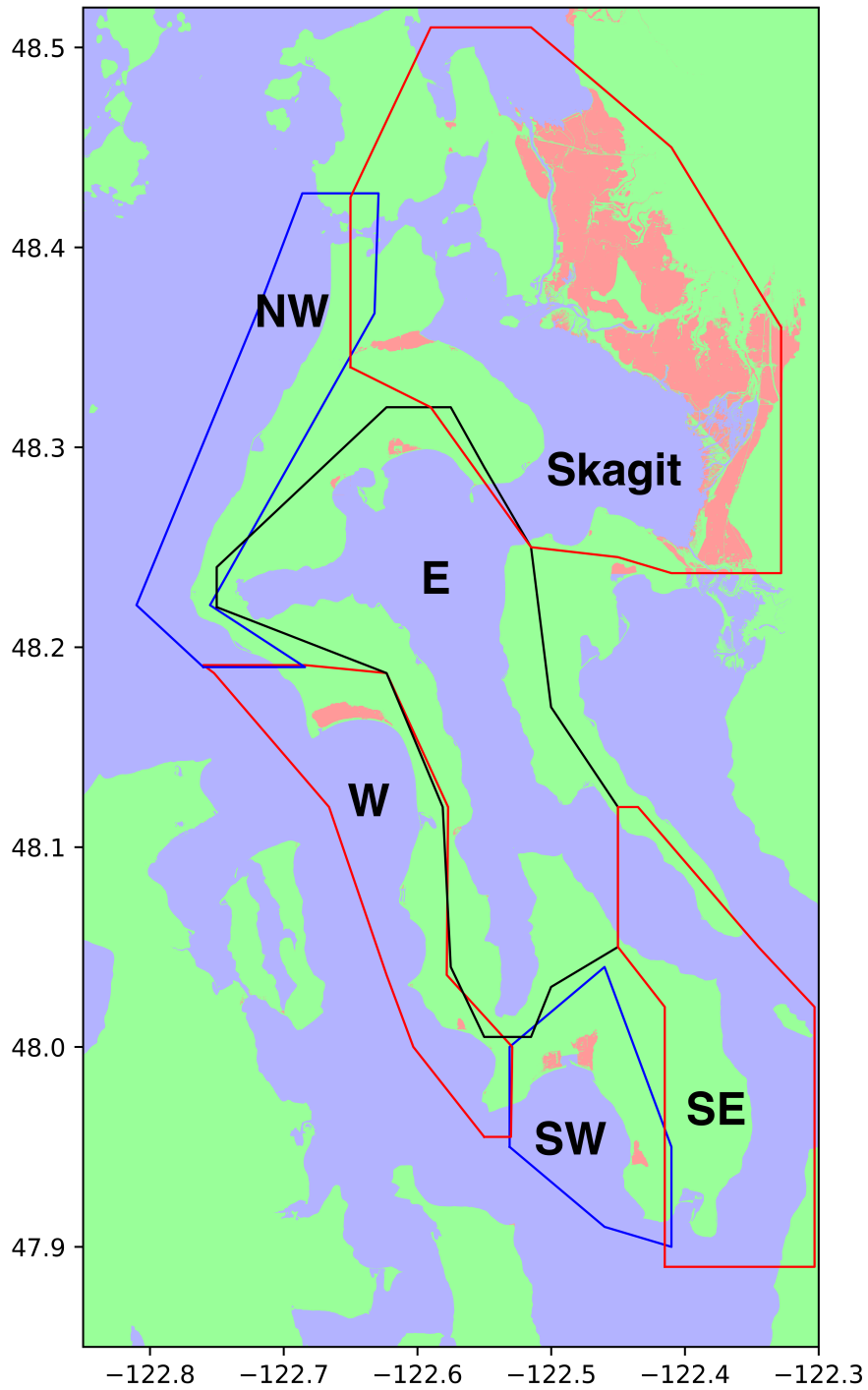


Figure 1: The study region as subdivided into 6 polygons. The regions are labeled SW_Whidbey, W_Whidbey, NW_Whidbey, E_Whidbey, SE_Whidbey, and Skagit, as indicated. Green indicates dry land above MHW. The pink regions are dry land with elevation below MHW, as determined using the algorithm described in Section 5.1.

2 Earthquake Sources

Three earthquake sources were considered for this study: a Cascadia Subduction Zone (CSZ) megathrust event with moment magnitude Mw9.0 (denoted CSZ-L1), a potential Seattle Fault rupture denoted SF-L, and an Aleutian Subduction Zone event off the coast of Alaska with magnitude 9.24, denote AKmaxWA.

Other potential sources have not been considered in this study. Several other fault zones cross Puget Sound, but potential sources from these faults have not been considered. In particular the South Whidbey Island Fault (SWIF) and Devil’s Mountain Fault directly cross the study region, but peer-reviewed sources thought to be representative of events on these faults are not available.

2.1 Cascadia megathrust event CSZ-L1

The probability that an earthquake of magnitude 8 or greater will occur on the Cascadia Subduction Zone (CSZ) in the next 50 years has been estimated to be 10-14% (Petersen, et. al., 2002 [20]). The last such event occurred in 1700 (Satake, et al., 2003 [21]; Atwater, et al., 2005 [3]) and future events are expected to generate a destructive tsunami that will inundate Washington Pacific coast communities within tens of minutes after the earthquake main shock.

The CSZ-L1 event used in this study creates very large waves along the outer coast and a substantial wave that propagates through the Strait of Juan de Fuca (SJdF) and into Puget Sound, reaching the western edge of Whidbey Island about 1.5 hours after the earthquake, with wave heights in excess of 5 meters at some points. No subsidence or uplift is produced by CSZ-L1 in the study region.

The potential CSZ event used in this study is the L1 scenerio developed by Witter, et al. (2013) [23]; crustal deformation for the region of interest is shown in Figure 2. The L1 source is one of 15 seismic scenarios used in a hazard assessment study of Bandon, OR, based on an analysis of data spanning 10,000 years. This scenario has been adopted by Washington State as the “maximum considered case” for many inundation modeling studies and subsequent evacuation map development; it is used because the standard engineering planning horizon is 2500 years and Witter, et al. (2013) [23] estimated that L1 has a mean recurrence period of approximately 3333 years, with the highest probability of occurrence of all events considered with magnitude greater than Mw 9.

The original L1 source was developed for studies on the Oregon coast and was truncated at around 48N. An extension of this was developed by the NOAA Center for Tsunami Reasearch (NCTR) group in the Pacific Marine Environment Laboratory (PMEL) in Seattle. The seafloor deformation is shown in Figure 2. As prescribed by DNR, we used this extended source, the same version of the CSZ-L1 source as used in our other recent tsunami hazard assessments, [12, 1, 22].

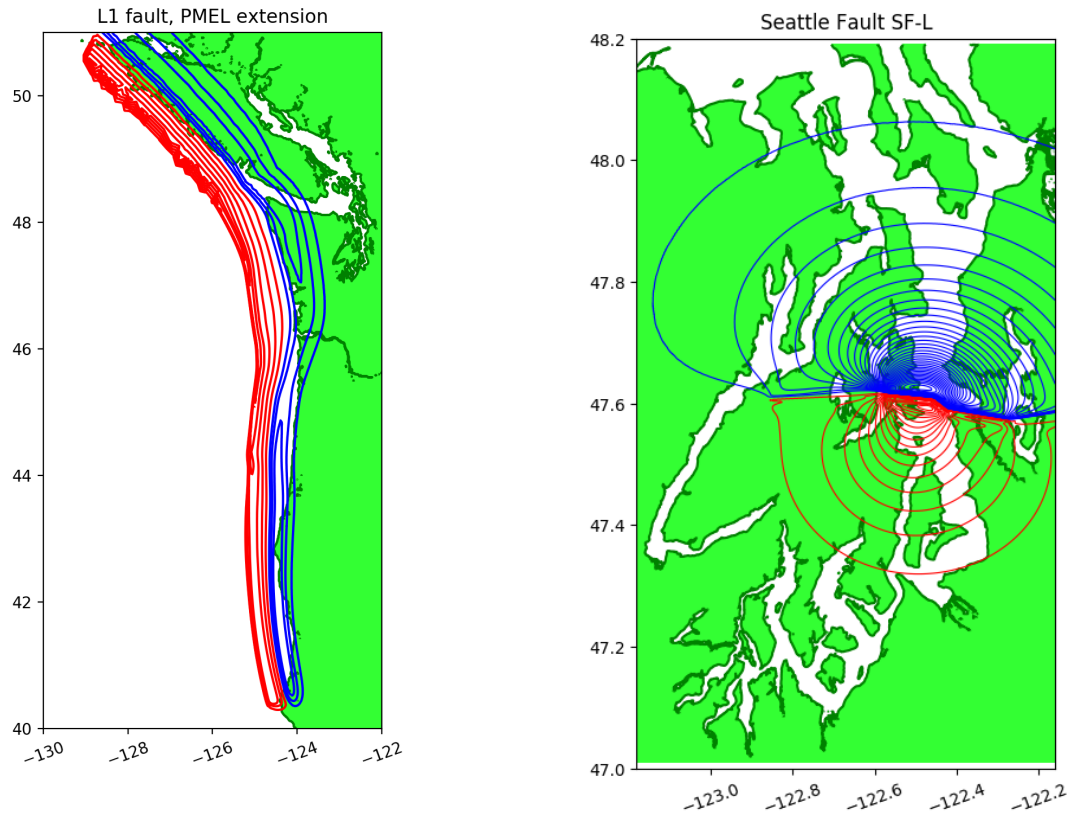


Figure 2: Left: Surface deformation of the L1 source, with maximum uplift 15.08 m and maximum subsidence -3.98 m. Red contours show uplift (2 meter interval), blue contours show subsidence (1 meter interval). Right: Surface deformation of the SF-L source, with maximum uplift 8.37 m and maximum subsidence -1.78 m. Red contours show uplift at levels 0.5, 1, 1.5, ... meters, blue contours show subsidence at levels -0.05 , -0.1 , ... meters.

2.2 Seattle Fault event SF-L

The Seattle Fault cuts across Puget Sound (through Seattle and Bainbridge Island) and can create a tsunami that affects the southern portion of Whidbey Island within 45 minutes after the earthquake.

Figure 2 shows contours of uplift and subsidence due to a hypothetical event on the Seattle fault that we denote by SF-L. There is a small amount of subsidence due to this event on southern Whidbey Island (less than 15 cm) but none in the rest of the study region. This event gives a tsunami with wave heights up to 2 meters in some places on the southwest Whidbey coast, with relatively little inundation elsewhere in the study region.

This is the same version of the Seattle Fault source as in our other recent tsunami hazard assessments, [12, 1, 22]. Earlier tsunami hazard studies have referred to this as a Mw 7.3 event. However, when we tried to recreate the deformation field by applying the Okada model to the subfault parameters listed in [5], we determined that the magnitude should be Mw 7.54, as discussed in Appendix E of the Snohomish County report, [12]. Regardless of the proper magnitude, we are using the deformation file provided by PMEL that has been used for the previous tsunami hazard analyses of Everett [5].

Due to uncertainty about the magnitude, in [12] we adopted the SF-L notation for this larger Seattle Fault scenario, and continue to use that here. The deformation was originally chosen to match observed uplift and subsidence at a few points around Puget Sound. Since the original specification of this deformation, many new observations have been made and improved models for the subfault geometry have also been produced. A new model for SF-L is now under development and in the future this could perhaps be used to update the results of the current study.

In our Snohomish County study we also considered a smaller event denoted SF-S, which was deemed too small to be of further interest for tsunami modeling. The Snohomish County report [12] contains additional information about this source and discussion of some of the confusion in the literature about the exact specification and magnitude of this source.

2.3 Aleutian Subduction Zone event AKmaxWA

The Aleutian Subduction Zone event denoted by AKmaxWA in this study is based on a hypothetical earthquake developed by PMEL in the work reported in [6], shown in Figure 3. This source was designed to have a similar magnitude and location as the 1964 Alaska Earthquake (Mw 9.2) but to have uniform slip of 20 m specified over a set of 20 “unit source” subfaults from the NOAA SIFT database. The set of unit sources used were chosen by running tsunami simulations with all combinations subject to some constraints and choosing the set that gave the maximum impact on the Washington coast. The magnitude based on the subfault dimensions and slip (and assuming a crustal shear modulus, or rigidity, of 40 GPa) works out to Mw 9.24. Since magnitudes are generally rounded off to 1 digit in reporting them, this was viewed as a “maximal Mw 9.2” event, thus having the same magnitude as the 1964 event with maximal impact on Washington.

We include the subfault parameters for the event we used in Table 1 to be clear exactly what we used and for future reference. We generated the surface deformation by applying the Okada model to these subfault parameters, but we also acquired a deformation file from PMEL that they have used in other tsunami simulations, and confirmed that these agree.

Various other hypothetical events similar to Alaska 1964 have been used in other tsunami hazard assessments, with some confusion in the literature regarding the nomenclature and their magnitudes. In the supplementary materials [13, 14] we include a Jupyter notebook developed in the course of this work to explore some of these sources, with the help of several others from PMEL and DNR. In particular, note that the AKmaxWA source we are using is distinct from the “AKmax” source used in Allan et al. [2], which was designed to maximize impact in Oregon. It is also distinct from the AASZ sources used by Witter et al. [23] and in other PTHA studies such as [10].

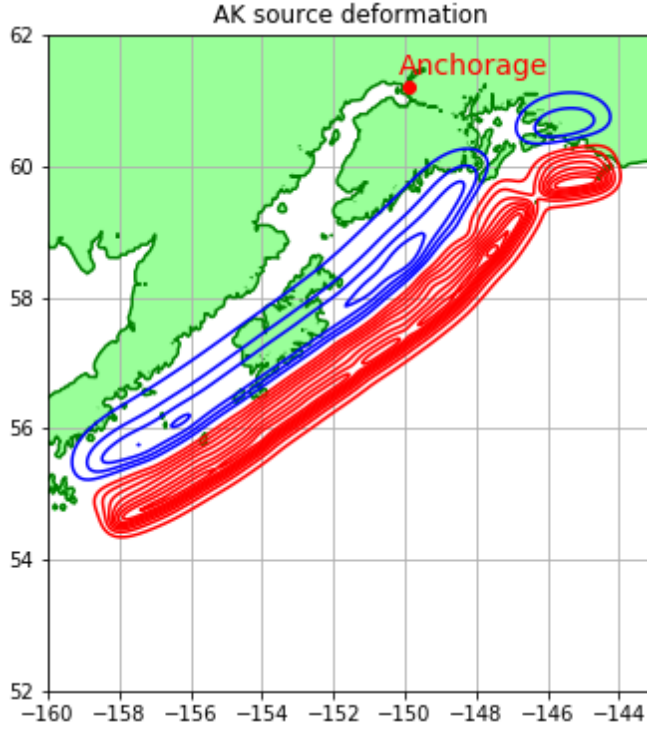


Figure 3: Surface deformation of the AKmaxWA source, with maximum uplift 9.7 m and maximum subsidence -4.9 m. Red contours show uplift, blue contours show subsidence (1 meter intervals in each case).

Unit Source	Longitude	Latitude	Depth (km)	Strike (degrees)
acsza29	-157.7390	55.1330	17.94	247.0000
acszz29	-158.1203	55.4908	30.88	246.2137
acsza30	-156.3960	55.5090	17.94	240.0000
acszz30	-156.8479	55.8534	30.88	240.4869
acsza31	-155.1050	55.9700	17.94	236.0000
acszz31	-155.5685	56.3016	30.88	235.6690
acsza32	-153.7920	56.4730	17.94	236.0000
acszz32	-154.2120	56.8210	30.88	235.4756
acsza33	-152.4630	56.9750	17.94	236.0000
acszz33	-152.8909	57.3227	30.88	235.4119
acsza34	-151.0629	57.5124	17.94	236.0000
acszz34	-151.5802	57.8213	30.88	234.6891
acsza35	-149.7403	58.0441	17.94	230.0000
acszz35	-150.3575	58.3252	30.88	230.1971
acsza36	-148.6751	58.6565	17.94	218.0000
acszz36	-149.4588	58.8129	30.88	217.3327
acsza37	-147.7495	59.2720	17.94	213.7100
acszz37	-148.3921	59.5820	30.88	214.2669
acsza38	-145.3445	60.1351	17.94	260.0800
acszz38	-145.4638	60.5429	30.88	259.0313

Table 1: Subfault parameters for the AKmaxWA event used in this study, from [6]. All subfaults have length 100 km, width 50km, dip = 15° , rake = 90° , and slip = 20 meters. The subfaults are taken from the NOAA Unit Source database [16, 9]. With crustal rigidity (shear modulus) set to $\mu = 40$ GPa, this gives a Mw 9.24 event (see [13, 14]).

3 Topography and Bathymetry

3.1 1/3 Arc-second DEMs

Output from the model was requested at grid points spaced 1/3" in longitude and 1/3" in latitude, with the points aligned with cell centers of the 1/3" DEM files that are available for the Puget Sound region. (Note that 1/3" in latitude is approximately 10.3 m. At this latitude, 1/3" in longitude is approximately 6.9 m).

GeoClaw uses finite volume methods with adaptive mesh refinement, and the finest grid resolution near regions of interest was set to the desired resolution of 1/3" by 1/3". It is important to note, however, that in the finite volume formulation the given DEM files are used to construct a piecewise bilinear function interpolating at the DEM points, and averages of this function over grid cells are then used as the topography values in the numerical method. Hence a cell that is centered at a DEM point overlaps 4 bilinear functions meeting at this point and the "GeoClaw topography" used in this grid cell will depend on the DEM values at 9 neighboring points. Moreover, if there is co-seismic subsidence (or uplift) in a cell the final GeoClaw topography value in this cell (which we denote by B) will include this deformation. For these reasons we provide both B and the DEM value Z at the same point in the netCDF files of model output, along with the co-seismic deformation dZ ; see Appendix A.

The study region lies partly in the region covered by two different 1/3" DEMs developed by NCEI. The Port Townsend 1/3" MHW Coastal Digital Elevation Model [17] (referred to below as PT-DEM) covers all of the study region, but was developed in 2011 and does not have the best available data in some regions. The newer (2014) Puget Sound 1/3" MHW Coastal Digital Elevation Model [18] (referred to below as PS-DEM) contains better data for the southern portion of Whidbey Island, but only extends up to 48.19N. The two DEMs often disagree in regions of overlap.

At our request, NCEI kindly provided a DEM that covers the full study area and that has the best currently available data in all locations, also north of 48.19N, including portions of the Skagit River Delta, critical in this study since much of this land is below MHW and protected by dikes. Remaining issues with this DEM are discussed further in Appendix D, but the quality was deemed sufficient for this study. This new merged 1/3" DEM is referred to as PTPSm-DEM, and will be archived on the NCEI data catalog.

3.2 Coarser DEMs

The 1/3" PT-DEM and PS-DEM discussed above were coarsened to obtain 2" DEMs. These DEMs are more efficient to use in GeoClaw on coarser grid levels where all the details of the 1/3" DEMs are not required. In addition to these two DEMs, for simulations of the CSZ-L1 event, a 2" DEM of the Strait of Juan de Fuca was used that was obtained by coarsening the 1/3" Strait of Juan de Fuca DEM [19].

Outside of the Strait and Puget Sound, etopo 1-minute topography for the Pacific Ocean and outer coasts was used for simulating the L1 event that initiates on the Cascadia Subduction Zone and the AKmaxWA event that is generated off Alaska.

The extent of all of these topo files (except the 1-minute topo) are depicted in Figure 4 below.

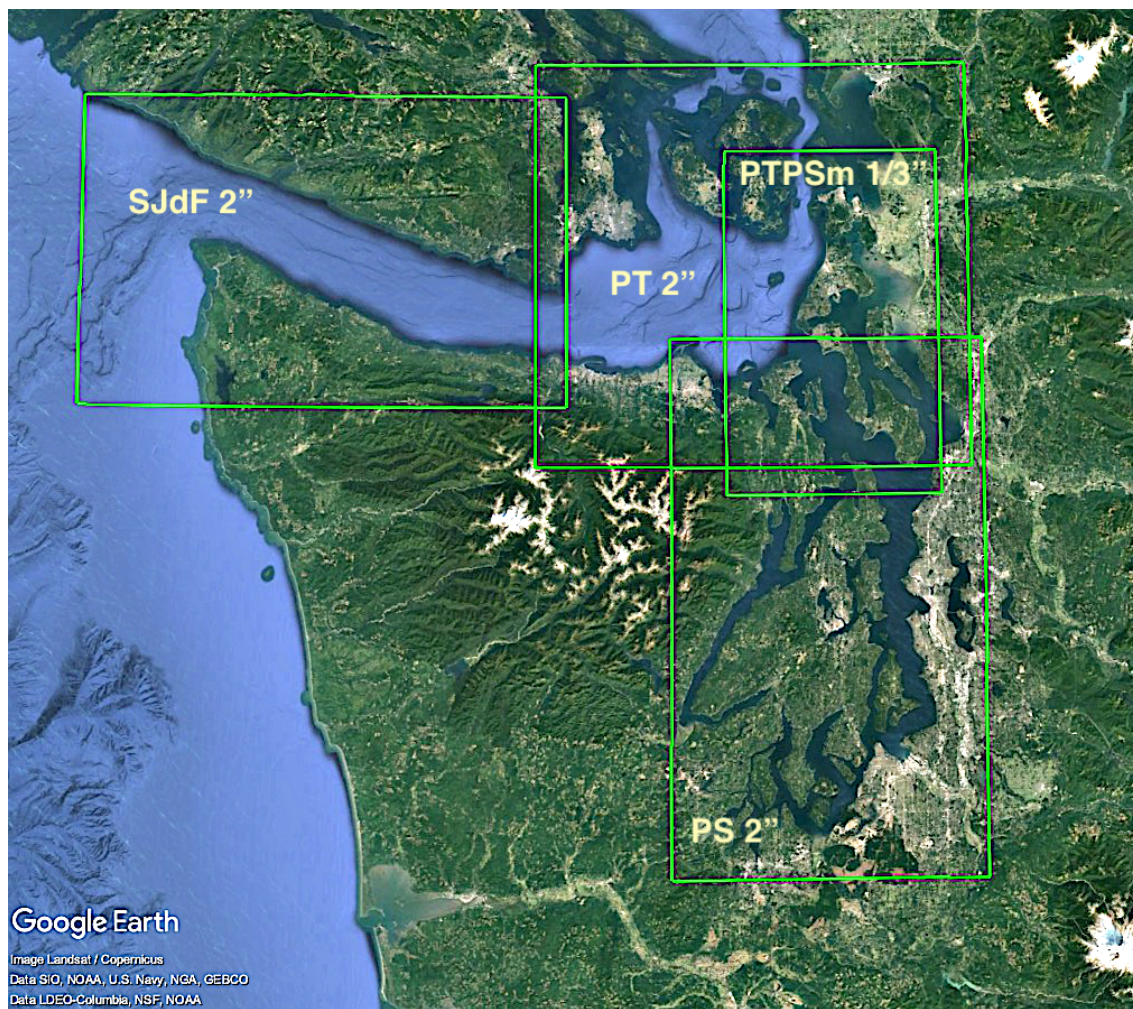


Figure 4: Topography files used for this project. The western most region is the 2" SJDF-DEM, the southern most is the 2" PS-DEM, and the remaining region covering the eastern most part of the Strait of Juan de Fuca is the 2" PT-DEM. The PTPSm-DEM corresponds to the new merged 1/3" DEM used for inundation modeling. All these DEMs were used for CSZ-L1 and AKmaxWA computations, and all but SJDF-DEM were used for the Seattle Fault SF-L results. In addition, etopo1 1-minute resolution DEMs were used for the Pacific Ocean and for the part of the Salish Sea and Strait of Georgia north of the extent of PT-DEM.

4 Modeling uncertainties and limitations

The simulations of tsunami generation, propagation and inundation were conducted with the GeoClaw model. This model solves the nonlinear shallow water equations, has undergone extensive verification and validation (e.g. [4, 15]), and has been accepted as a validated model by the U.S. National Tsunami Hazard Mitigation Program (NTHMP) after conducting multiple benchmark tests as part of an NTHMP benchmarking workshop [11].

Several important geophysical parameters must be set in the GeoClaw software, and some physical processes are not included in these simulations, which use the two-dimensional shallow water equations. These are discussed below along with their potential effect on the modeling results.

4.1 Tide stage and sea level rise

The simulations were conducted with the background sea level set to MHW. This value is conservative, in the sense that the severity of inundation will generally increase with a higher background sea level. Larger tide levels do occasionally occur, but the assumption of MHW is standard practice in studies of this type. Potential sea level rise over the coming decades was not taken into account in this modeling.

The 1/3" DEMs used in this study are all referenced to MHW, meaning so that $Z = 0$ corresponds to the shoreline at MHW.

4.2 Subsidence

The Seattle Fault event SF-L gave a small amount of subsidence (less than 15 cm) in the southwest portion of Whidbey Island, as shown in Figure 2. Elsewhere there was no subsidence from any event. The subsidence (or uplift) is accounted for in the GeoClaw modeling in the areas closer to the sources. The initial DEM provided for the region is modified by the earthquake deformation.

4.3 Structures

Buildings were not included in the simulations, the topographic DEMs provided for this study are “bare earth”. The presence of structures will alter tsunami flow patterns and generally impede inland flow. To some extent the lack of structures in the model is therefore a conservative feature, in that their inclusion would generally reduce inland penetration of the tsunami wave. However, as in the case of the friction coefficient, impeding the flow can also result in deeper flow in some areas. It can also lead to higher fluid velocities, particularly in regions where the flow is channelized, such as when flowing up streets that are bounded by buildings.

4.4 Bottom friction

Mannings coefficient of friction was set to 0.025, a standard value used in tsunami modeling that corresponds to gravelly earth. This choice of 0.025 is conservative in some sense, because the presence of trees, structures and vegetation would justify the use of a larger value, which might tend to reduce the inland flow. On the other hand, larger friction values can lead to deeper flow in some areas, since the water may pile up more as it advances more slowly across the topography. A sensitivity study using other friction values has not been performed.

4.5 Tsunami modification of bathymetry and topography

Severe scouring and deposition are known to occur during a tsunami, undermining structures and altering the flow pattern of the tsunami itself. Again, this movement of material requires an expenditure of tsunami energy that tends to reduce the inland extent of inundation. On the other hand, if natural berms or ridges

along the coastline (or man-made levies or dikes) are eroded by the tsunami, then some areas can experience much more extensive flooding. There is no erosion or deposition included in the simulations presented here.

5 Study regions

Figure 1 shows the coast of Island and Skagit Counties subdivided into the six polygons covering the study region. These regions will be referred to as *fgmax regions* since these are regions on which a fixed set of points is defined (independent of adaptive refinement) on which the maximum of each quantity of interest is monitored during the course of the simulation. The quantities monitored are the flow depth, flow speed, and momentum flux, along with the time at which the maximum is attained and the first arrival time of significant waves at each grid point.

Within each fgmax region, a set of fgmax points were defined as described below, the points where the maxima need to be monitored. For each tsunami source, a separate job run was then done for each region in which adaptive mesh refinement (AMR) was used to focus fine computational grids around the fgmax region. Due to the large extent of the study region and complicated coastline, it was not possible to do a single run with 1/3" resolution around all the fgmax regions. Table 2 gives an overview of the six regions.

Region label	Count	Plots and Results
SW_Whidbey	758,485	Section 6.1
W_Whidbey	1,487,849	Section 6.2
NW_Whidbey	1,407,122	Section 6.3
E_Whidbey	2,842,086	Section 6.4
SE_Whidbey	1,625,609	Section 6.5
Skagit	5,327,605	Section 6.6
Total	13,448,756	

Table 2: The fgmax regions. The fgmax points are aligned with the DEM in the regions specified, with 1/3" spacing in longitude and 1/3" in latitude. The column labeled "Count" gives the number of fgmax points in each region. See Section 6 for plots of the fgmax points and of sample results for each region.

The fgmax points lie on a grid with spacing 1/3" by 1/3" that is aligned with the DEM grids. An improvement to GeoClaw developed for a previous project [12] allows selecting only the grid points in each region for which the topography elevation is below some limit. For the current project we have made additional improvements to the code that now allow us to select only the points from the 1/3" grid that satisfy all of these conditions:

- The point lies within a specified polygon,
- The point has a topography elevation below a specified maximum Z_{\max} ,
- There is a path of points with elevation below Z_{\max} connecting the point to the coast.

In addition, any grid point in the polygon that lies within 10 grid cells of the coast is selected as an fgmax point, insuring that there is a band of fgmax points all along the coast, even in regions where the topography rises very steeply.

These improvements were necessary in order to reduce the total number of fgmax points to a manageable number. Our previous approach used in [12, 1, 22] did not enforce a band of fgmax points along the coast and so Z_{\max} was set to 40 m to insure that some onshore points were included even in regions of steep topography. With the new approach we have set $Z_{\max} = 15$ m, since we know that no event creates run-up exceeding this value. Moreover, the new approach avoids selecting points that are below Z_{\max} in elevation but separated from the coast by higher ground (e.g. a local depression), since we know that the tsunami cannot reach these points. This also helps to reduce the number of fgmax points selected.

In addition, we improved the code to allow specifying a certain type of polygon as the fgmax region from which to select fgmax points. (These "Ruled Rectangles" are described in Appendix B.) In our previous

work we first specified rectangles and then selected points below elevation Z_{\max} . That approach did not carry over well to the complicated geometry of the current study region. In particular, we have specified polygons for the fgmax regions `E.Whidbey` and `SE.Whidbey` that cover the coast on the east side of Whidbey Island and the west side of Camano Island, while three other polygons cover the west side of Whidbey Island (see Figure 1). In each case we want to select fgmax points only from one side of the island and use fine 1/3" computational grids only on that side of the island. Specifying rectangles that cover the desired regions would be impossible. (The AMR procedures in GeoClaw have also been improved to allow specifying refinement to the finest level only in certain Ruled Rectangles; see Appendix B.)

Even with these improvements, the total number of fgmax points over the entire study region is still more than 13 million. Table 2 gives a breakdown by region. In order to efficiently run the code with so many fgmax points, it was also necessary to make some improvements in the way fgmax points are handled internally in the GeoClaw code, resulting in a substantial speedup while still monitoring values in the same manner as in previous versions of GeoClaw.

All of these improvements are discussed in more detail in Appendix B. They will eventually be incorporated into the open source GeoClaw package for use by others as well, and all the code used in this project is archived at [14].

If only onshore inundation and near shore currents need to be modeled, then one could also set a lower threshold, e.g. -60 m, and only select fgmax points within the polygons where the bathymetry elevation is both above this value and less than Z_{\max} . For this project we included all water points in each polygon in order to model currents farther from shore.

5.1 Issues with land below MHW

Several coastal areas in the study region contain dry land that is below MHW, but protected by dikes and/or levees from inundation under normal conditions. In particular, the Skagit River Delta contains more than 150 km^2 of land below MHW, mostly farmland but also many structures and several communities, including much of the town of La Conner, WA (see Figure 1 and further discussion in Appendix D). The standard GeoClaw software would initialize these points with water up to the level of MHW at the start of the simulation, flooding all of this area even if no tsunami arrives. This would be quite misleading since much of this area does not flood for the tsunami events considered here. Moreover, even in regions the tsunami does reach, it would have very different dynamics if it moved over an initially flooded artificial lake than moving over dry land, and the maximum depths recorded would not be at all correct; water entering a large artificial lake will spread out rapidly and eventually raise the level everywhere by a small amount, whereas the same quantity of water overtopping a dike and moving across dry land will quickly decelerate due to high bottom friction, giving higher maximum depth near the dike and little or no flooding farther inland.

To deal with this problem, a new capability was developed in the course of modeling Whatcom County [1], where the same problem arose to a lesser extent. For the current project, an improved version of this approach has been developed.

The general idea is to pre-process the 1/3" topography DEM to generate a mask array `allow_wet_init` that covers the same region (or at least some subset of the DEM that contains all regions where dry land below MHW exists). This mask array indicates at each DEM point if this is a point that should be viewed as dry when using the DEM to initialize GeoClaw, regardless of its elevation, or if this point should be handled in the usual way in GeoClaw (described below), which allows it to be initially wet. Below we use A_{ij} to denote the value of this `allow_wet_init` array in the (i, j) grid cell.

Recall that GeoClaw generates cell-averaged topography values in each finite volume grid cell by integrating a piecewise bilinear function defined by the DEM. So even if the finite volume cells on the finest level are exactly aligned with the 1/3" DEM, as enforced in this project, the GeoClaw topography value B_{ij} in a cell will not agree with the DEM value Z_{ij} at the center of the cell. The "usual way" to initialize water depth in a cell is to set the depth $h_{ij} = 0$ if $B_{ij} \geq \text{sea_level}$ (a dry cell) and to $h_{ij} = \text{sea_level} - B_{ij} > 0$ if $B_{ij} < \text{sea_level}$ (a wet cell). Hence the surface elevation $\eta_{ij} = B_{ij} + h_{ij}$ is equal to `sea_level` in the wet cells. Here `sea_level` represents the desired initial sea level for the tsunami simulation, relative to the vertical datum of the DEM. For this project, the 1/3" DEMs are referenced to MHW, which is the desired

initial water level, and so we set `sea_level` = 0. (To model the effect of the tsunami arriving at a different tide stage, or to account for expected future sea level rise, a different value of `sea_level` might be chosen in the GeoClaw run.)

When the mask array `allow_wet_init` $\equiv A$ covers a grid cell, the above procedure is used if $A_{ij} == 1$, but if $A_{ij} == 0$ then we set $h_{ij} = 0$ regardless of B_{ij} .

The approach used to create the mask array consists of setting $A_{ij} = 1$ wherever $Z_{ij} < -5$ m (or some sufficiently deep value that any point satisfying this is offshore). At other points A_{ij} is set to a special value indicating `unset`. A value of `sea_level_mask` is then chosen and the idea is to flood the topography outwards from the points already set by setting $A_{ij} = 1$ at any points neighboring the currently set points if they satisfy $Z_{ij} < \text{sea_level_mask}$. (Note that `sea_level_mask` might be different from `sea_level`, as discussed below.) An iterative “marching front” algorithm is used to expand the front outwards in each iteration until no additional points can be so marked. Normally this will march up to the shoreline and not beyond. All inland points will still be `unset`. If an impermeable dike exists that subdivides the region, then the marking will stop at the dike and points behind the dike will be `unset` even if $Z_{ij} < \text{sea_level_mask}$. At this point all `unset` points are marked as forced to be dry, by setting $A_{ij} = 0$ at these points.

This procedure does not always work exactly as hoped, for several reasons:

- A 1/3” DEM has grid spacing of about 10 m in latitude and 7 m in longitude (at the latitude of Puget Sound). Some dikes are so narrow that they are not well represented in the DEM, particularly if they cut through the grid at an angle. Hence even a “perfect” DEM at this resolution may have gaps consisting of DEM points with $Z_{ij} < \text{sea_level}$ that allow the marching algorithm to pass through the dike and eventually erroneously mark all points on the inland side with $A_{ij} = 1$, allowing GeoClaw to initialize this region with wet cells.
- The DEMs are not always perfect and may have values $Z_{ij} < \text{sea_level}$ even at points where the dike exists and should be above `sea_level` over a sufficiently wide region to be leak-free at 1/3” resolution. These erroneous gaps can again result in large regions being improperly flooded initially.
- Even if the DEMs are perfect and the dikes are sufficiently wide, the referencing to MHW may not be perfect and so a dike that should extend above `sea_level` may fall slightly short. It should be remembered that although a vertical datum like NAVD88 is well defined at each point on earth, the MHW vertical datum requires computing an offset relative to NAVD88 that varies spatially, since the tide is greatly affected by the local topography, particularly in a complex region like Puget Sound. The Port Townsend 1/3” DEM covering the Skagit River Delta, for example, covers a large portion of the Sound and no single offset from NAVD88 is correct.

The Skagit River Delta contains more than 200 km of dikes and levies and so it should not be surprising that they are not all gap-free in the 1/3” DEM, particularly when the possible offset from true MHW is taken into account.

In the `Skagit` region, in order to obtain an `allow_wet_init` mask that does a sufficiently good job (as judged by comparing the points forced to be dry with satellite imagery from Google Earth), we applied the marching algorithm with a value `sea_level_mask` = -0.6 m, instead of using `sea_level_mask` = 0. After lowering the specified sea level by 60 cm, the marching algorithm does stop at nearly all dikes along the coast. (Lowering by only 50 cm still gave incorrect results in some areas near La Conner.)

In the GeoClaw simulation we still initialize everywhere using `sea_level` = 0, so that the simulation is still at MHW (as defined by the DEM). We only used the lowered `sea_level_mask` to determine the mask array used to force some GeoClaw cells to be dry even though $B_{ij} < 0$. Note that any gaps in the dike relative to MHW still exist, and in the GeoClaw simulation water will still leak in through these gaps. Moreover, even if there are no gaps in the DEM topography, recall that the B_{ij} values used in GeoClaw come from integrating piecewise bilinear functions defined by the DEM, and this introduces a smoothing that can cause a lowering of the dikes and additional leakiness in the GeoClaw simulation.

However, this leakage will be very slow since the elevation in the gaps is close to MHW (hence the water depth is small and subject to large frictional drag) and the water is flowing into initially dry areas. If run

long enough, the water would eventually fill all the land behind the leaky dike, at least until it runs into non-leaky levies, but in practice for large initially dry areas this would take much longer than the time scale of the tsunami inundation in our simulations.

For regions close to the leaky dikes, however, it is possible that some flooding will be observed due to the leakiness in regions that should not be flooded by the tsunami. We believe this is only an issue for the SF-L event in the *Skagit* region, since this tsunami has little offshore wave height in this region and perhaps should not flood beyond the dikes at all. Hence some caution should be used when interpreting these results. See Section 6.6 for more discussion of the issues in this region.

6 Results – Maximum flow depth and speeds

We have not attempted to produce high quality graphics of the results, since Washington State DNR is producing the maps that will be published elsewhere. However, we provide some plots to give an indication of the sort of flooding and flow speeds observed, and for future reference if the simulations are re-run at a later date.

For each region we first show the fgmax points that were selected for that region. These plots also show regions (if any) where the topography DEM value showed the point as below MHW but the algorithm described in Section 5.1 identified the point as an initially dry point.

The maximum flow depth plots show the maximum depth of water recorded during the computation over the full simulation time of 6, 8, or 14 hours (for SF-L, CSZ-L1, and AKmaxWA, respectively). This depth is shown only in regions that were originally dry in the simulation, and those points colored green remained dry. White regions are where there was initially water, or else there were no fgmax points. In the speed plots the maximum speed is shown both in the water and for initially dry points that became wet at some point. White regions are where there were no fgmax points.

In addition to the plots shown in this report, we have also produced high-resolution png files in a form that has been embedded in kml files to facilitate viewing the input data and results on Google Earth, for example. The low resolution figures in this report cannot possibly show all the details whereas with the kml files the user can zoom in to explore the results in more detail. These kml files are archived at [14], along with the Python code that produced them.

The raw results are contained in netCDF files archived at [14], and these can be downloaded and plotted in different ways or with different color maps, either using modifications of our Python scripts, or with sophisticated GIS tools.

6.1 Region SW_Whidbey

See Figure 1 to see the location of the SW_Whidbey region in the context of the full study region. Figure 5 below shows the fgmax points selected within this region, with points colored by elevation relative to MHW. Figure 6 also shows the fgmax points but with those determined to be dry land below MHW colored pink.

Figure 7 shows some sample results for each of the three regions, as described at the start of Section 6.

Noteworthy in this region.

- The SW_Whidbey region contains two areas of extensive dry land below MHW. One region near Maxwelton is at roughly latitude 46.95 and is well isolated behind the road running along the coast. There are houses along the road but the land below MHW appears to be mostly wetlands. This region was easily identified by the algorithm described in Section 5.1. The second region is at the north shore of Useless Bay, around Deer Lagoon at latitude 47.99. Much of this land is wetlands but the Useless Bay Golf & Country Club also lies in this region.
- The topography DEM around Deer Lagoon contains gaps in the dikes and/or low spots, as described in Section 5.1. In order to dry identify points in this region the marching front algorithm was applied with the `sea_level_mask` set to -0.5 m. The GeoClaw run is still performed with `sea_level` set to 0.

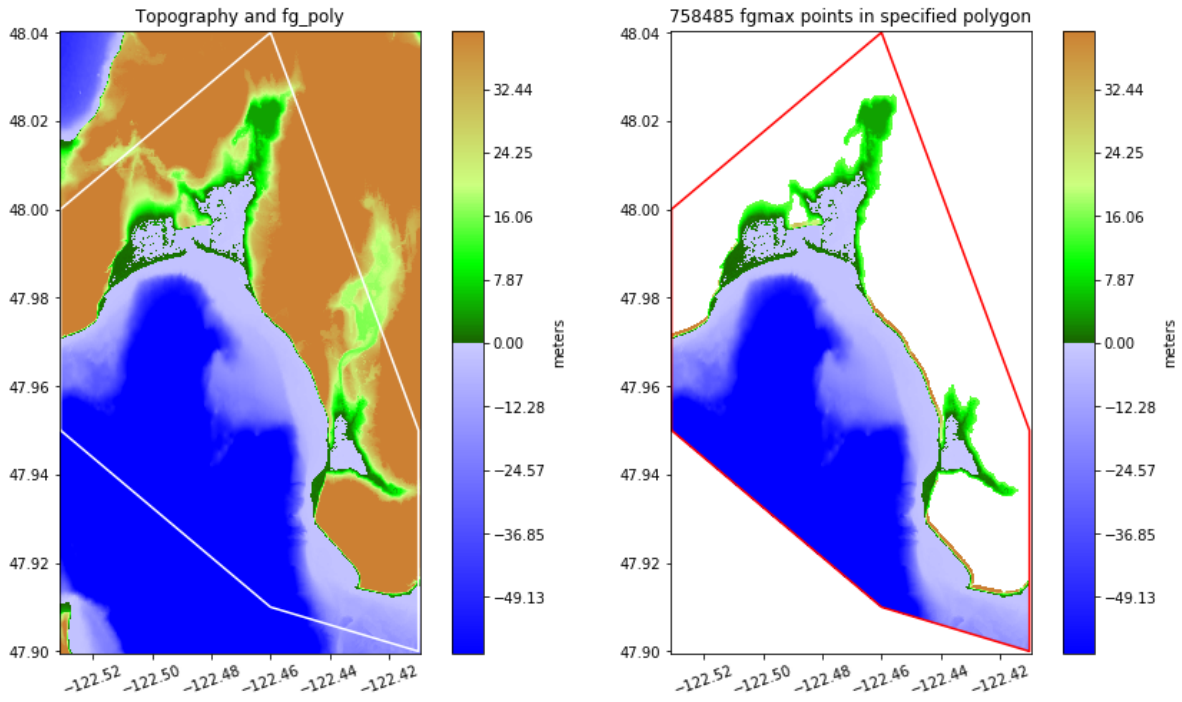


Figure 5: Left: Polygon used to select fgmax points for the Region SW_Whidbey. Right: Points selected.

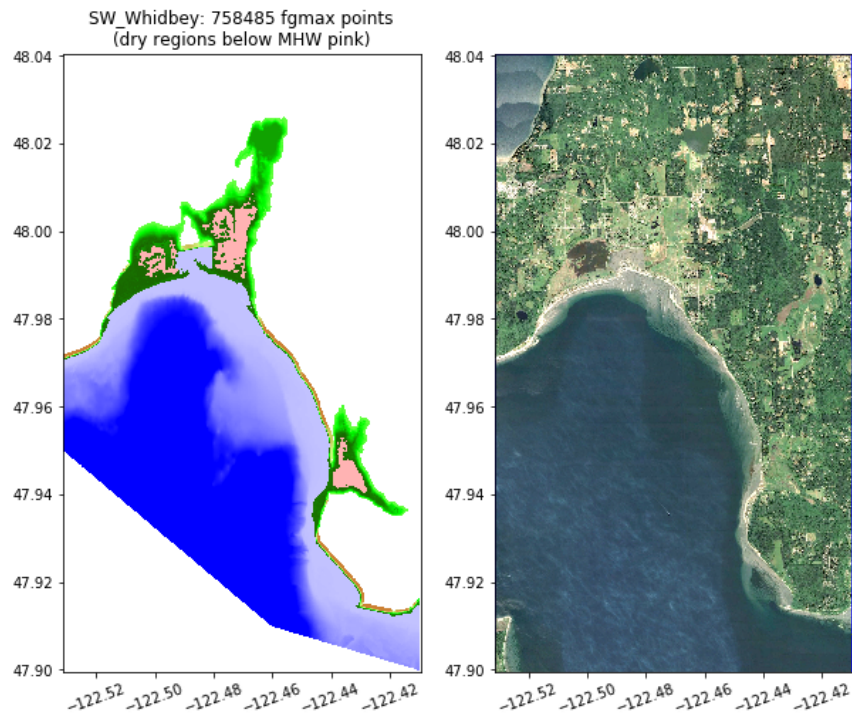


Figure 6: fgmax points selected in Region SW_Whidbey with points identified as dry but below MHW colored pink. For comparison the figure on the right shows a Google Earth image of this region.

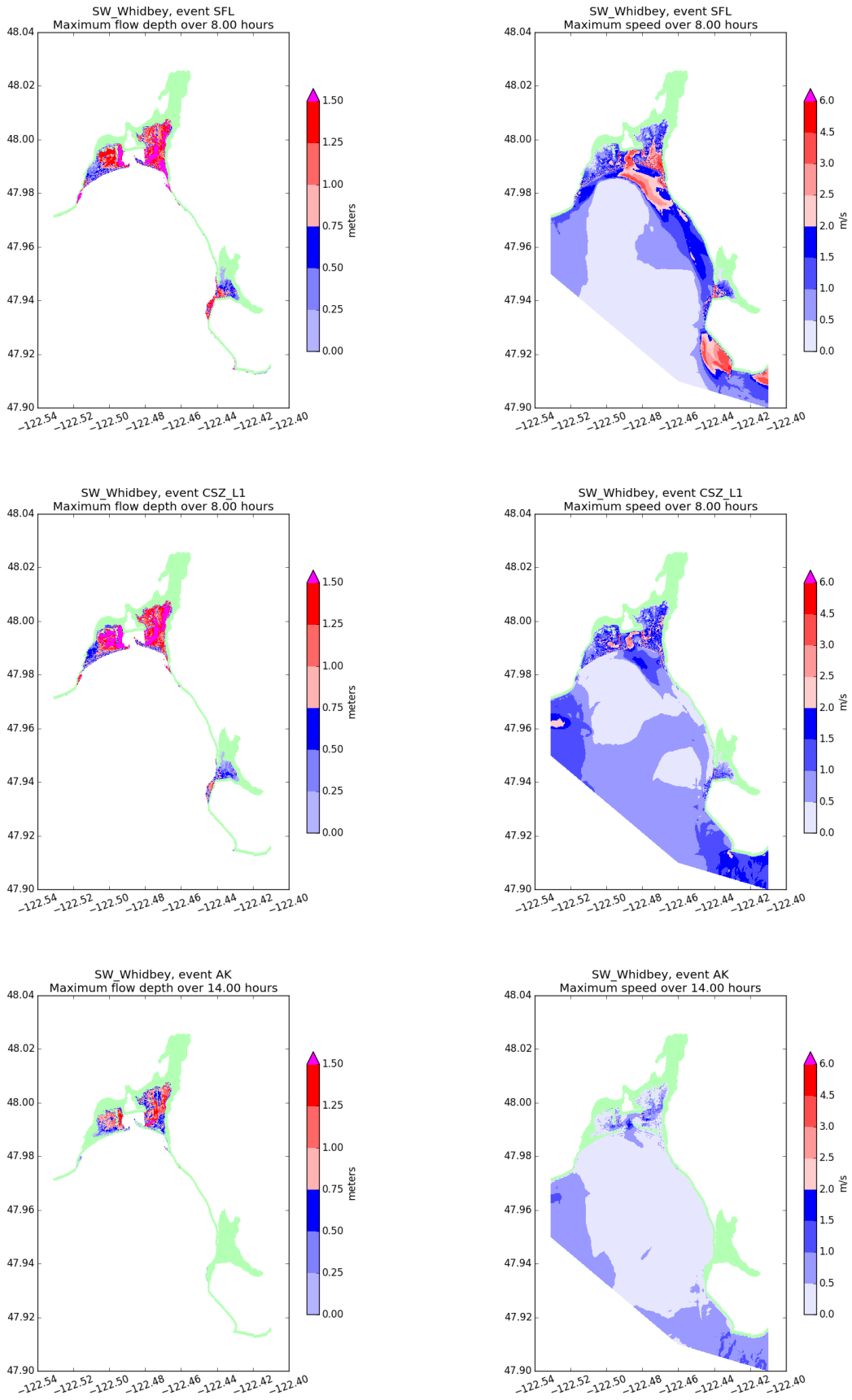


Figure 7: Sample results for the Region SW Whidbey. See the description in Section 6.
 20

6.2 Region W_Whidbey

See Figure 1 to see the location of the W_Whidbey region in the context of the full study region. Figure 8 below shows the f_{gmax} points selected within this region, with points colored by elevation relative to MHW. Figure 9 also shows the f_{gmax} points but with those determined to be dry land below MHW colored pink.

Figure 10 shows some sample results for each of the three regions, as described at the start of Section 6.

Noteworthy in this region.

- There is a large area of land below MHW at the north edge of this region, between Keystone and Fort Casey, that is predominantly behind a dike. This area is partly wetland and includes Crockett Lake. This area was initialized as dry in the GeoClaw simulation, including the lake bed.
- The Keystone Ferry Terminal lies in this region, and Gauge 23 shows time series at this location.

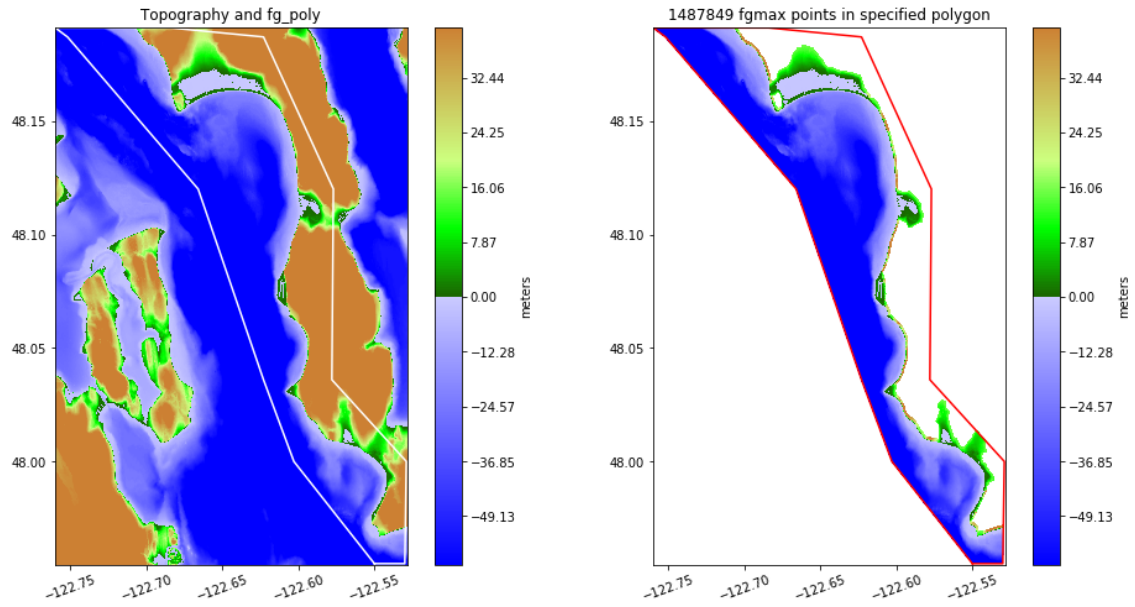


Figure 8: Left: Polygon used to select fgmax points for the Region W.Whidbey. Right: Points selected.

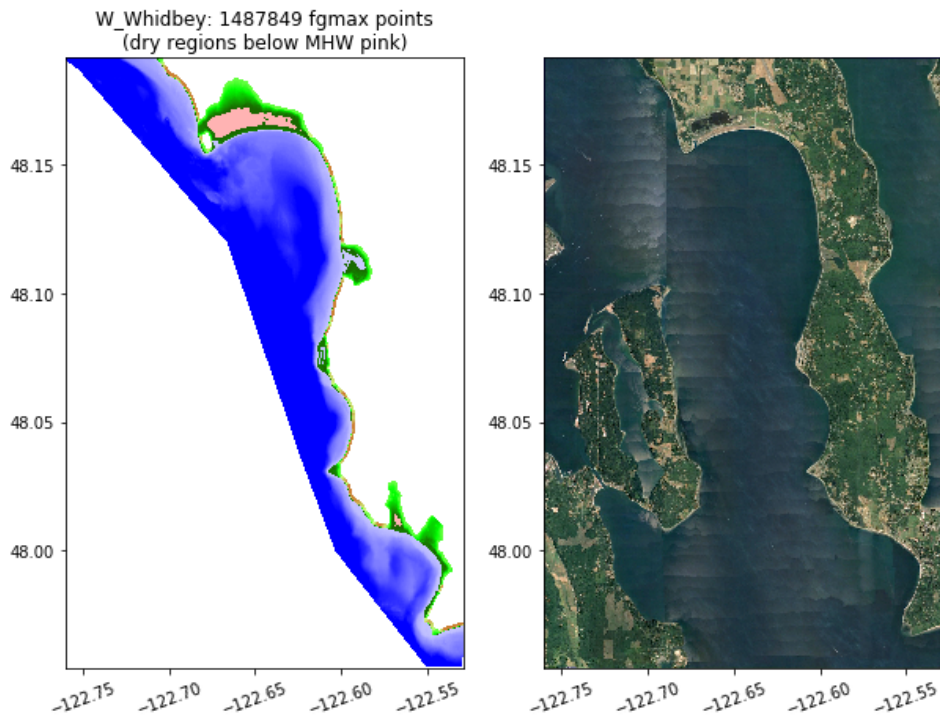


Figure 9: fgmax points selected in Region W.Whidbey with points identified as dry but below MHW colored pink. For comparison the figure on the right shows a Google Earth image of this region.

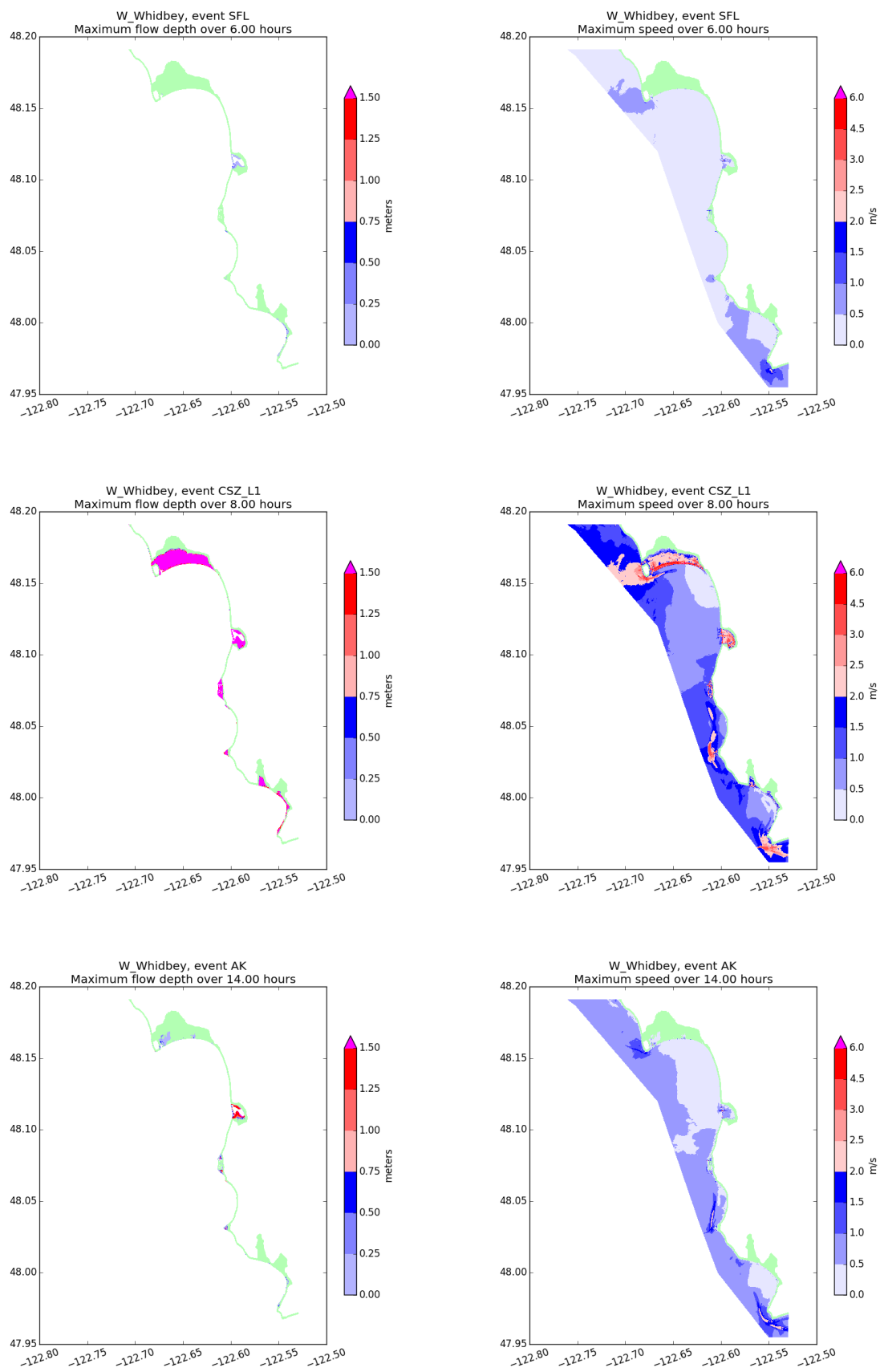


Figure 10: Sample results for the Region W_Whidbey. See the description in Section 6.

6.3 Region NW_Whidbey

See Figure 1 to see the location of the NW_Whidbey region in the context of the full study region. Figure 11 below shows the fgmax points selected within this region, with points colored by elevation relative to MHW. Figure 12 also shows the fgmax points but with those determined to be dry land below MHW colored pink (none in this region).

Figure 13 shows some sample results for each of the three regions, as described at the start of Section 6.

Noteworthy in this region.

- No areas below MHW in this region were determined to be dry land and so in this region the standard GeoClaw procedure was used to initialize all cells in which $B < 0$ as initially wet.
- Naval Air Station Whidbey Island (Ault Field) lies in this region and is partly inundated by the CSZ-L1 event.

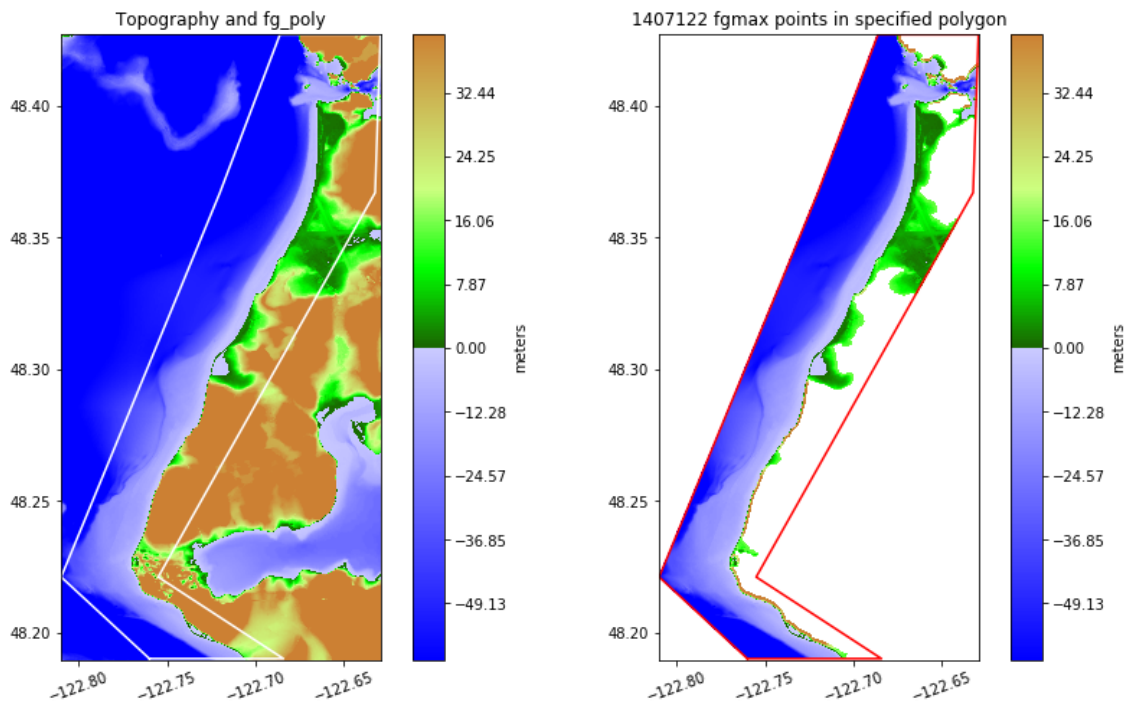


Figure 11: Left: Polygon used to select fgmax points for the Region NW Whidbey. Right: Points selected.

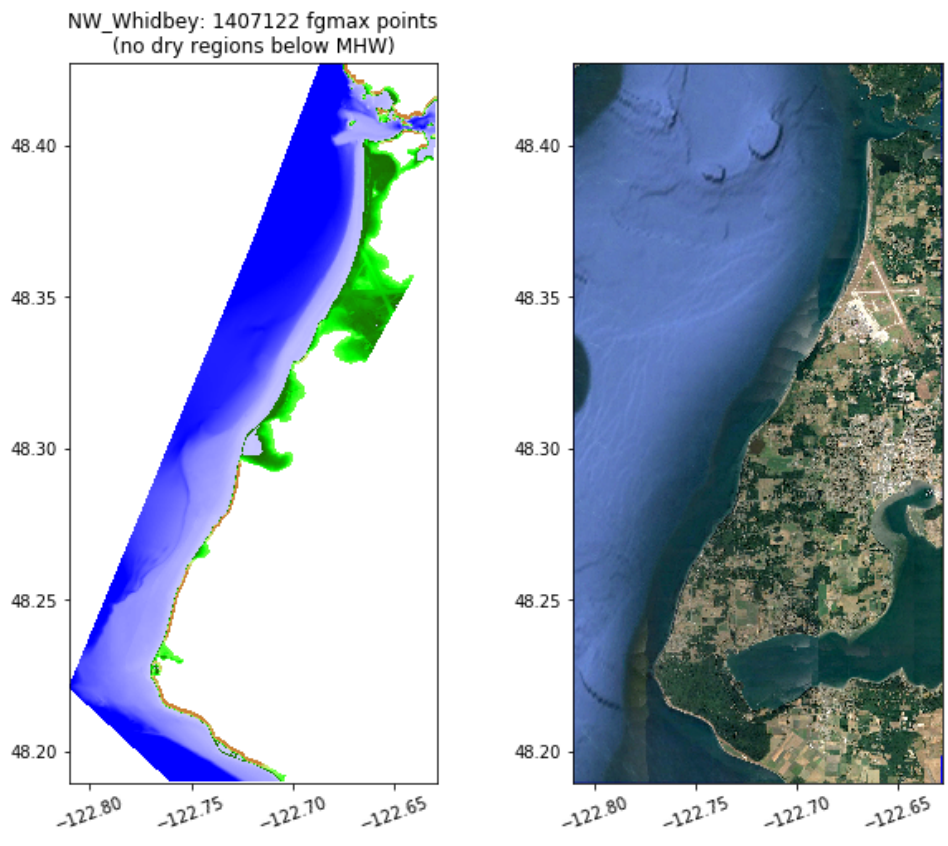


Figure 12: fgmax points selected in Region NW Whidbey with points identified as dry but below MHW colored pink (none in this region). For comparison the figure on the right shows a Google Earth image of this region.

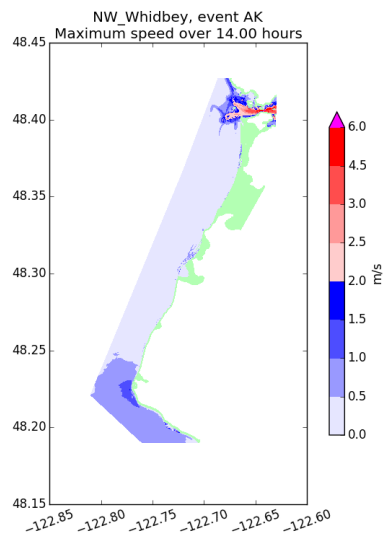
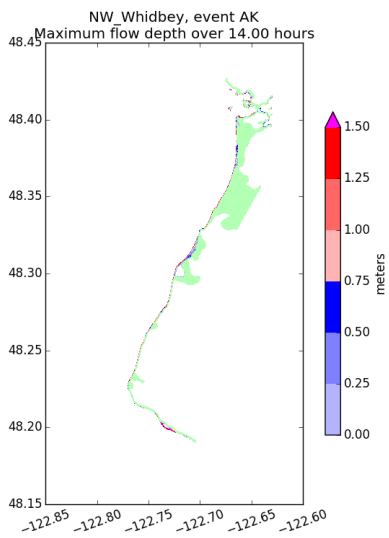
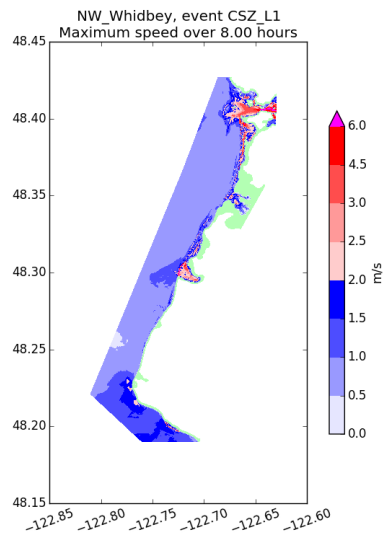
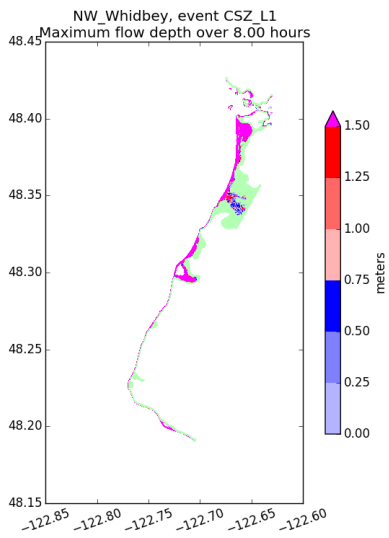
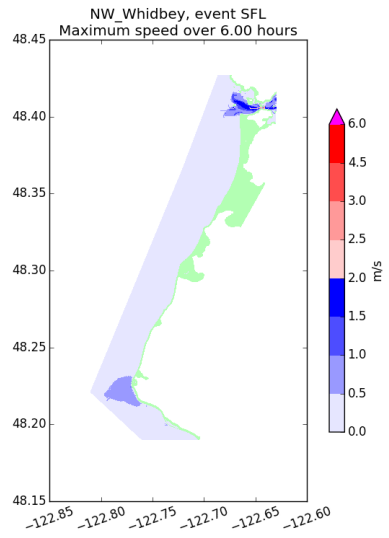
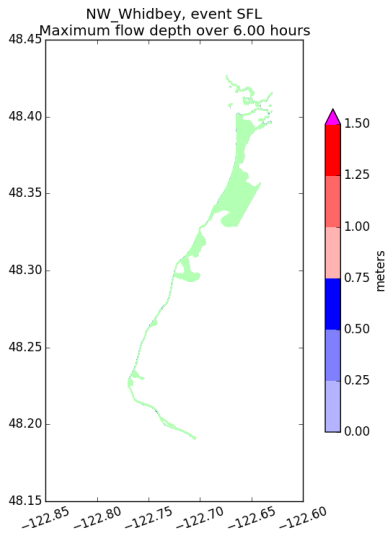


Figure 13: Sample results for the Region NW_Whidbey. See the description in Section 6.
26

6.4 Region E_Whidbey

See Figure 1 to see the location of the E_Whidbey region in the context of the full study region. Figure 14 below shows the fgmax points selected within this region, with points colored by elevation relative to MHW. Figure 15 also shows the fgmax points but with those determined to be dry land below MHW colored pink.

Figure 16 shows some sample results for each of the three regions, as described at the start of Section 6.

Noteworthy in this region.

- The E_Whidbey region covers the waterway on the east side of Whidbey Island, which is partly bounded by the west coast of Camano Island. There is only one small region at the northern extent of this region near Oak Harbor that was identified as below MHW but protected by dikes.
- Tsunami waves primarily reach this region from the south, traveling between the southern tip of Whidbey Island and Everett, either directly from the Seattle Fault event, or after passing through Admiralty Inlet for the CSZ and AKmaxWA events. In principle waves traveling through Deception Pass, at the northern tip of Whidbey Island, can also reach this region. However, our tests showed that these waves are small relative to those arriving from the south.

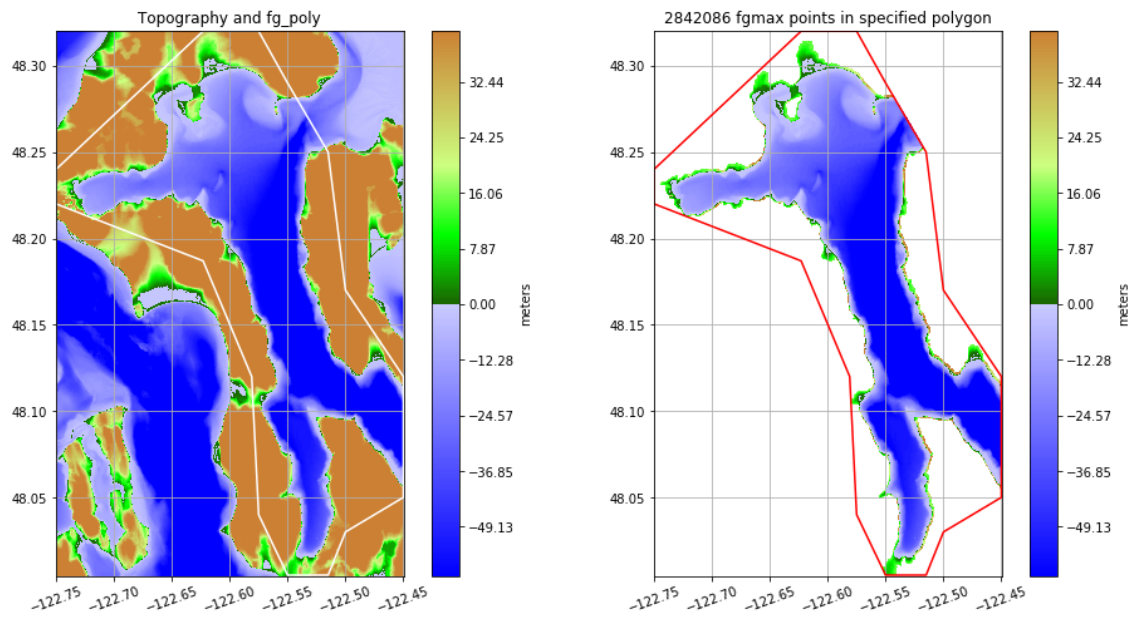


Figure 14: Left: Polygon used to select fgmax points for the Region E.Whidbey. Right: Points selected.

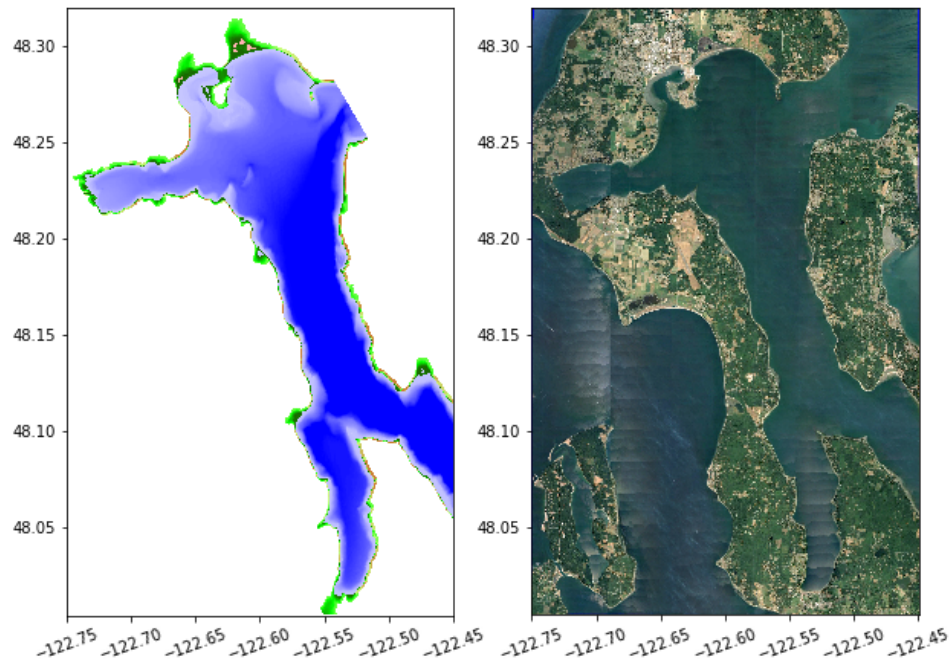


Figure 15: fgmax points selected in Region E.Whidbey with points identified as dry but below MHW colored pink. For comparison the figure on the right shows a Google Earth image of this region.

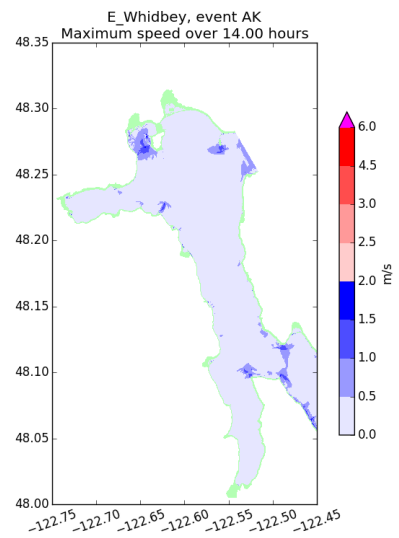
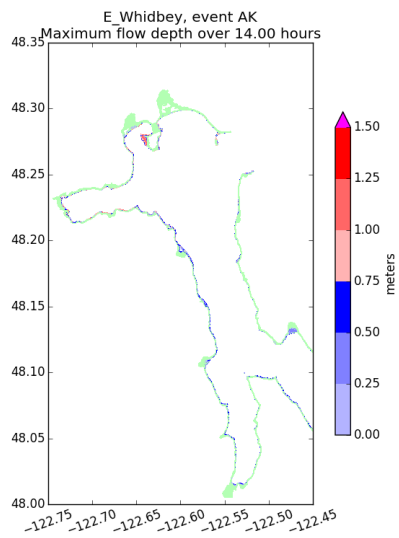
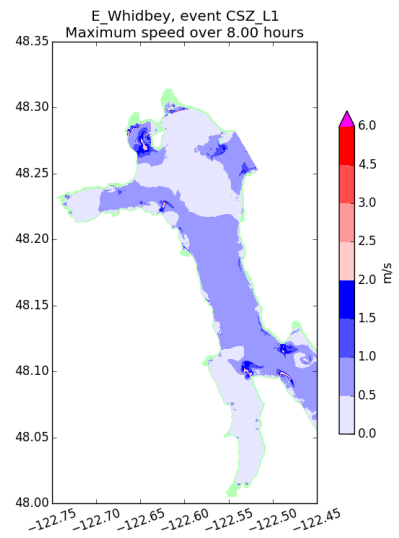
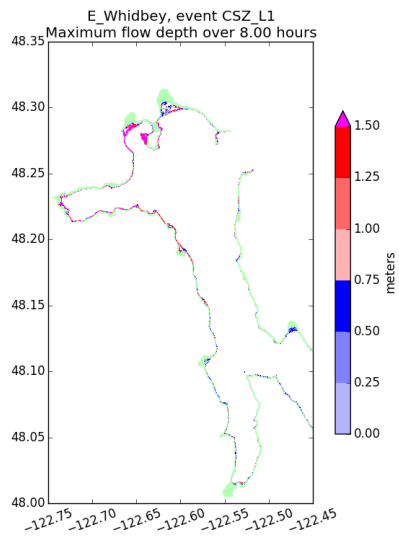
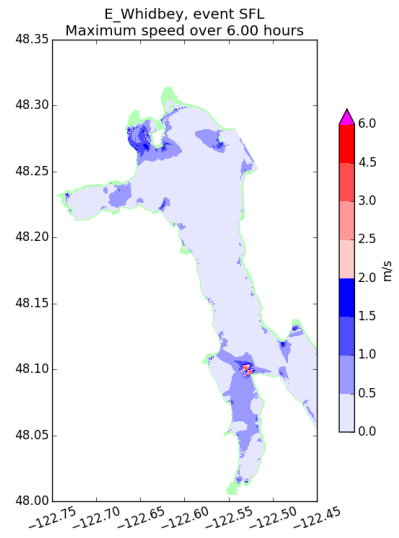
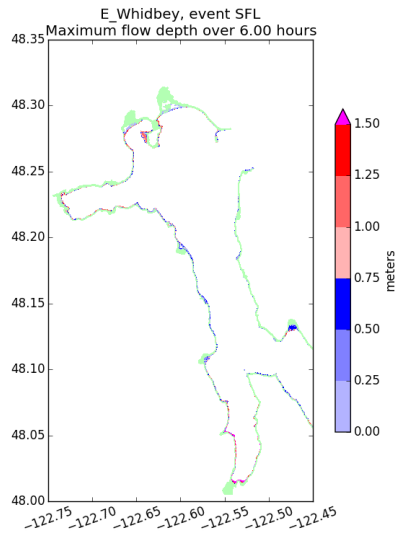


Figure 16: Sample results for the Region E_Whidbey. See the description in Section 6.
29

6.5 Region SE_Whidbey

See Figure 1 to see the location of the SE_Whidbey region in the context of the full study region. Figure 17 below shows the fgmax points selected within this region, with points colored by elevation relative to MHW. Figure 18 also shows the fgmax points but with those determined to be dry land below MHW colored pink (none in this region).

Figure 19 shows some sample results for each of the three regions, as described at the start of Section 6.

Noteworthy in this region.

- No areas below MHW in this region were determined to be dry land and so in this region the standard GeoClaw procedure was used to initialize all cells in which $B < 0$ as initially wet.
- This region was already modeled as part of the previous Snohomish County project [12]. However, it has been redone as part of this work so that all of Whidbey Island will be covered. In the future we plan to redo all of the Snohomish County project with the latest version of GeoClaw since elsewhere in the County there are significant regions of dry land below MHW.

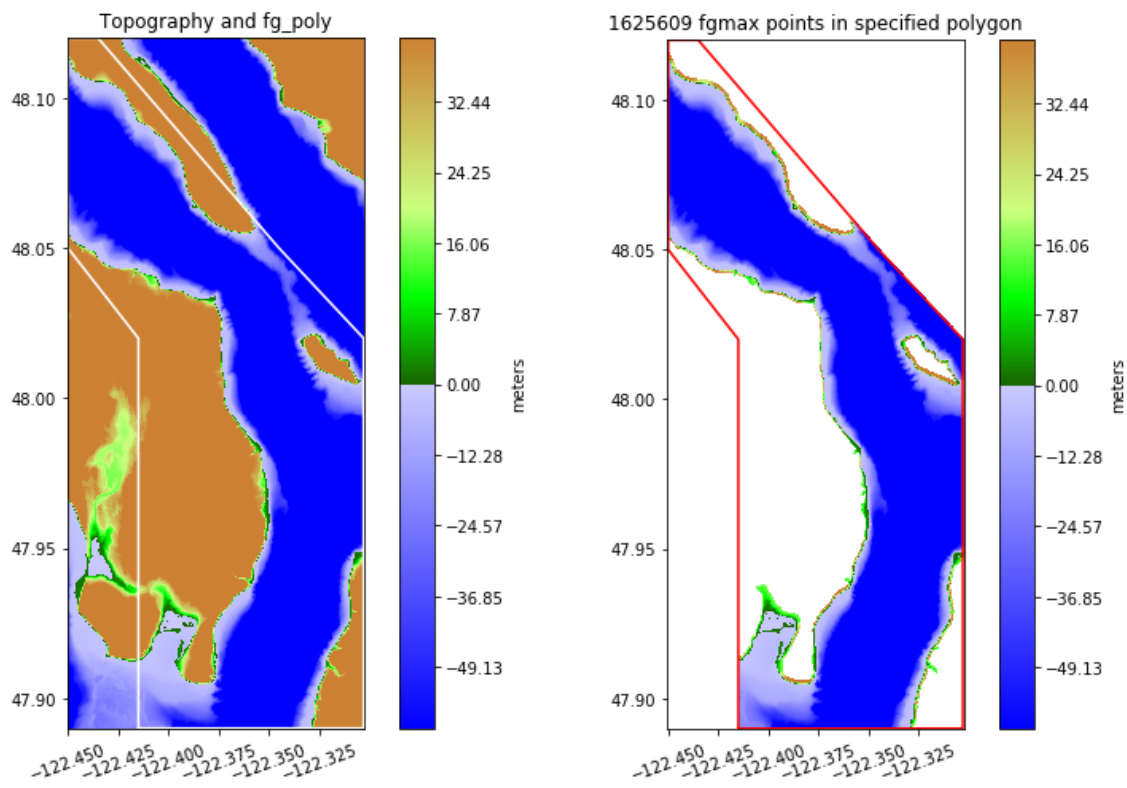


Figure 17: Left: Polygon used to select fgmax points for the Region SE Whidbey. Right: Points selected.

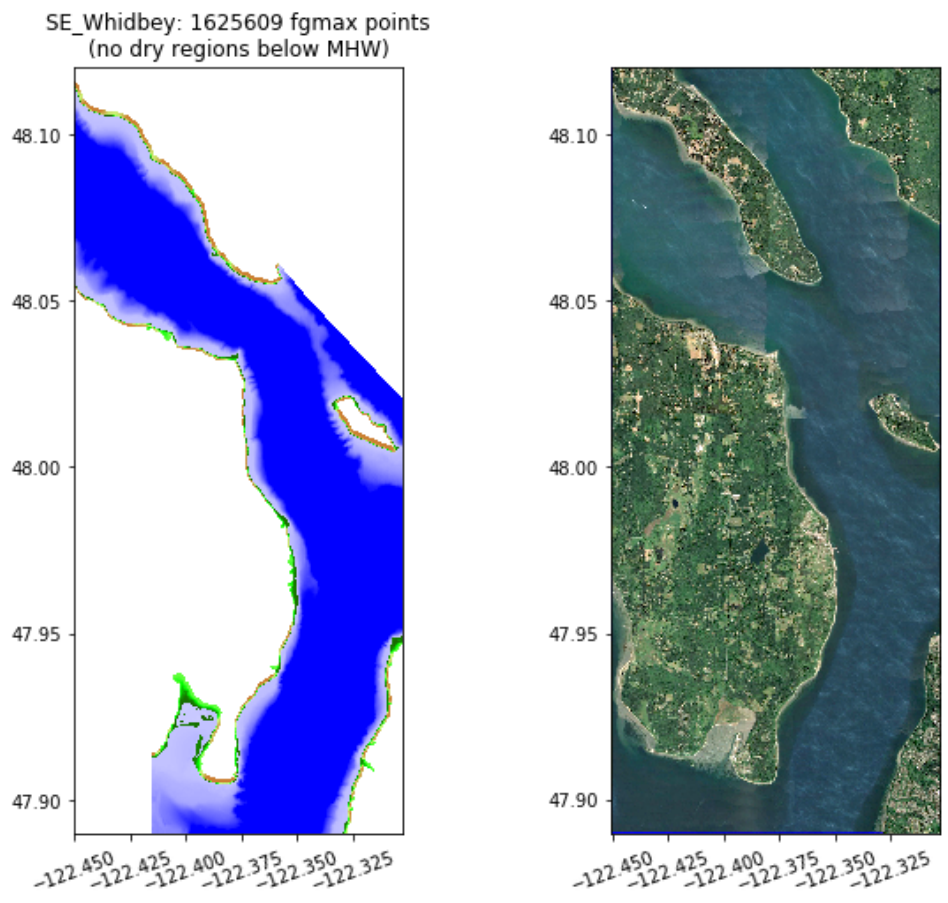


Figure 18: fgmax points selected in Region SE Whidbey. For comparison the figure on the right shows a Google Earth image of this region.

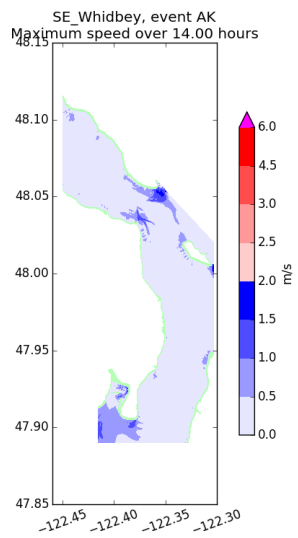
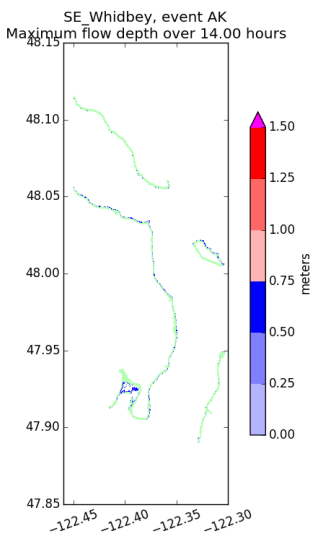
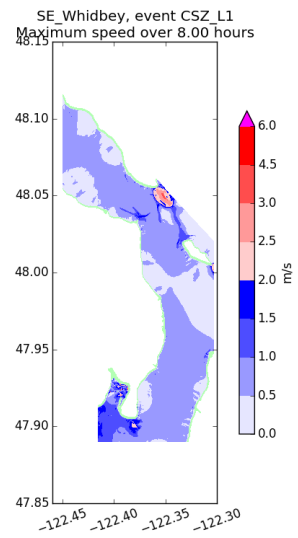
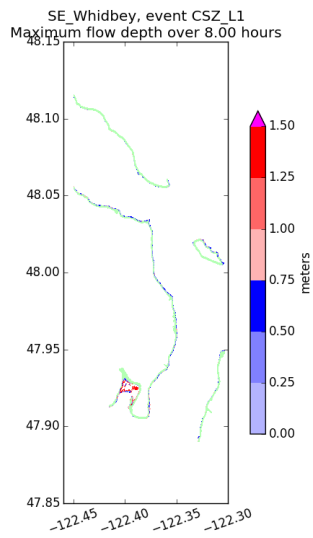
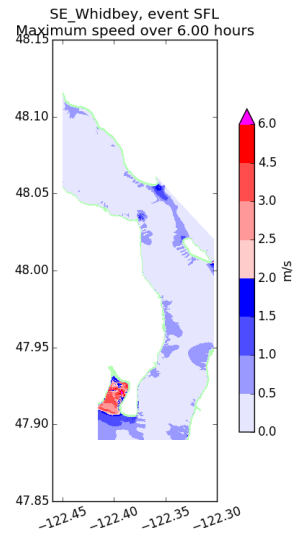
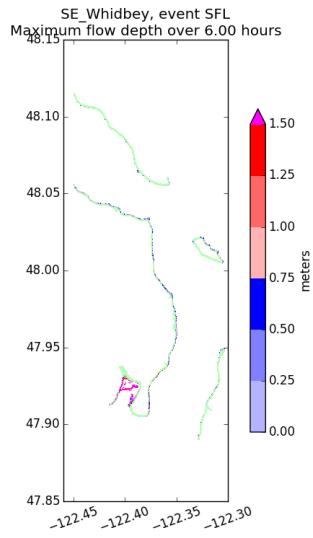


Figure 19: Sample results for the Region SE_Whidbey. See the description in Section 6.

6.6 Region Skagit

See Figure 1 to see the location of the **Skagit** region in the context of the full study region. Figure 20 below shows the fgmax points selected within this region, with points colored by elevation relative to MHW. Figure 21 also shows the fgmax points but with those determined to be dry land below MHW colored pink.

Figure 19 shows some sample results for each of the three regions, as described at the start of Section 6.

Noteworthy in this region.

- There are extensive areas (more than 150 km²) of dry land below MHW in this region.
- The custom DEM PTPSm-DEM discussed in Section 3 differs from the original PT-DEM in some significant ways in this region, and appears to be more accurate.
- There are still gaps in some of the dikes, and/or MHW is not exactly correct so that water overtops in some places. In order to determine regions to initialize as dry, the algorithm of Section 5.1 was applied with `sea_level_mask` set to -0.6 m. Setting it slightly higher, to -0.5 m, give more extensive regions of incorrect initial flooding. With this value most dry land was correctly identified. See Appendix D for more discussion and additional figures.
- Waves enter this region in one of three ways: through Deception Pass (at the west edge near latitude 48.4), from the south (through region **E_Whidbey**), or from Padilla Bay in the north. The fgmax region was expanded to the north farther than originally planned in order to better model waves arriving through Padilla Bay. With both the CSZ and AKmaxWA events, these waves eventually overtop Highway 20, which runs along Padilla Bay to Anacortes.
- The CSZ results around Highway 20 differ from those obtained in 2016 by PMEL [8], where no overtopping was observed. Moreover the parking lot of the Swinomish Casino & Lodge (at roughly 48.4583N, 122.1595W) is partly inundated in our CSZ simulation, and was not in the 2016 work. Several differences in the modeling have been identified that could explain this. In particular, the 2016 work used a different version of the CSZ-L1 event that may not give as large waves, and the modeling resolution was 2/3 by 1/3 arcseconds rather than 1/3 by 1/3 and used Manning coefficient 0.03 rather than 0.025. Moreover, in the 2016 work any areas with elevation below MHW were initialized as wet, including the regions shown as pink in Figure 25.
- This Southeast corner of this region was already modeled as part of the previous Snohomish County project [12]. In the future we plan to redo all of the Snohomish County project with the latest version of GeoClaw since elsewhere in the County there are significant regions of dry land below MHW, including in the **Skagit** region. This area is best handled as part of this modeling study since inundation here may depend in part on how much of the Skagit River Delta farther north is flooded.

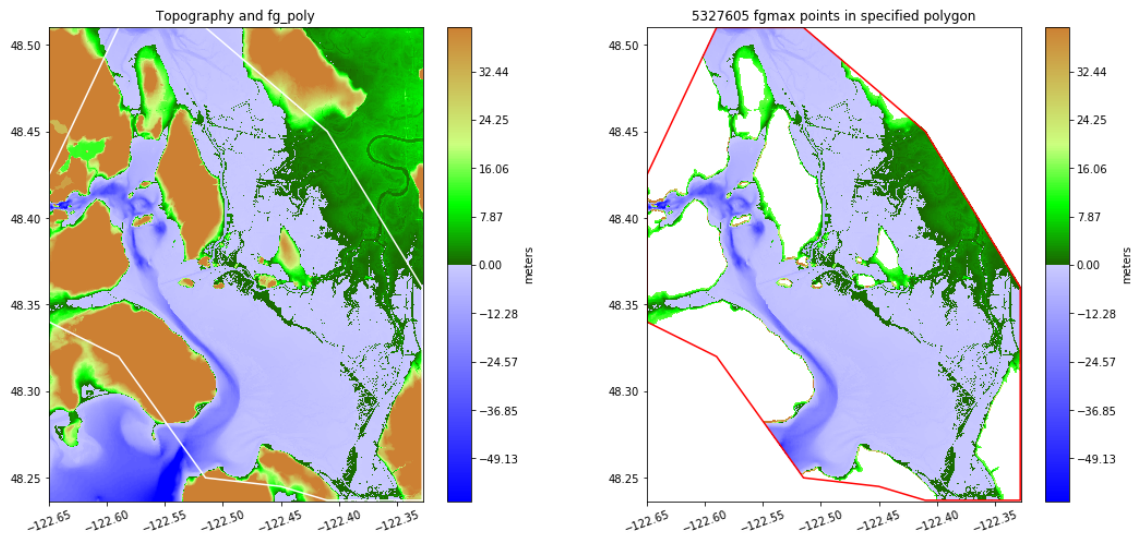


Figure 20: Left: Polygon used to select fgmax points for the Region Skagit. Right: Points selected.

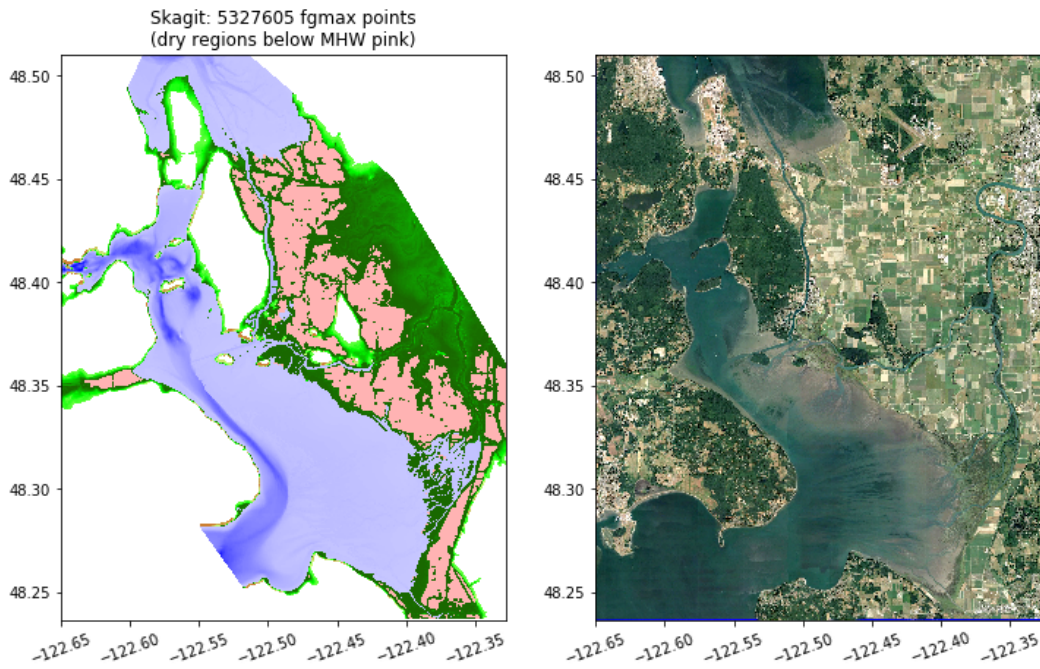


Figure 21: fgmax points selected in Region Skagit with points identified as dry but below MHW colored pink. For comparison the figure on the right shows a Google Earth image of this region.

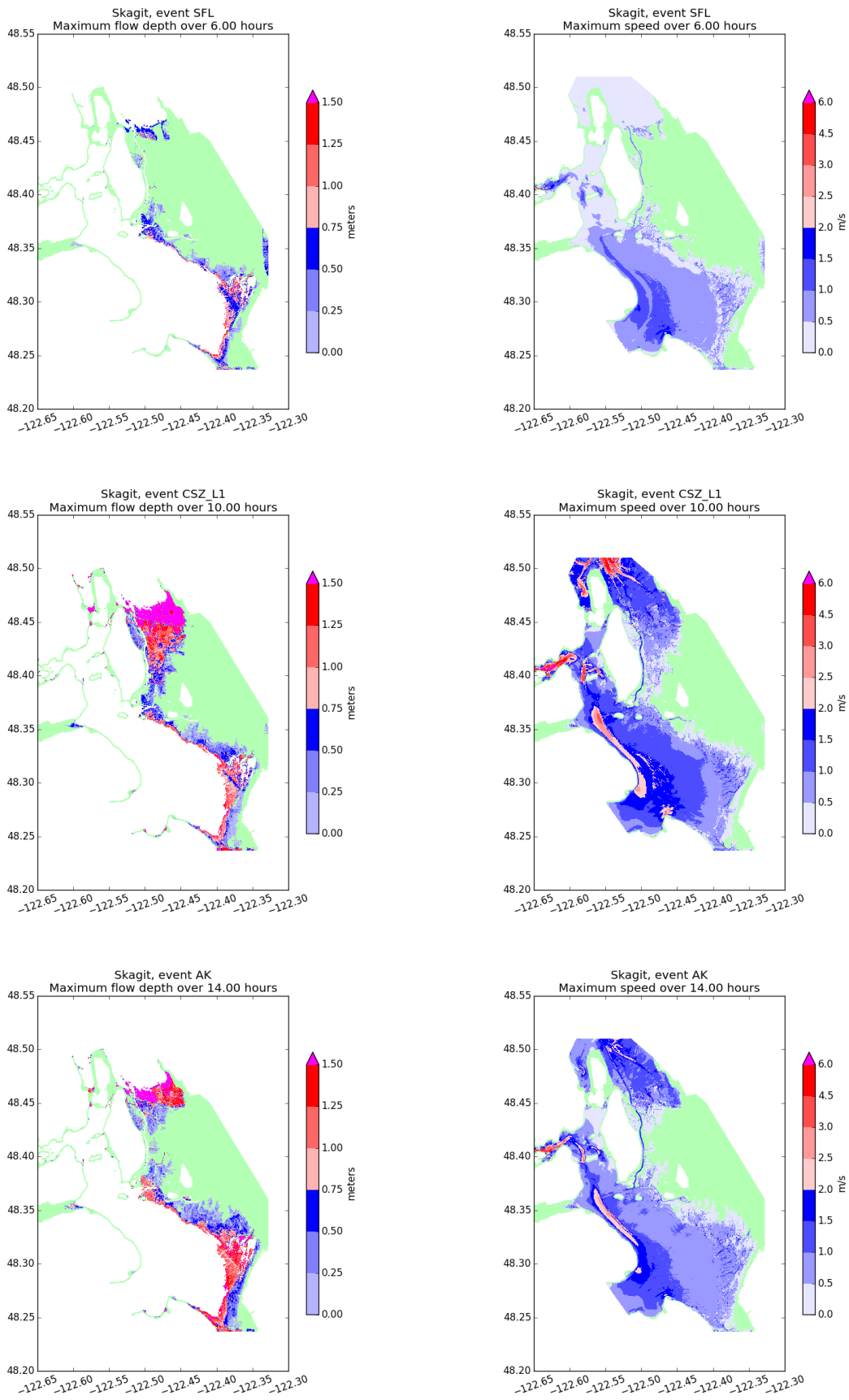


Figure 22: Sample results for the Region Skagit. See the description in Section 6.

7 Results – Gauge output

Figure 23 shows the location of the simulated gauges used to capture time series of the flow depth / surface elevation and of the current velocity over the course of each simulation, as specified by DNR and summarized in Table 3. Many of the gauges fall within the $1/3''$ by $1/3''$ *fgmax regions* listed in Table 2, so the time series for these were calculated from the run in that *fgmax* region. Others fall outside of any *fgmax* region and we present results from the run where the fine grid *fgmax* region was closest to the gauge, as also denoted in Table 3.

Examining these gauges gives an indication that the run times chosen for these simulations were sufficiently long to capture the maximum depth and speed at each point.

Additional notes:

- Gauge 8 is located in Deception pass, at the boundary between the *fgmax* regions *NW_Whidbey* and *Skagit*, and a region of very high current velocity. Appendix C.3 contains comparison plots at this gauge. The SF-L event is relatively weak here and best captured by the *Skagit* simulation, so more wave energy comes up from the east side of Whidbey Island than along the west side. On the other hand the CSZ-L1 and AKmaxWA events are better captured here in the *NW_Whidbey* simulation. Some comparisons are shown in Appendix C.3.
- Gauges 21, 22, and 27 in Admiralty Inlet are not within any *fgmax* region and so the grid resolution was $30''$ to $2''$ at this location for all runs. While the *W_Whidbey* simulation has been chosen as giving the “best” results, all regions recorded similar results, as confirmed in Appendix C.1 for Gauge 21. Note that for the AKmaxWA event the GeoClaw topography bounces around a bit as the grid resolution used fluctuates at the gauge location.
- Gauge 69 is at the boundary of the *E_Whidbey* and *Skagit* regions. In Appendix C.2 we present some comparisons of results at this gauge from the two sets of model simulations.

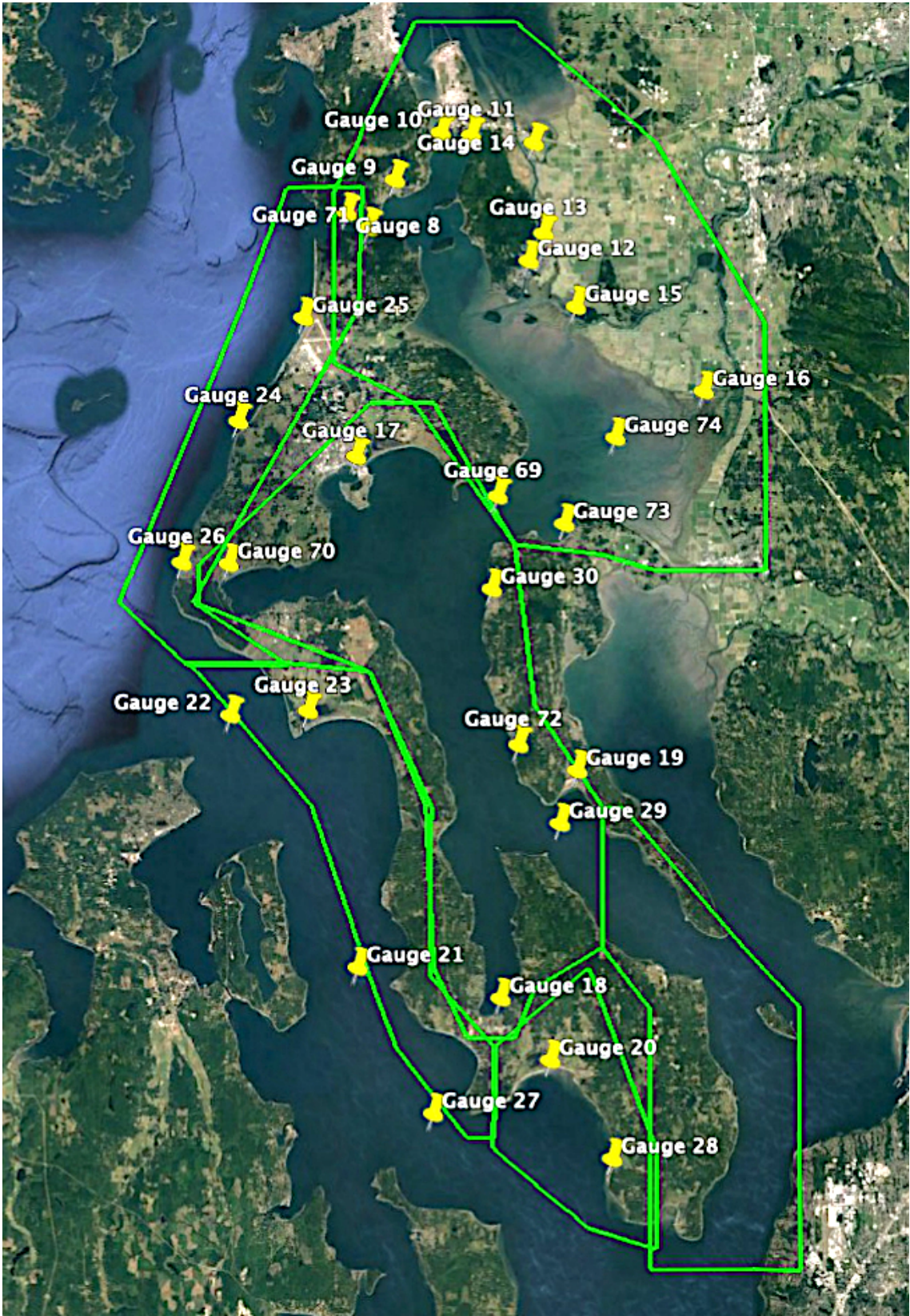


Figure 23: Synthetic gauge locations used for this study.

Number	Location	Longitude	Latitude	Region	Event	Resolution
8	Deception Pass	-122.6446154	48.40615643	Skagit	SFL	1/3 arcsec
8	Deception Pass	-122.6446154	48.40615643	NW_Whidbey	CSZ_L1	1/3 arcsec
8	Deception Pass	-122.6446154	48.40615643	NW_Whidbey	AK	1/3 arcsec
9	Dewey	-122.608597	48.42250637	Skagit	All	1/3 arcsec
10	West Similk Beach	-122.5742634	48.445988	Skagit	All	1/3 arcsec
11	East Similk Beach	-122.5514795	48.44475358	Skagit	All	1/3 arcsec
12	Shelter Bay entrance	-122.5083888	48.3823361	Skagit	All	1/3 arcsec
13	La Conner marina	-122.4974293	48.39592324	Skagit	All	1/3 arcsec
14	North Swinomish Channel	-122.5046077	48.44091253	Skagit	All	1/3 arcsec
15	NF Skagit River	-122.4730479	48.35965883	Skagit	All	1/3 arcsec
16	SF Skagit River	-122.3776417	48.31759572	Skagit	All	1/3 arcsec
17	Oak Harbor	-122.6370811	48.28513351	E_Whidbey	All	1/3 arcsec
18	Freeland	-122.5291308	48.01630332	E_Whidbey	All	1/3 arcsec
19	Elger Bay	-122.472247	48.12946374	E_Whidbey	All	1/3 arcsec
20	Useless Bay	-122.4923357	47.98548229	SW_Whidbey	All	1/3 arcsec
21	Admiralty Inlet	-122.6352602	48.03148226	W_Whidbey	All	2 – 30 arcsec
22	Admiralty Head	-122.7303854	48.15656397	W_Whidbey	All	2 – 30 arcsec
23	Keystone Ferry Terminal	-122.6726478	48.15882472	W_Whidbey	All	1/3 arcsec
24	Swantown	-122.7253316	48.30252036	NW_Whidbey	All	1/3 arcsec
25	Ault Field offshore	-122.6768363	48.35405271	NW_Whidbey	All	1/3 arcsec
26	Libbey Beach Park	-122.7670863	48.23225843	NW_Whidbey	All	1/3 arcsec
27	Admiralty Inlet	-122.5791306	47.95896414	W_Whidbey	All	2 – 30 arcsec
28	Maxwelton	-122.4464198	47.93657626	SW_Whidbey	All	1/3 arcsec
29	Saratoga Passage	-122.4850591	48.10313623	E_Whidbey	All	1/3 arcsec
30	Madrona Beach	-122.5358446	48.2194273	E_Whidbey	All	1/3 arcsec
69	passage off Polnell Point	-122.5314933	48.26545503	E_Whidbey	All	1/3 arcsec
70	Coveland	-122.7320237	48.23168851	E_Whidbey	All	1/3 arcsec
71	Cornet	-122.6280232	48.39871468	Skagit	All	1/3 arcsec
72	Cama Beach State Park	-122.5159274	48.14213969	E_Whidbey	All	1/3 arcsec
73	Ustalady Bay	-122.4818678	48.25169959	Skagit	All	1/3 arcsec
74	Skagit Bay	-122.4437215	48.29454833	Skagit	All	1/3 arcsec

Table 3: Location of synthetic gauges, see also the map in Figure 23. For each gauge we indicate which of the runs is used to computed the best gauge output (in the column “Region”). This is the same for all sources except for Gauge 8. The final column shows the grid resolution around the gauge location, which is 1/3” for gauges that lie within fgmax regions and for other gauges varies between 2–30” depending on the AMR algorithm.

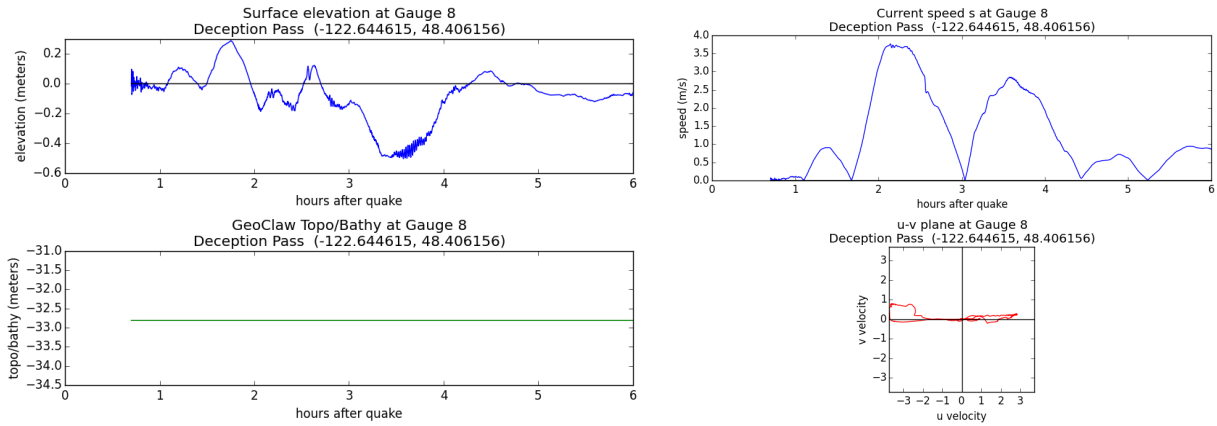
The figures on the next few pages show gauge output from the gauges. For each gauge, the figures show the surface elevation and speed, for each of the three events. The speed is shown both as a time series of speed $\sqrt{u^2 + v^2}$ vs. time, and also in the $u-v$ plane as the red curve in the lower right plot for each event. This plot allows one to see how the E–W component u of the speed compares to the N–S component v , and for some gauge locations shows a strong dominant direction of the current (e.g. predominantly E–W at Gauge 8 in Deception Pass). At other gauges the speed is less strongly one-dimensional.

Note that the vertical scale for each surface elevation and speed plot varies between locations and events in order to clearly show the results, and is set by the maximum amplitude in each case.

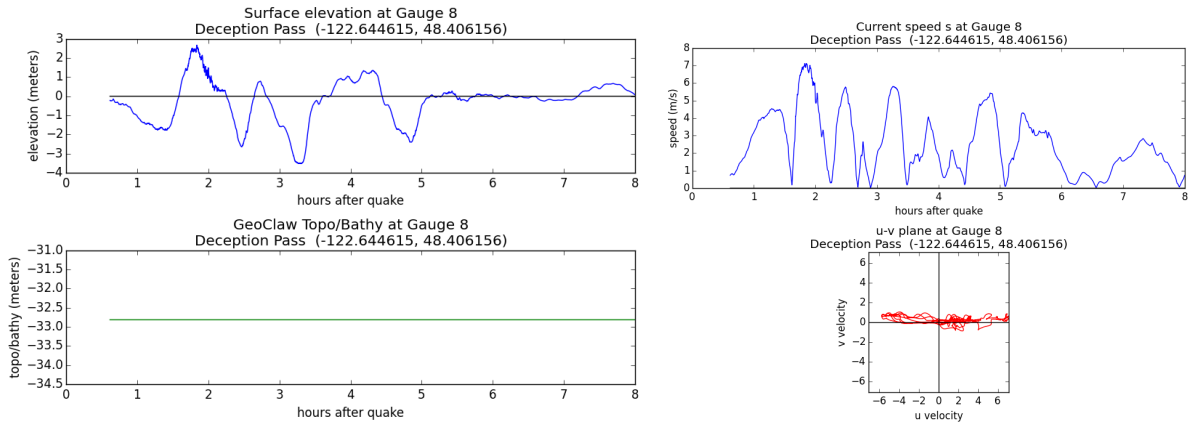
Gauge 8: Deception Pass.

Computed on region Skagit for SF-L and NW_Whidbey for L1 and AK.

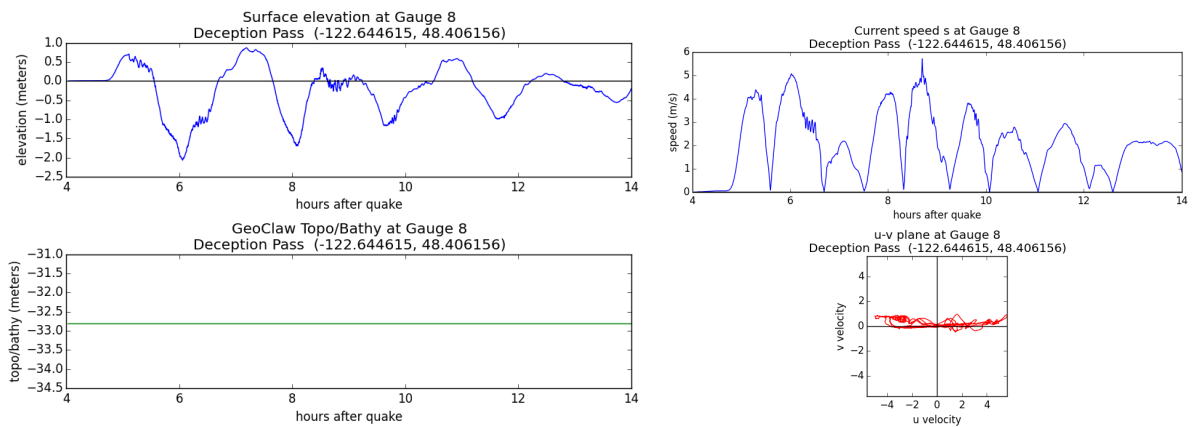
SF-L event:



CSZ L1 event:



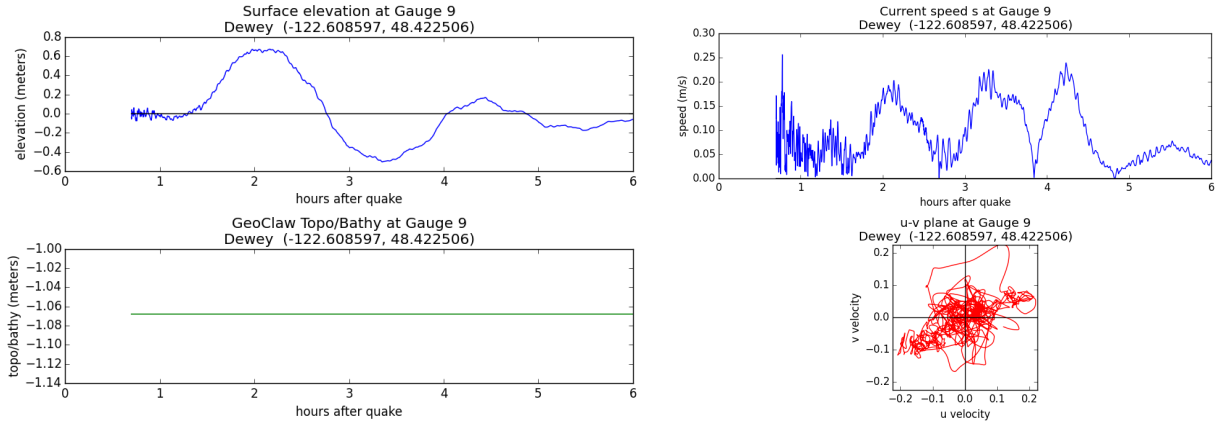
AK event:



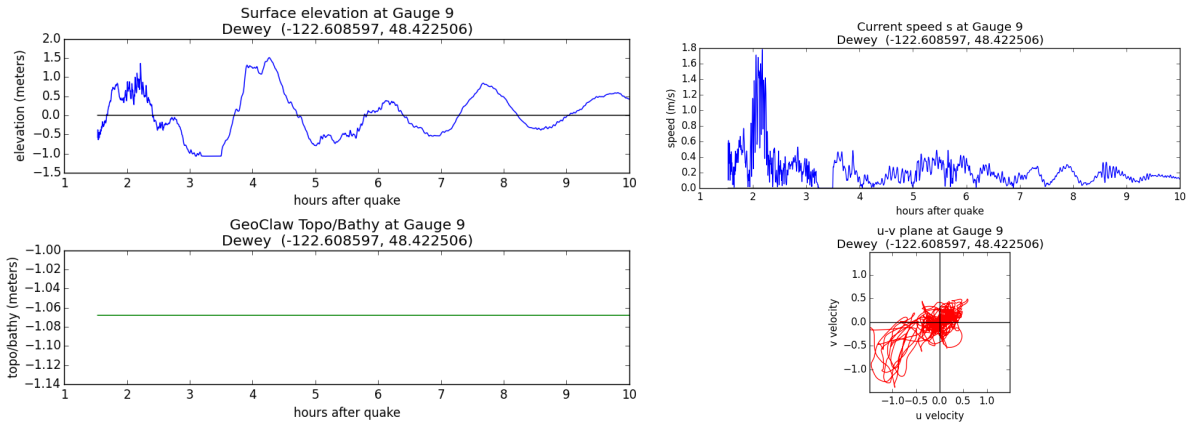
Gauge 9: Dewey.

Computed on region Skagit.

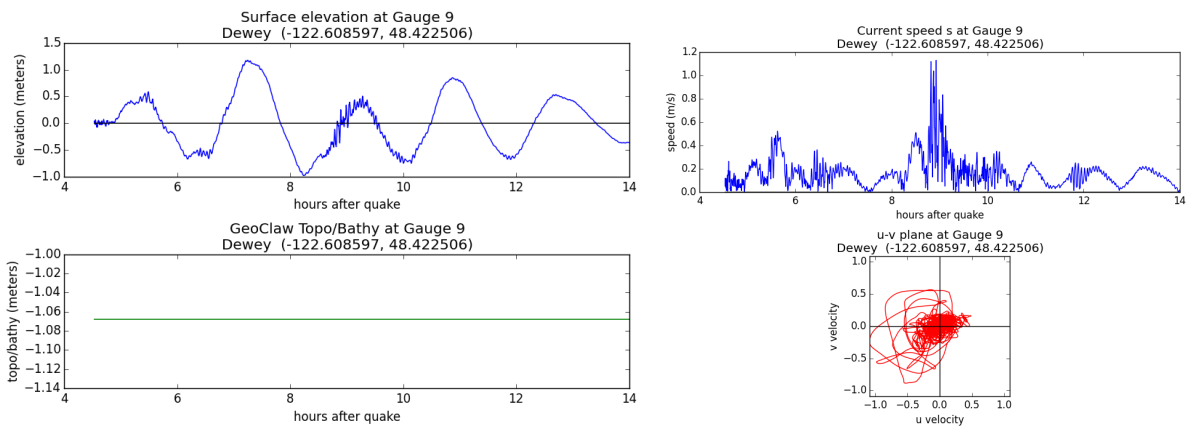
SF-L event:



CSZ L1 event:



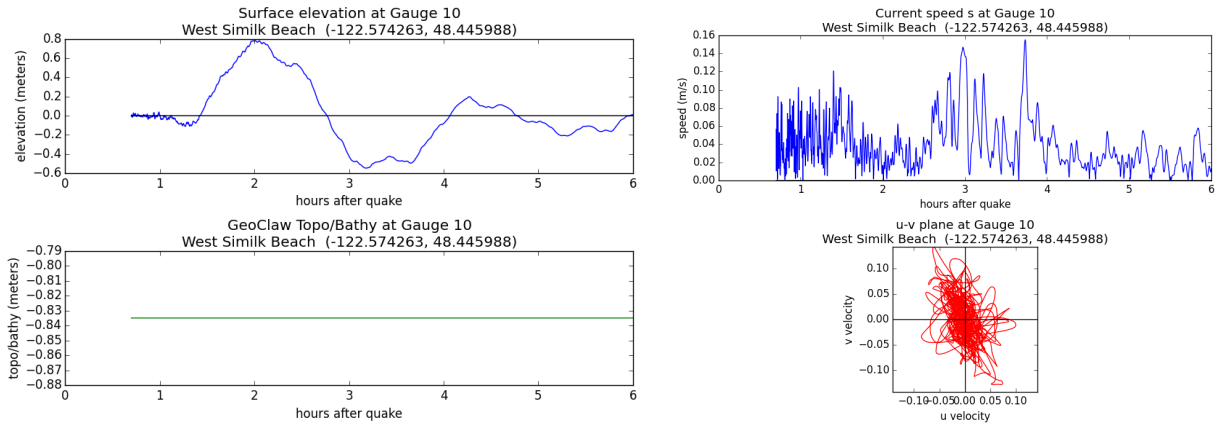
AK event:



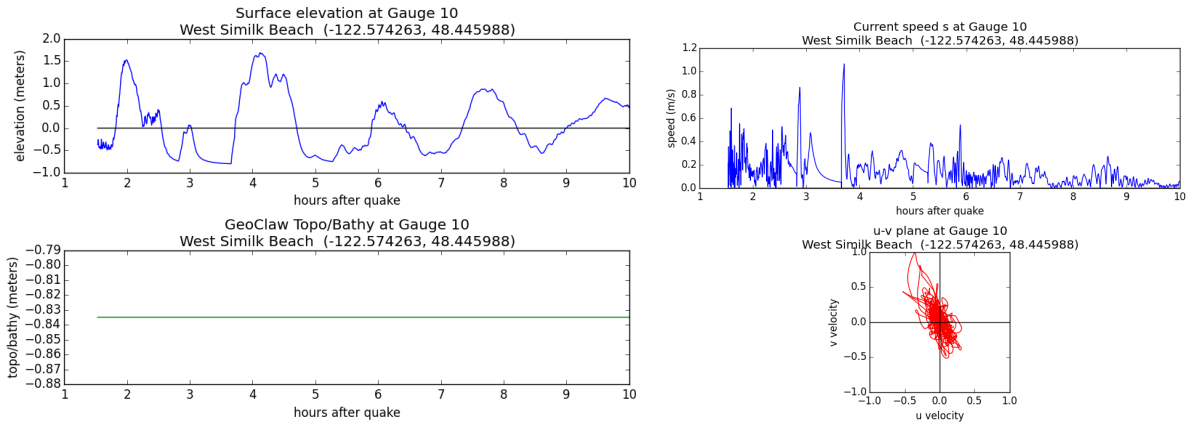
Gauge 10: West Similk Beach.

Computed on region Skagit.

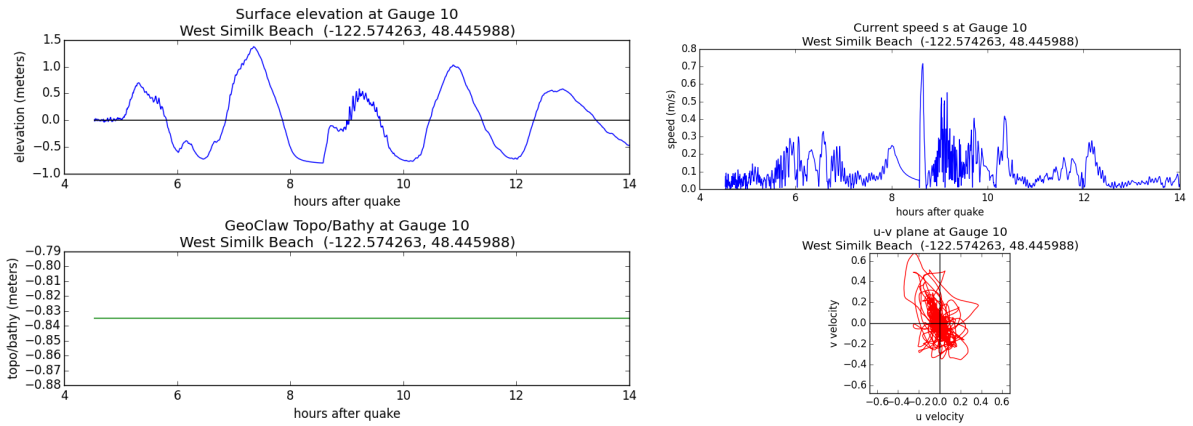
SF-L event:



CSZ L1 event:



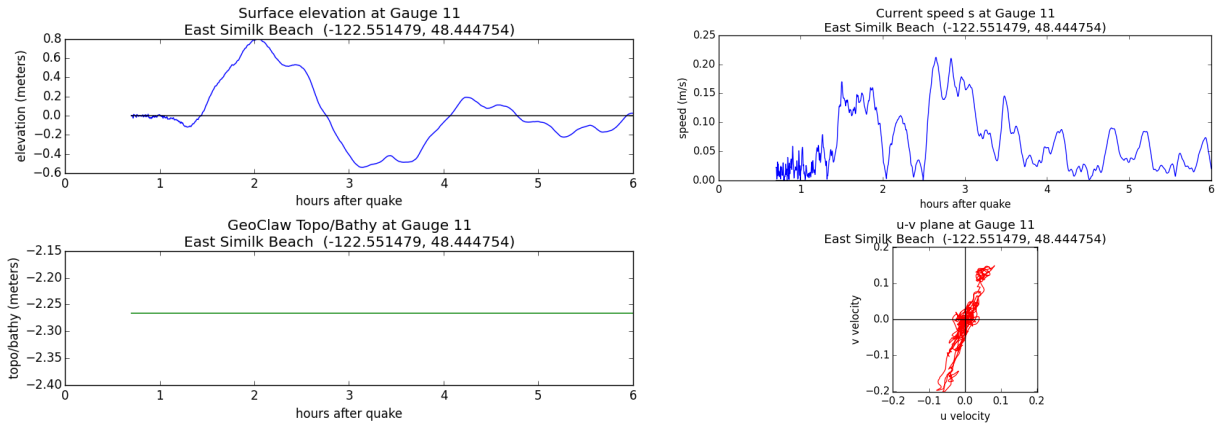
AK event:



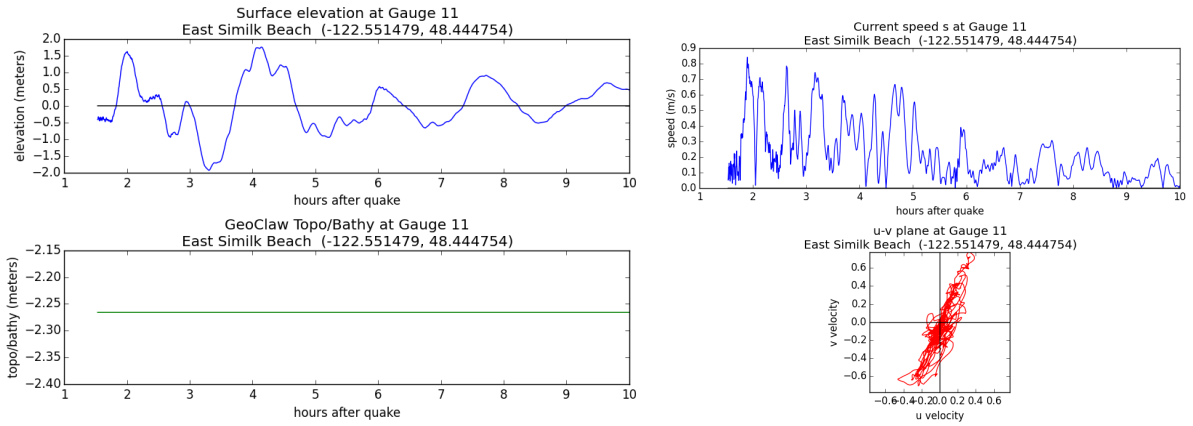
Gauge 11: East Similk Beach.

Computed on region Skagit.

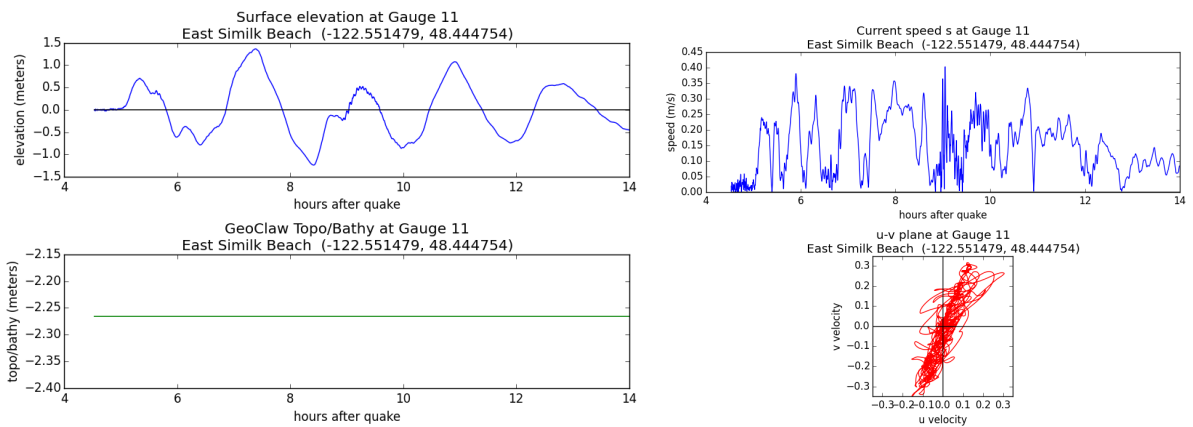
SF-L event:



CSZ L1 event:



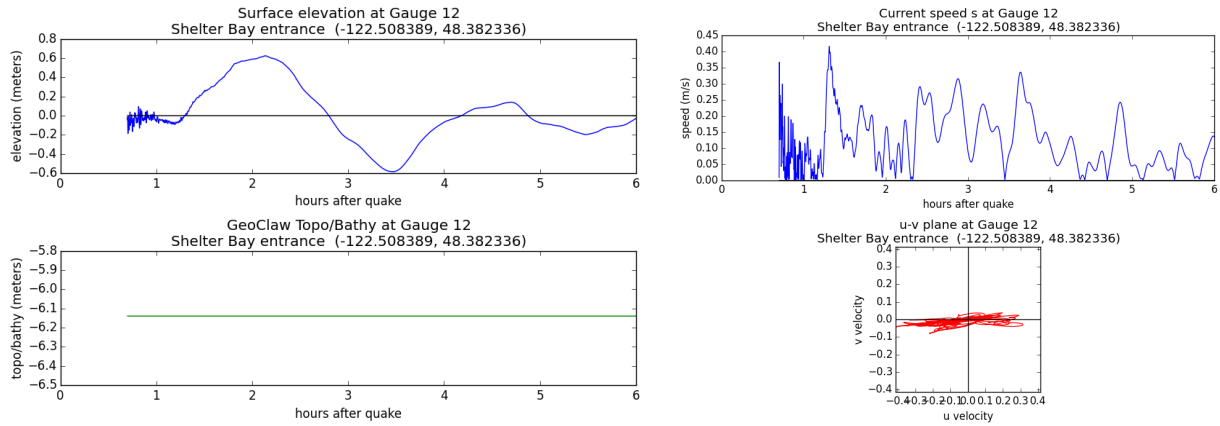
AK event:



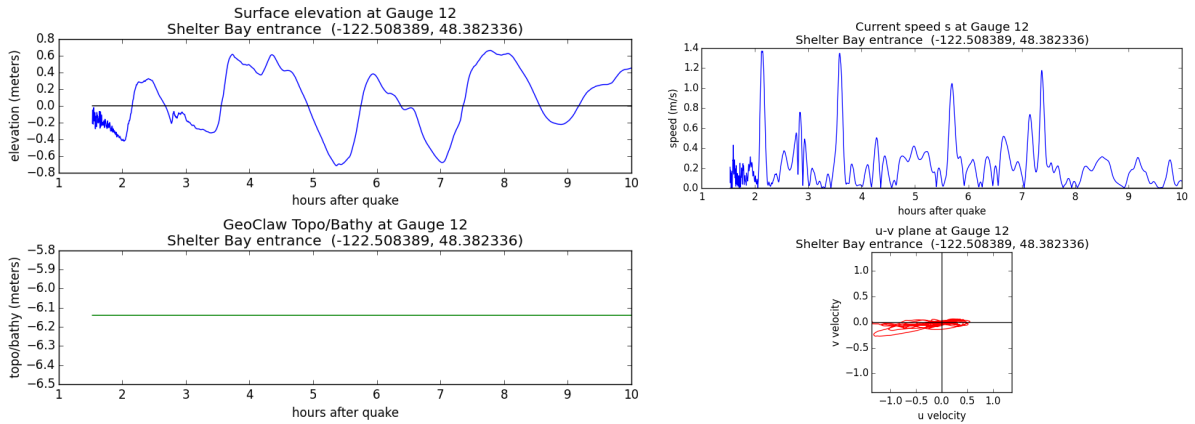
Gauge 12: Shelter Bay entrance.

Computed on region Skagit.

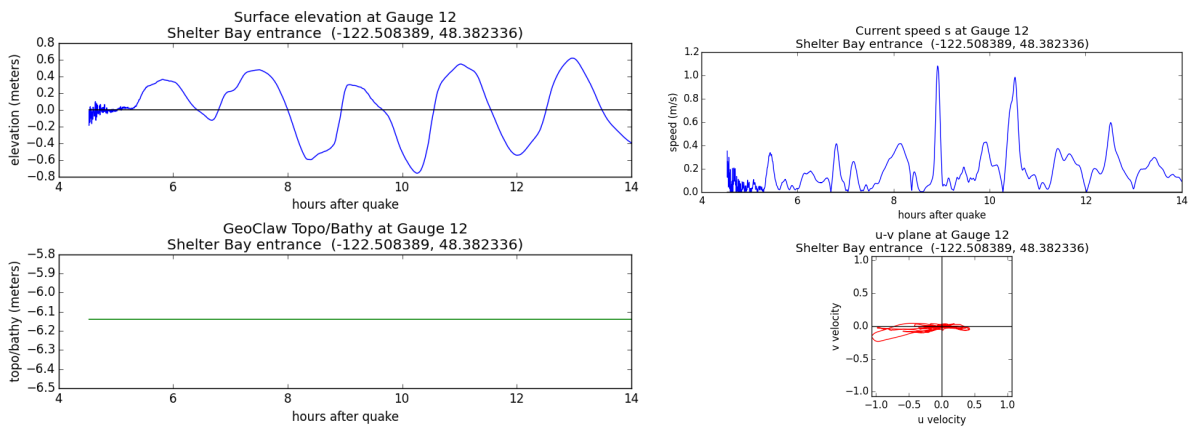
SF-L event:



CSZ L1 event:



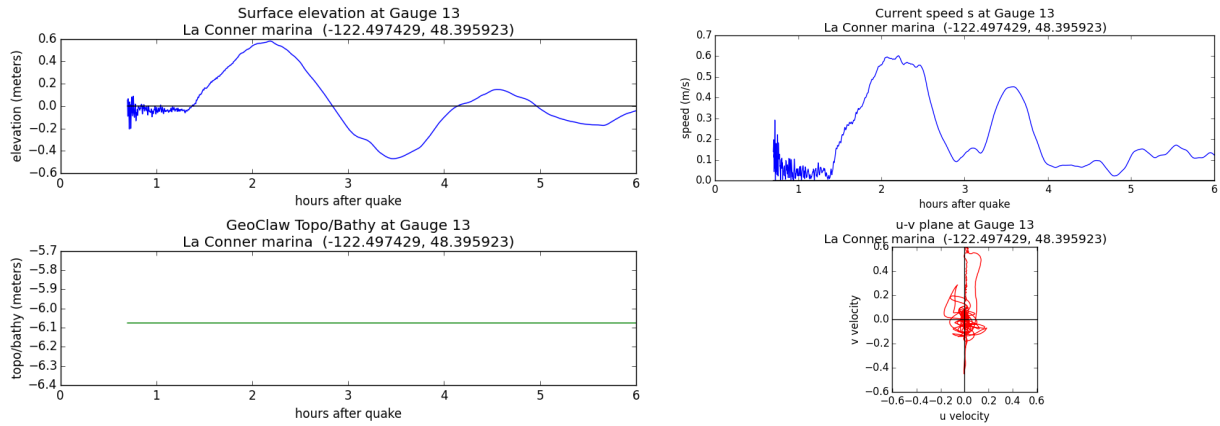
AK event:



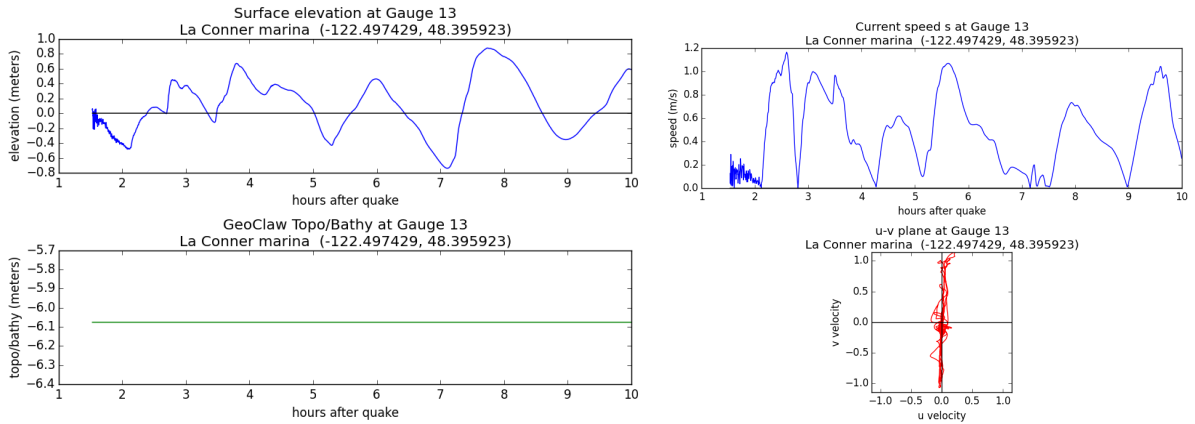
Gauge 13: La Conner marina.

Computed on region Skagit.

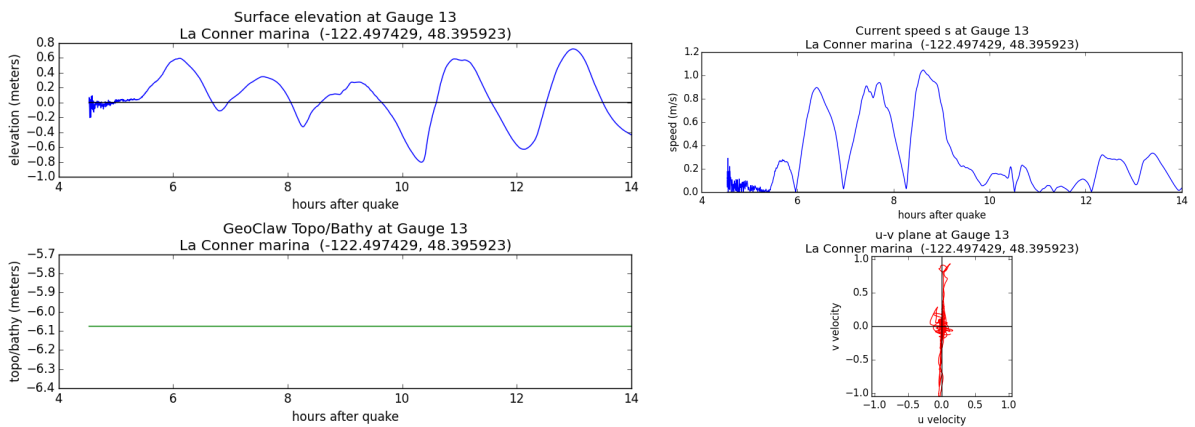
SF-L event:



CSZ L1 event:



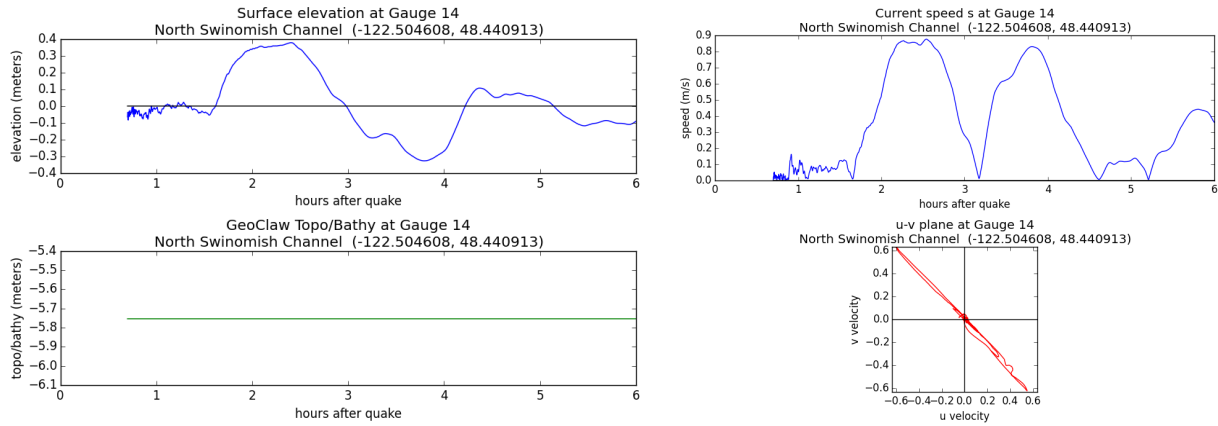
AK event:



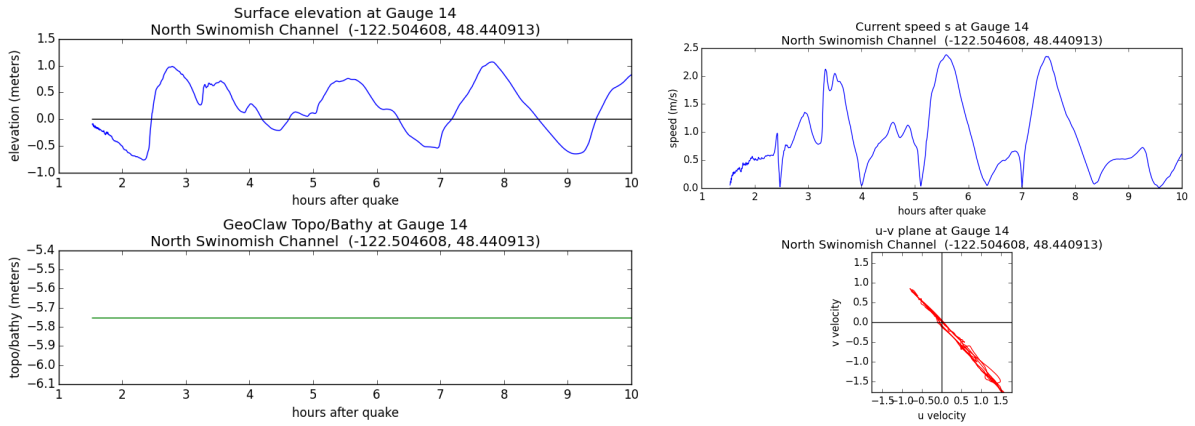
Gauge 14: North Swinomish Channel.

Computed on region Skagit.

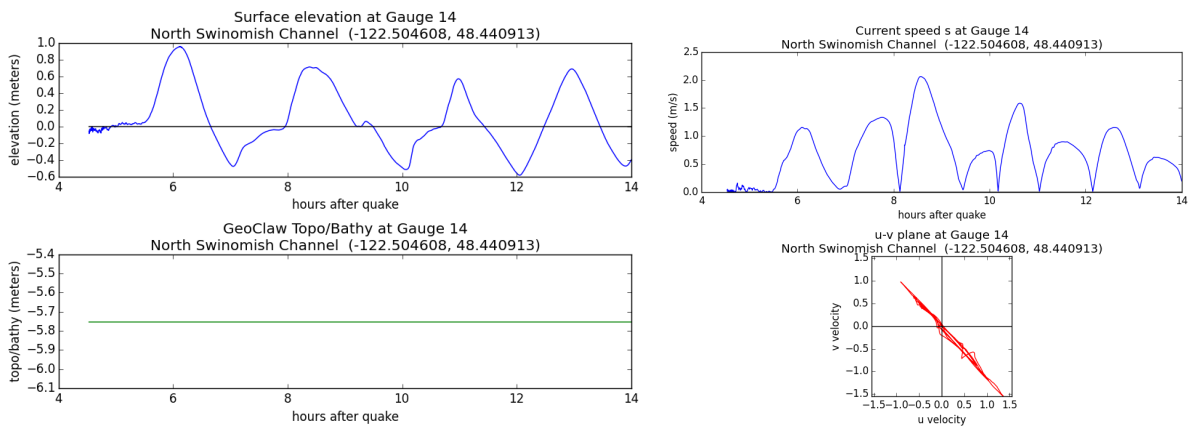
SF-L event:



CSZ L1 event:



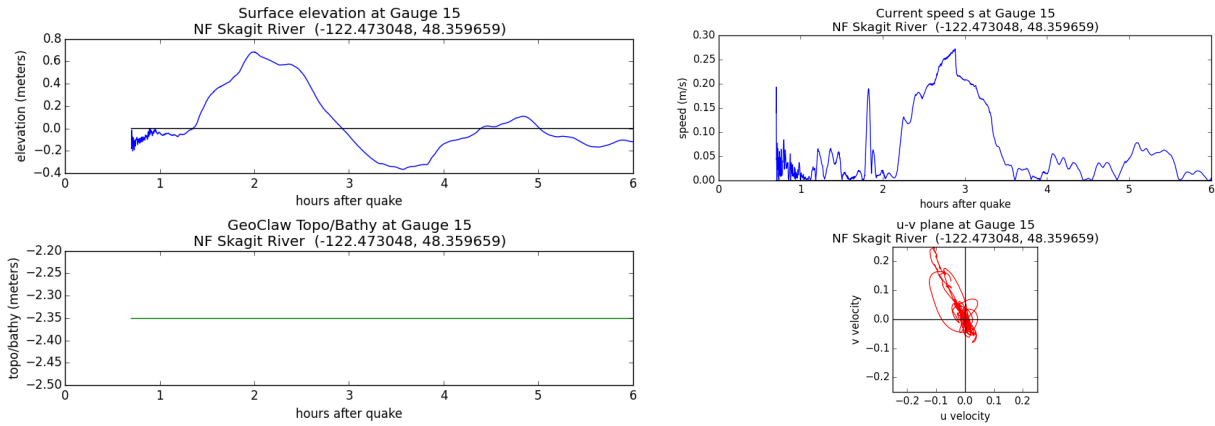
AK event:



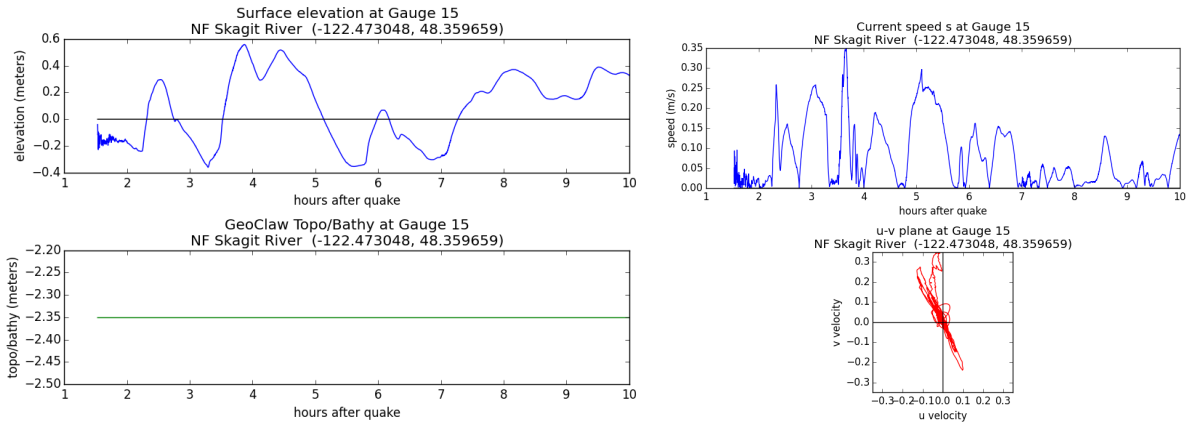
Gauge 15: NF Skagit River.

Computed on region Skagit.

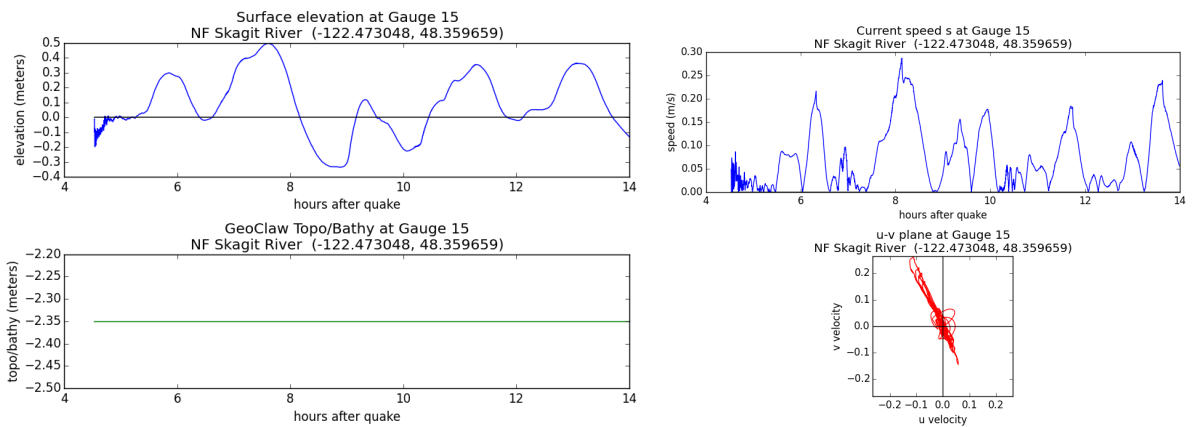
SF-L event:



CSZ L1 event:



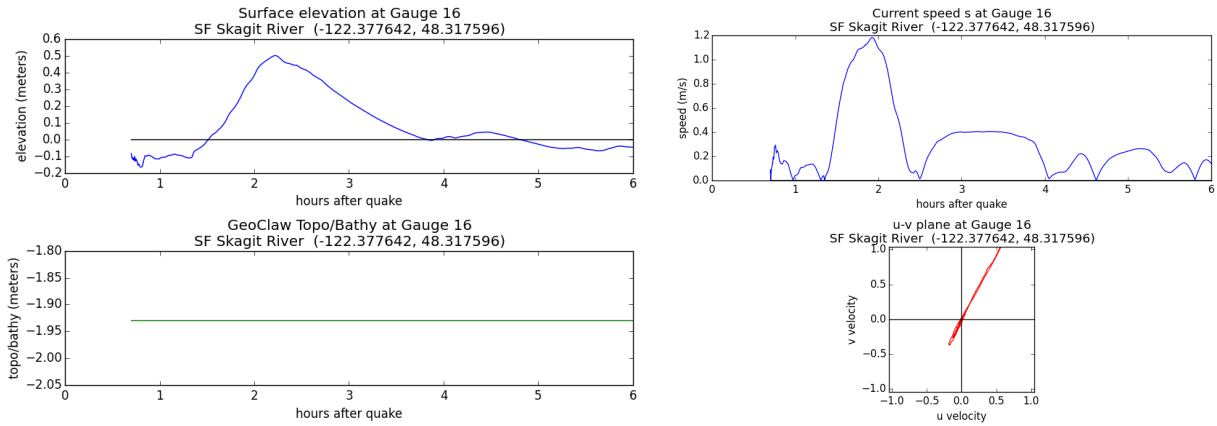
AK event:



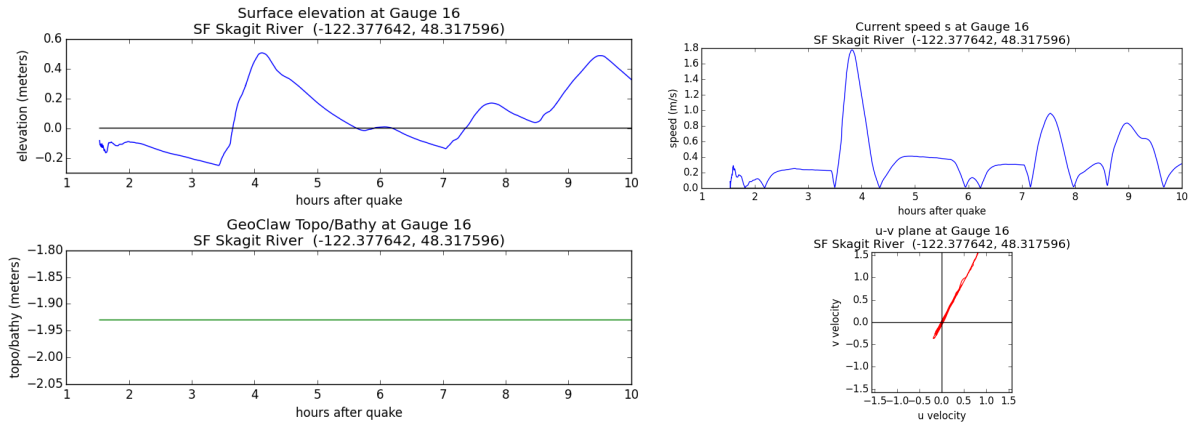
Gauge 16: SF Skagit River.

Computed on region Skagit.

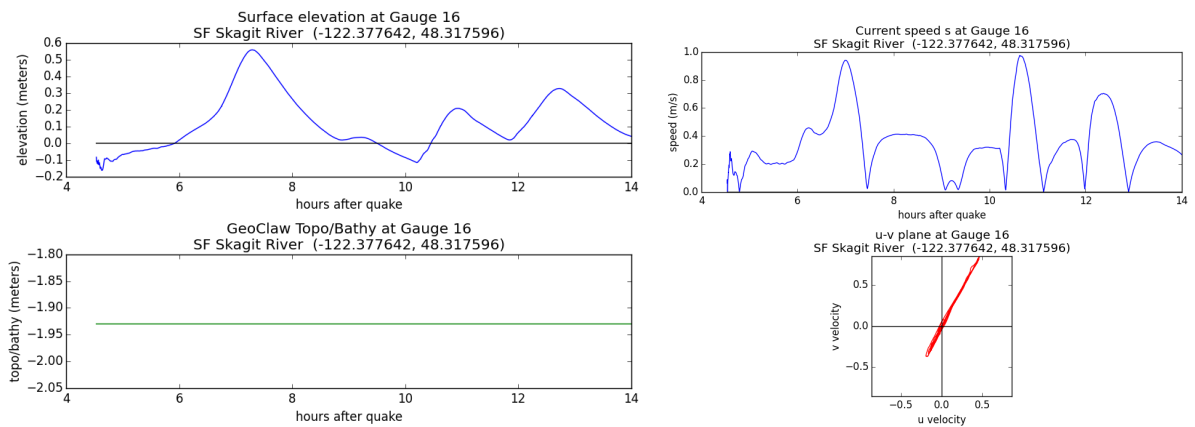
SF-L event:



CSZ L1 event:



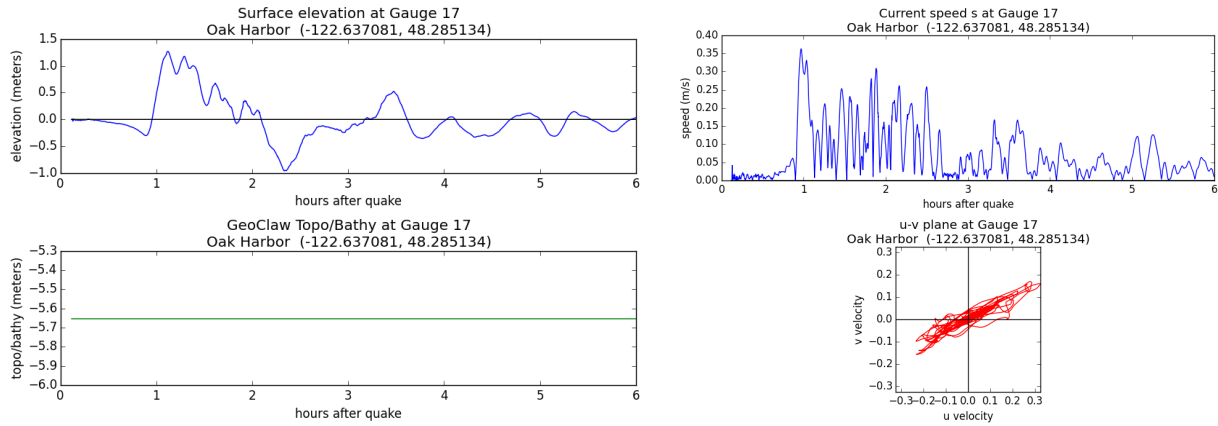
AK event:



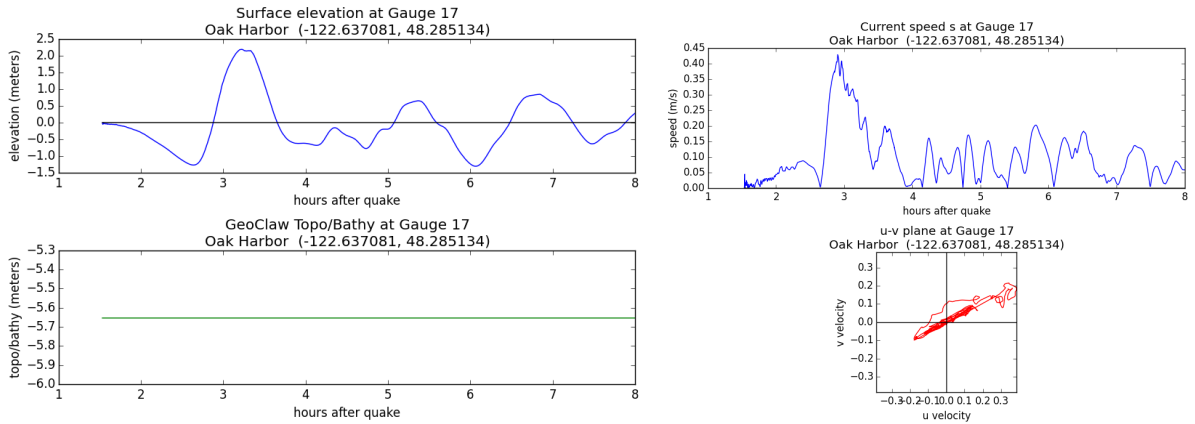
Gauge 17: Oak Harbor.

Computed on region E.Whidbey.

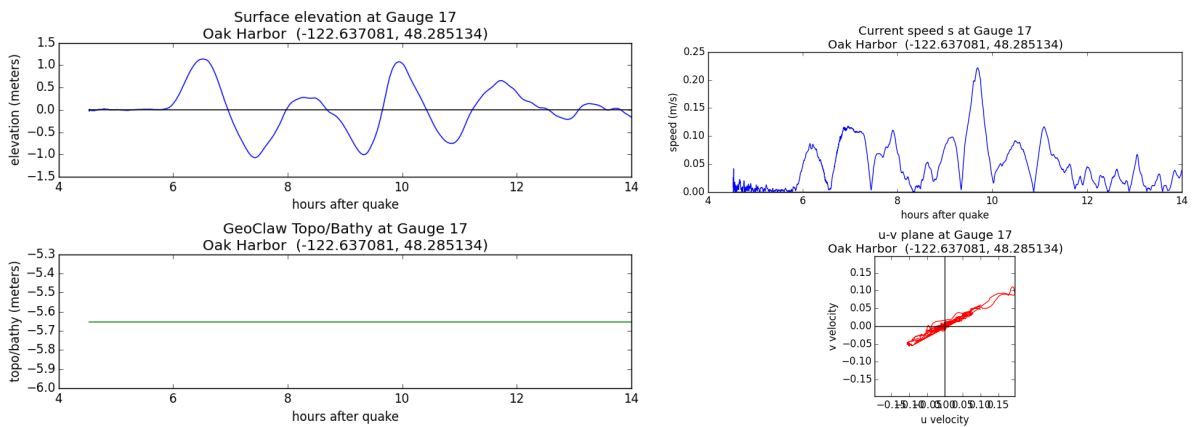
SF-L event:



CSZ L1 event:



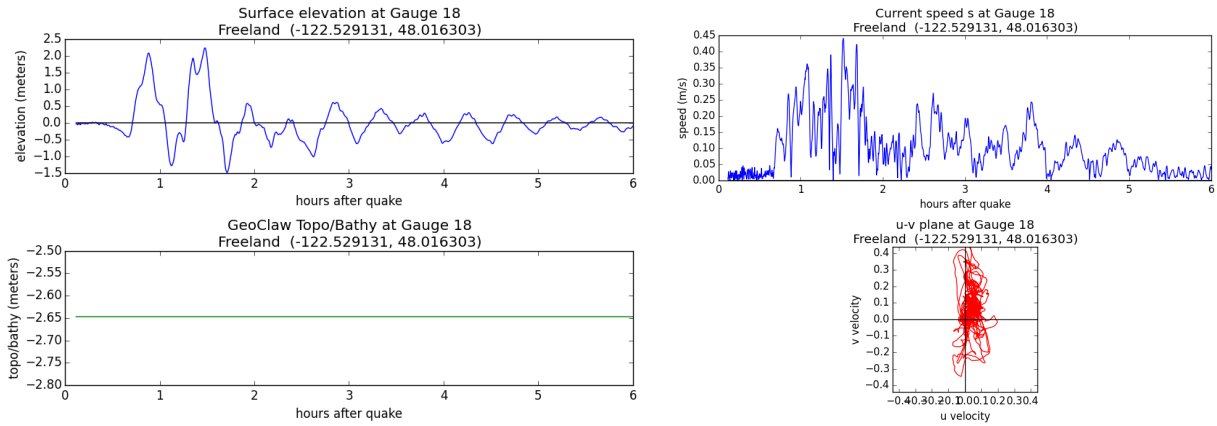
AK event:



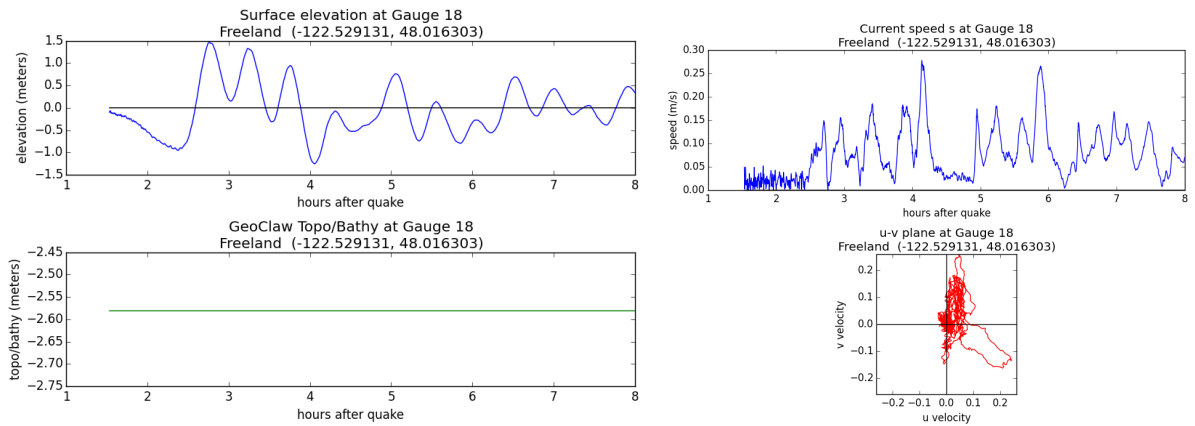
Gauge 18: Freeland.

Computed on region E.Whidbey.

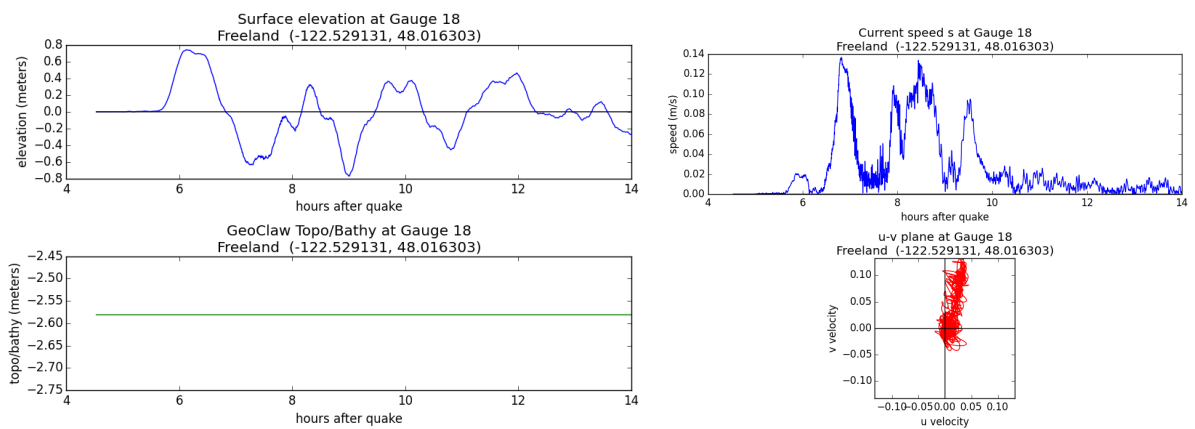
SF-L event:



CSZ L1 event:



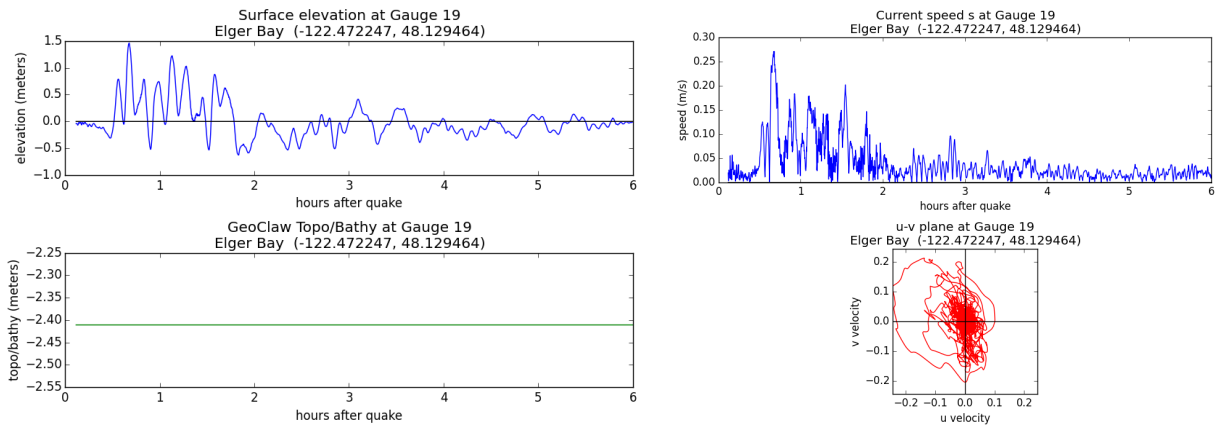
AK event:



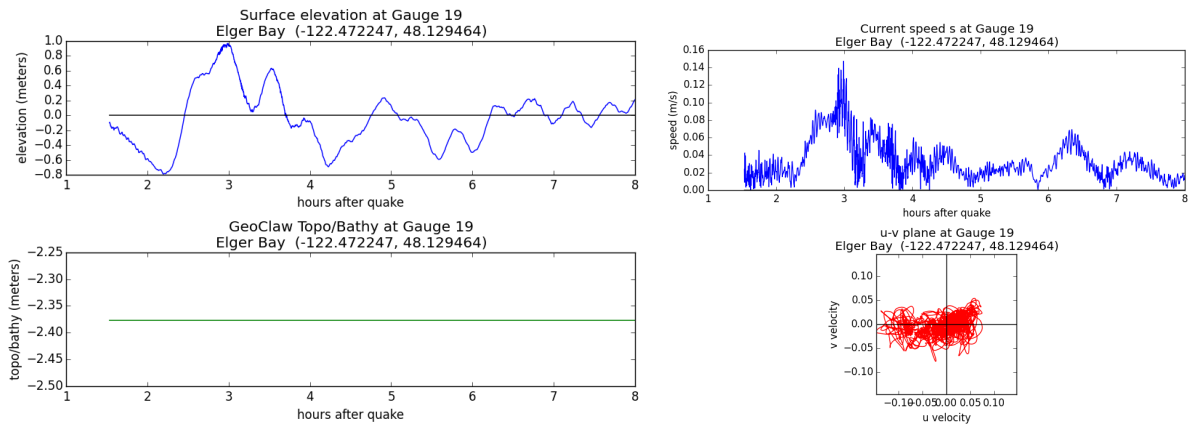
Gauge 19: Elger Bay.

Computed on region E.Whidbey.

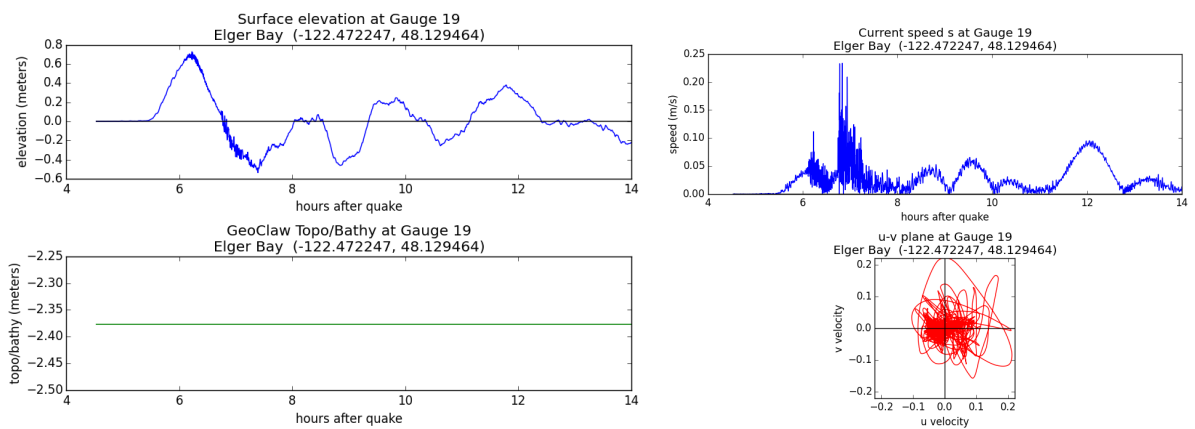
SF-L event:



CSZ L1 event:



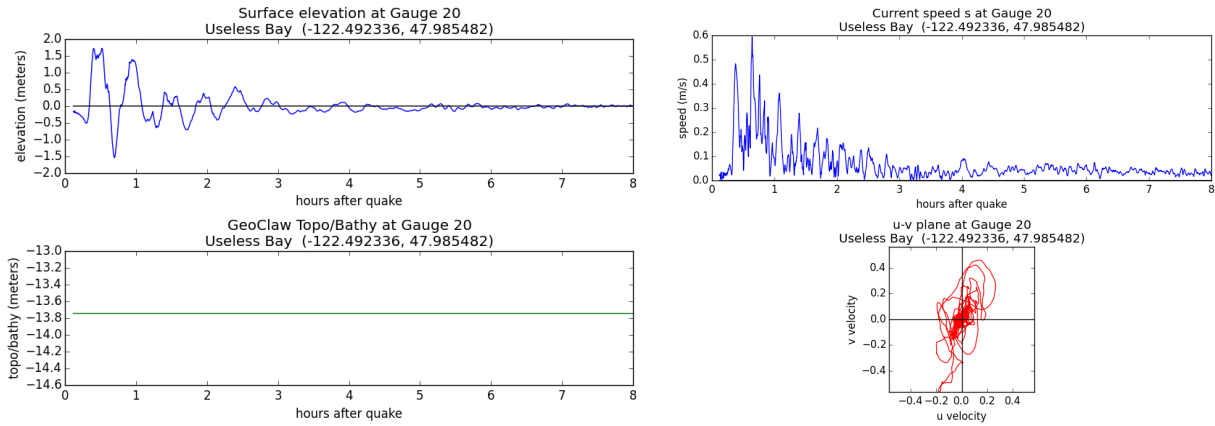
AK event:



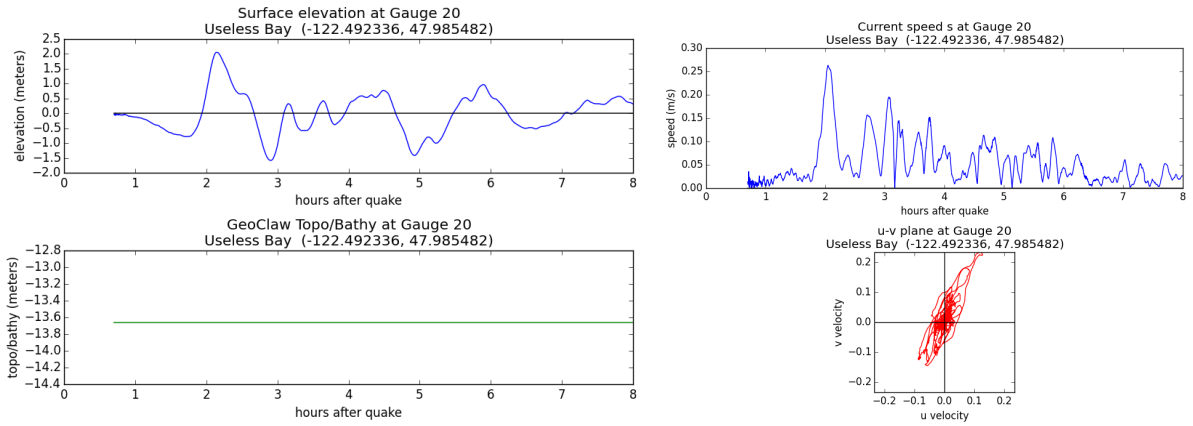
Gauge 20: Useless Bay.

Computed on region SW_Whidbey.

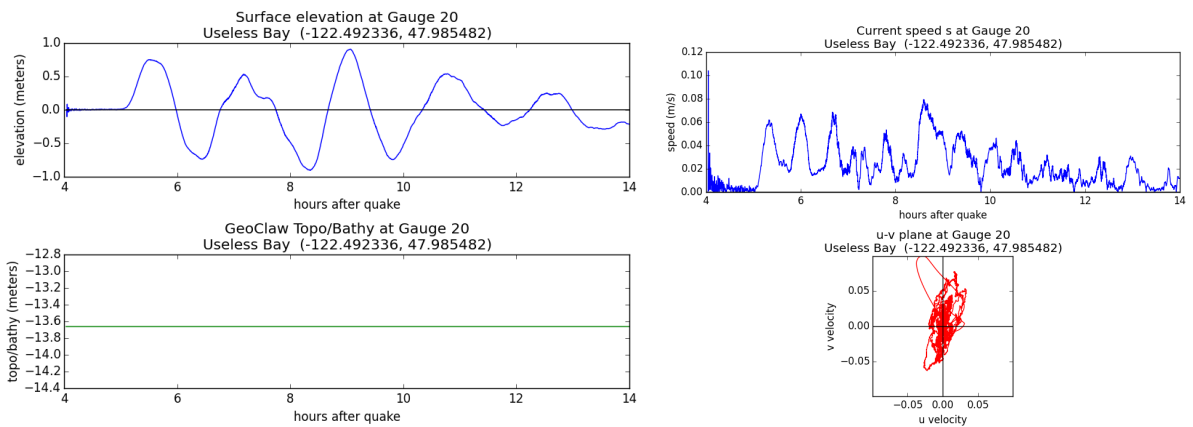
SF-L event:



CSZ L1 event:



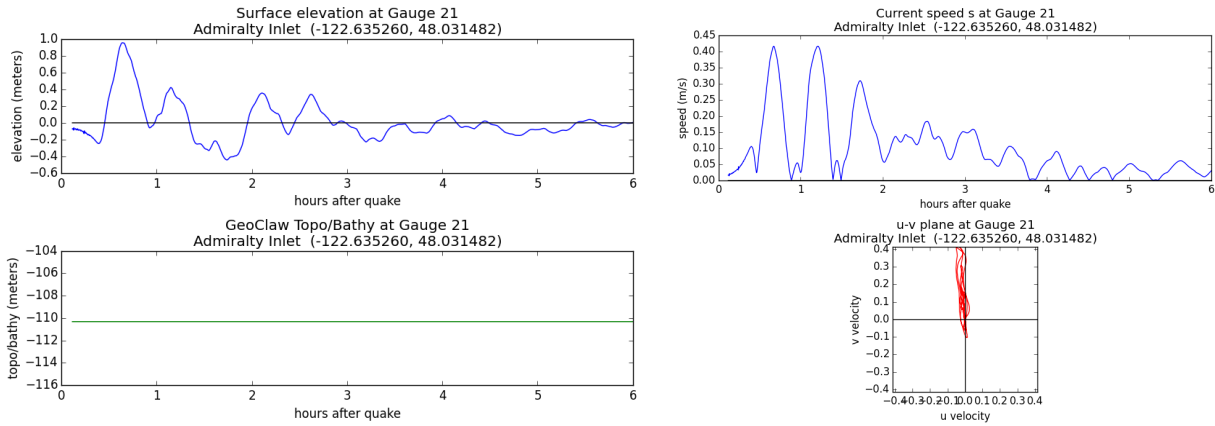
AK event:



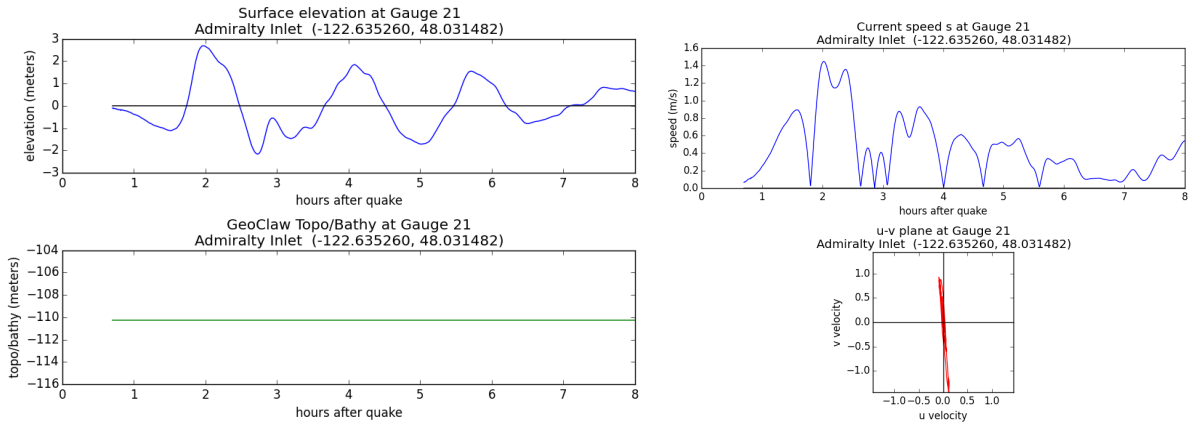
Gauge 21: Admiralty Inlet.

Computed on region W.Whidbey.

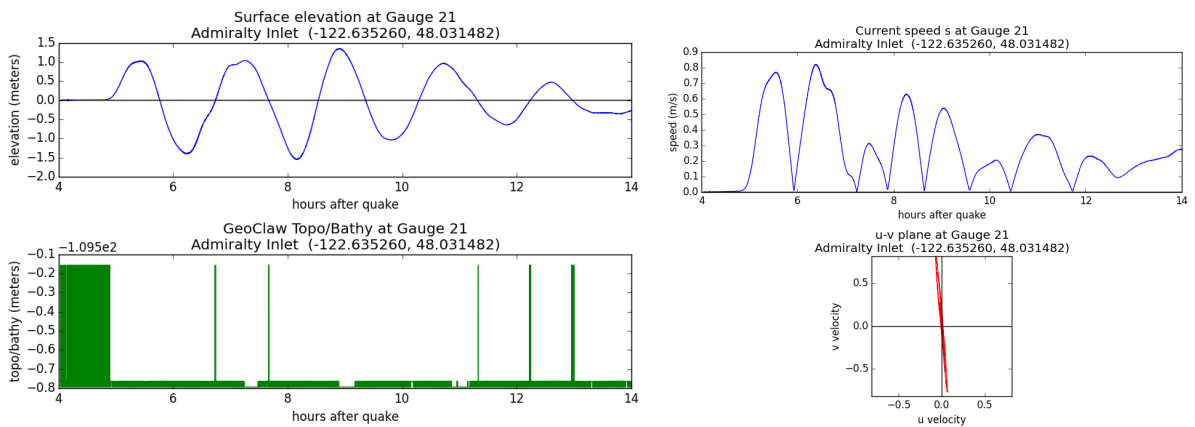
SF-L event:



CSZ L1 event:



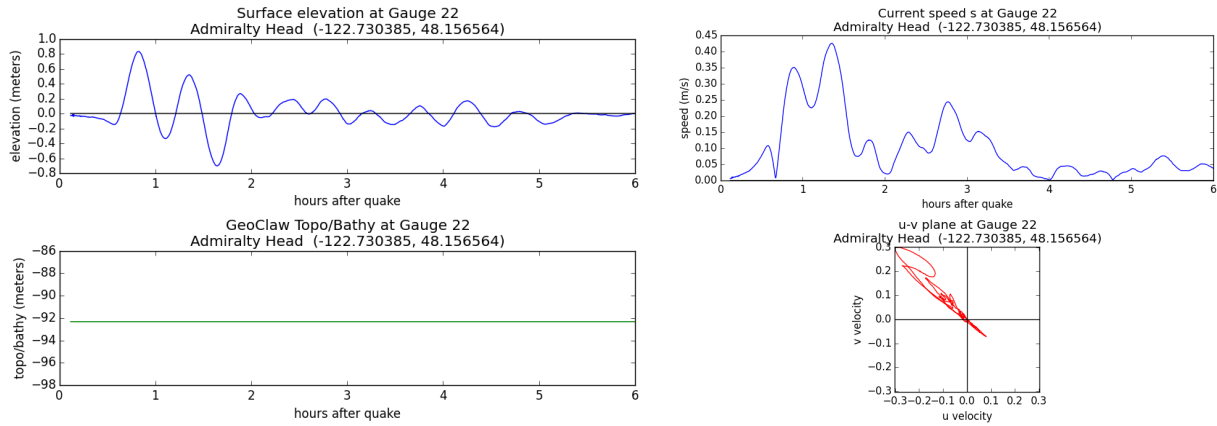
AK event:



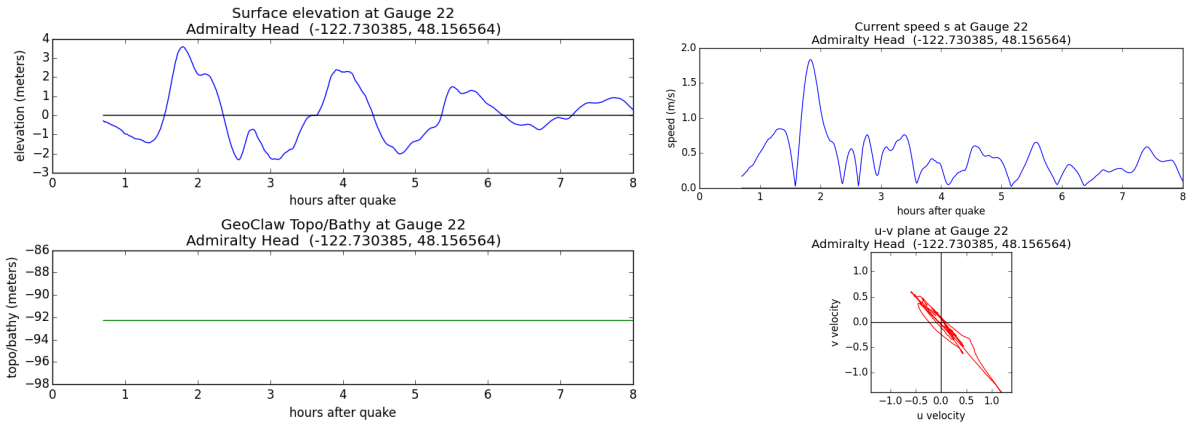
Gauge 22: Admiralty Head.

Computed on region W.Whidbey.

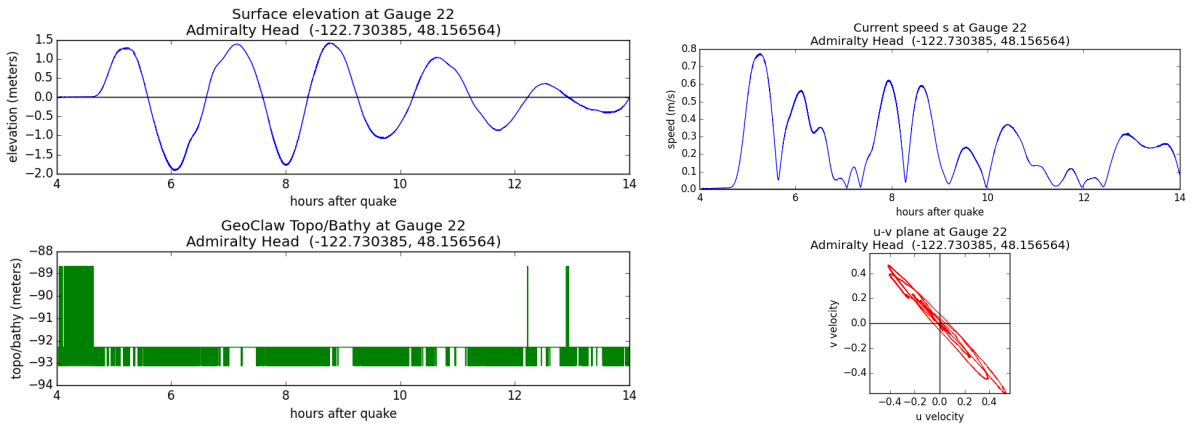
SF-L event:



CSZ L1 event:



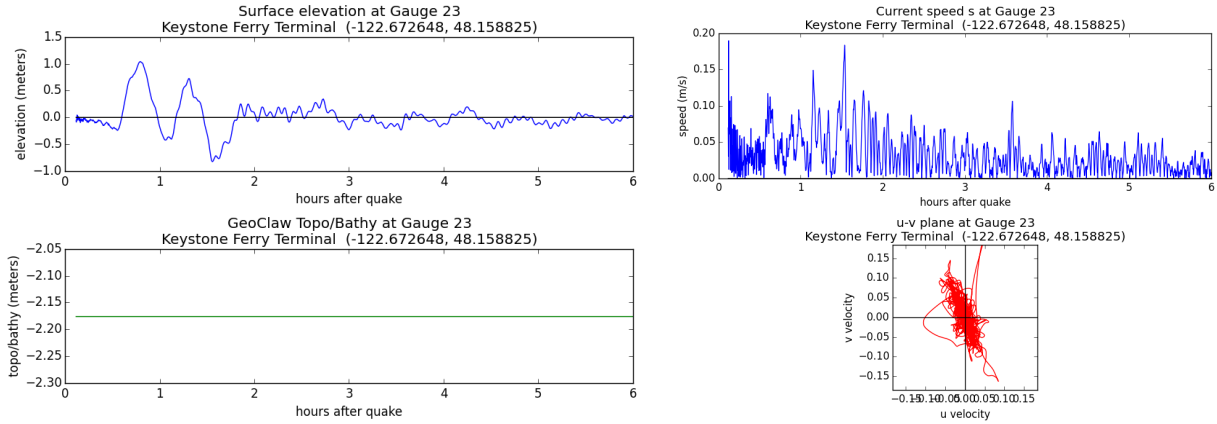
AK event:



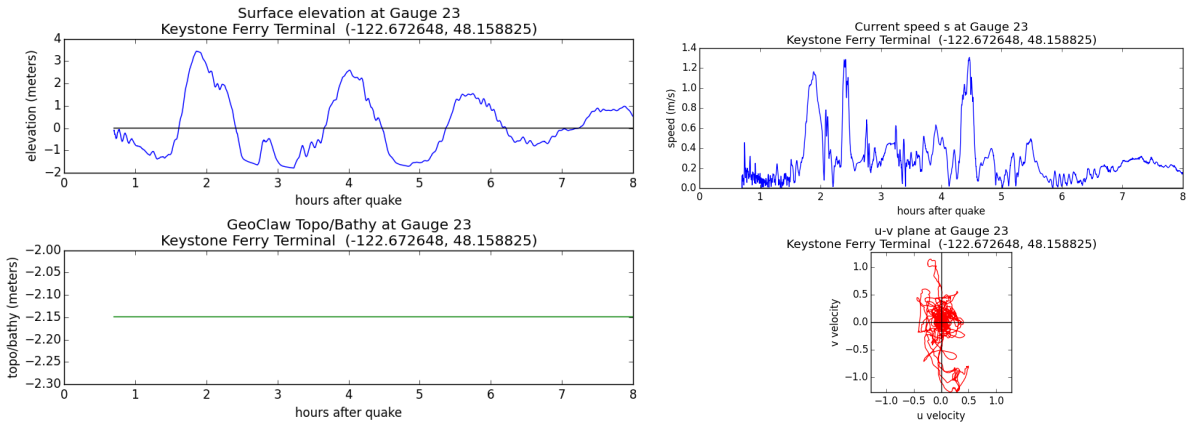
Gauge 23: Keystone Ferry Terminal.

Computed on region W.Whidbey.

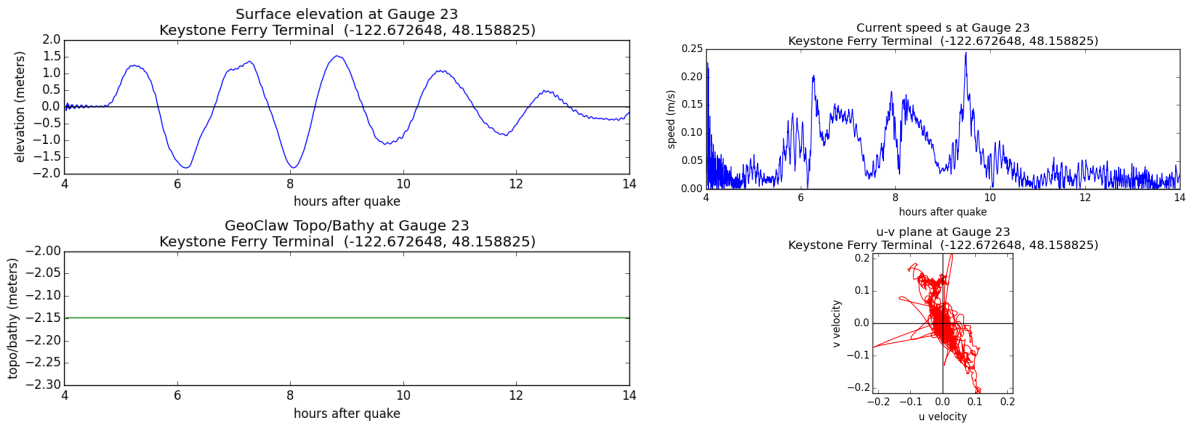
SF-L event:



CSZ L1 event:



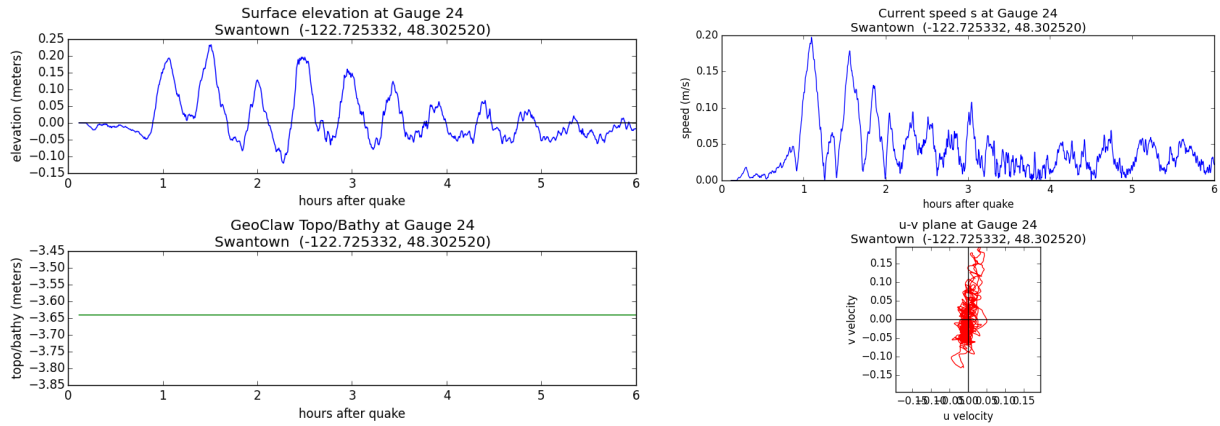
AK event:



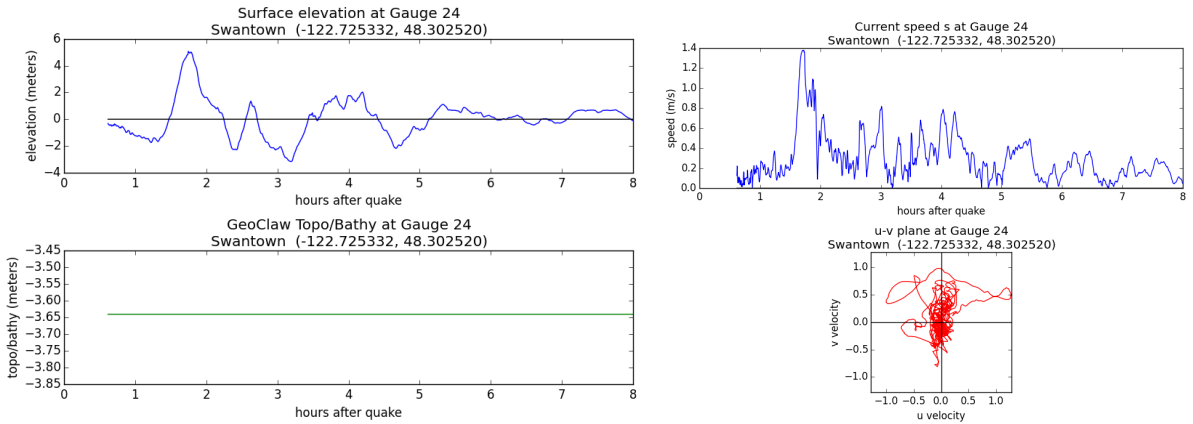
Gauge 24: Swantown.

Computed on region NW_Whidbey.

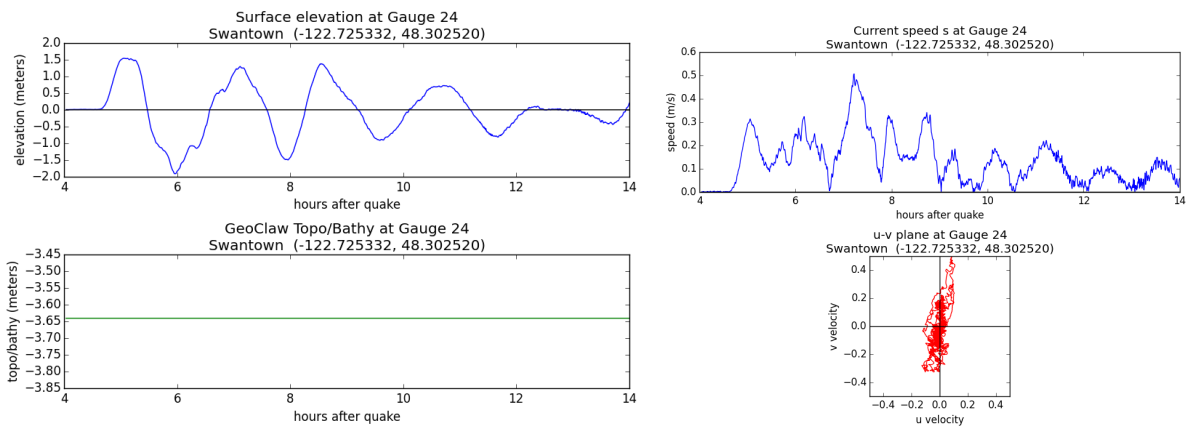
SF-L event:



CSZ L1 event:



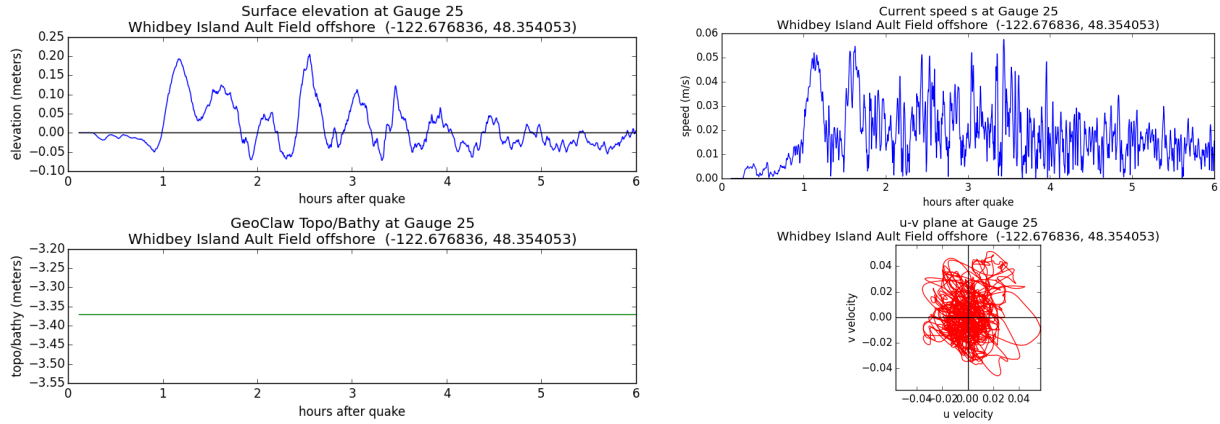
AK event:



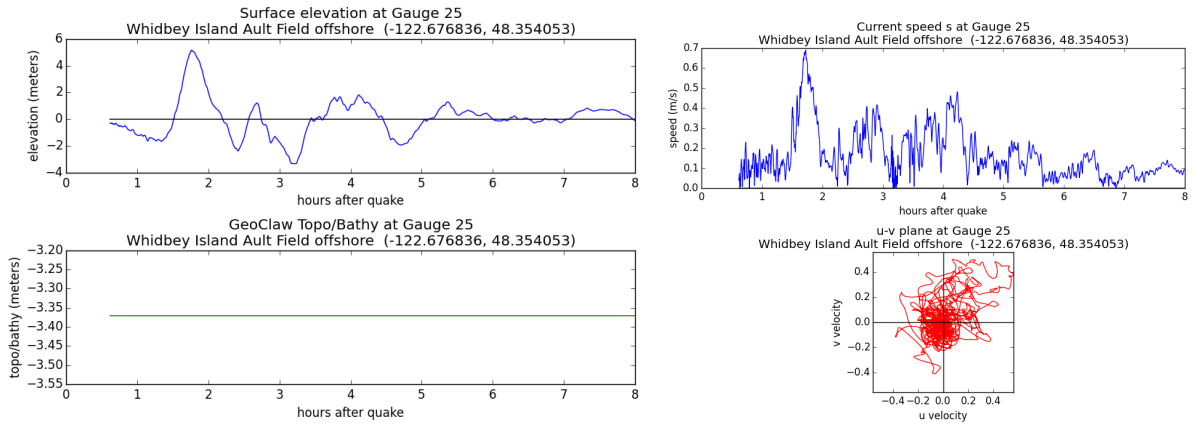
Gauge 25: Whidbey Island Ault Field offshore.

Computed on region NW_Whidbey.

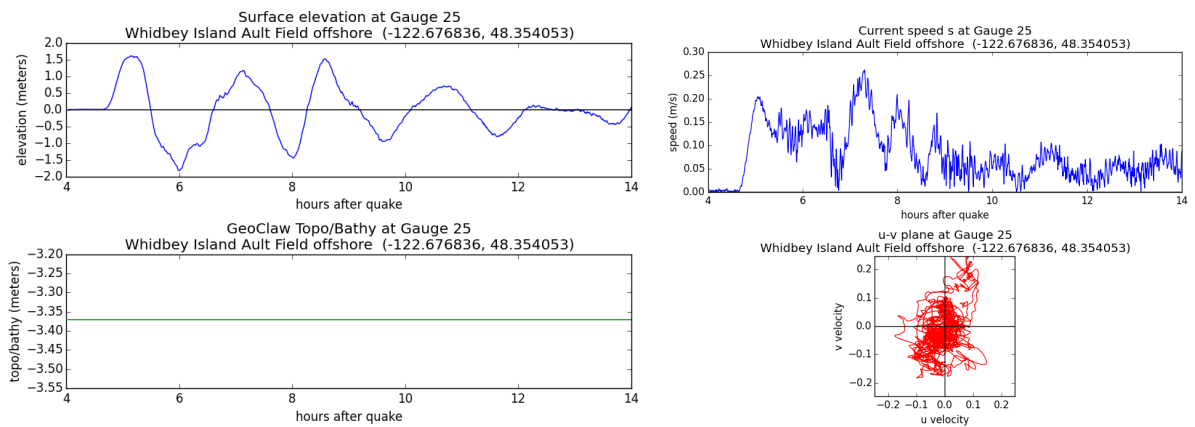
SF-L event:



CSZ L1 event:



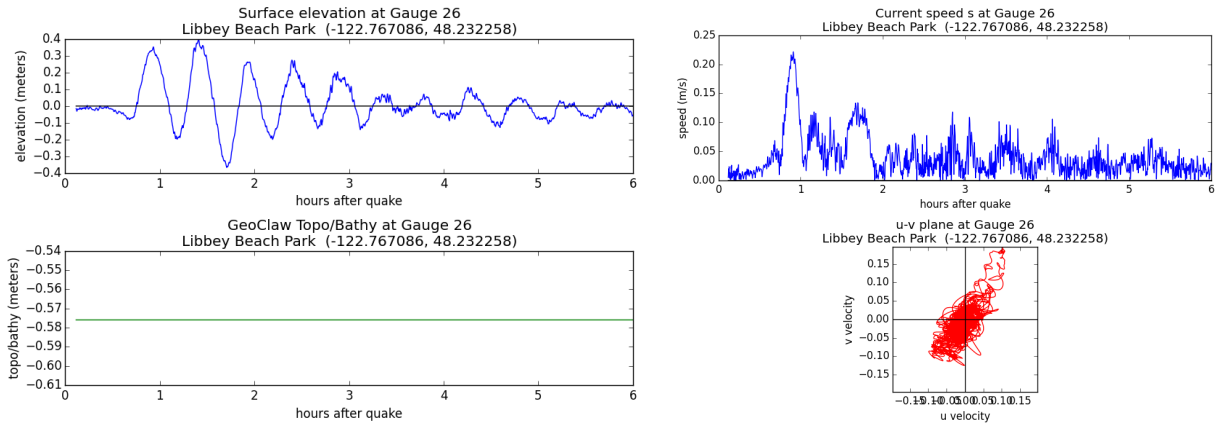
AK event:



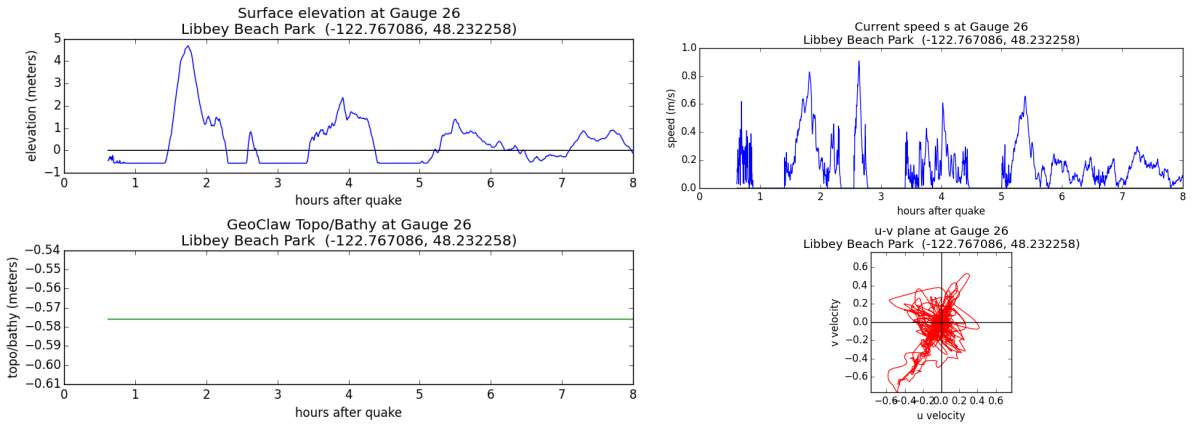
Gauge 26: Libbey Beach Park.

Computed on region NW_Whidbey.

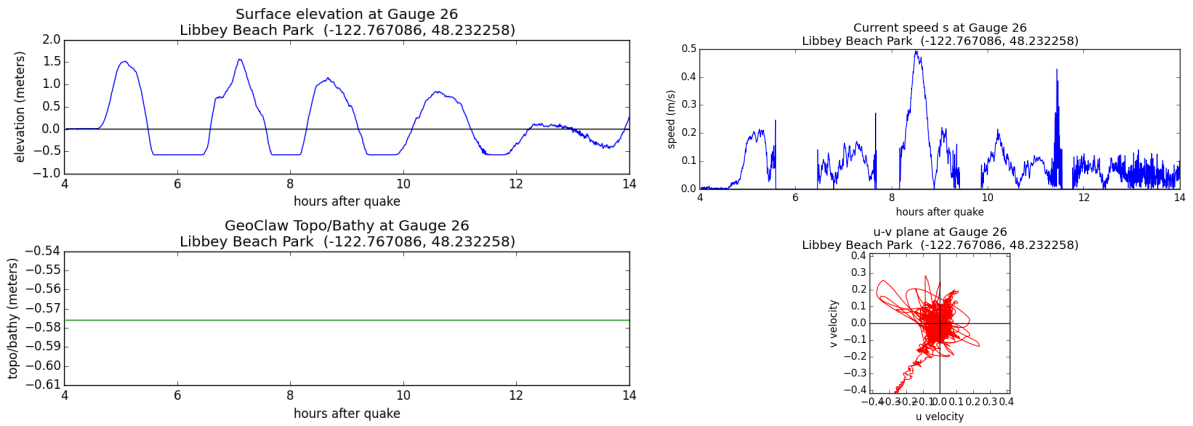
SF-L event:



CSZ L1 event:



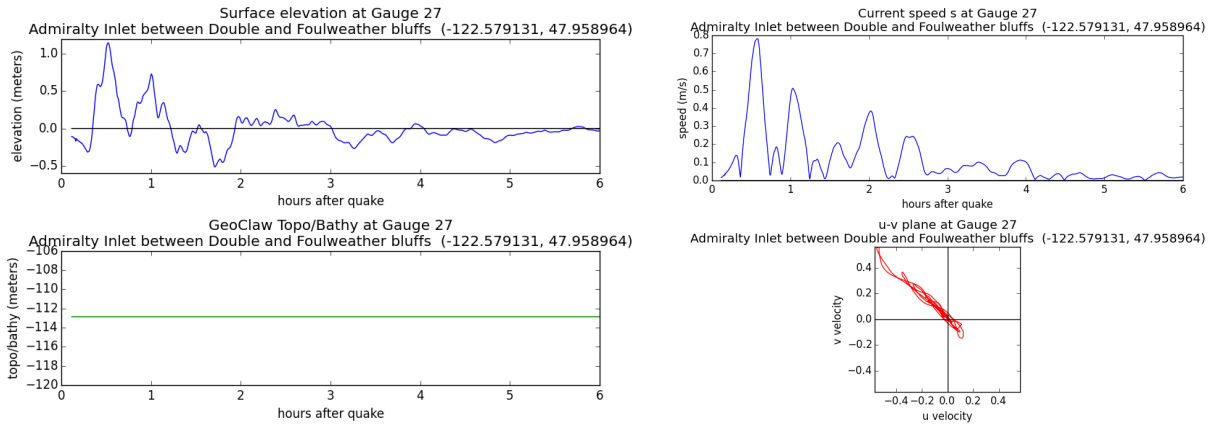
AK event:



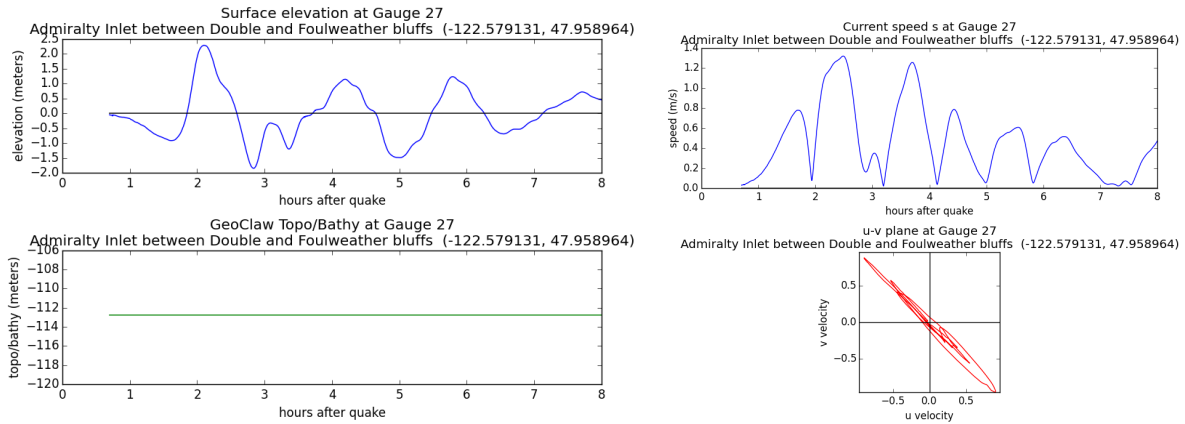
Gauge 27: Admiralty Inlet between Double and Foulweather bluffs.

Computed on region W.Whidbey.

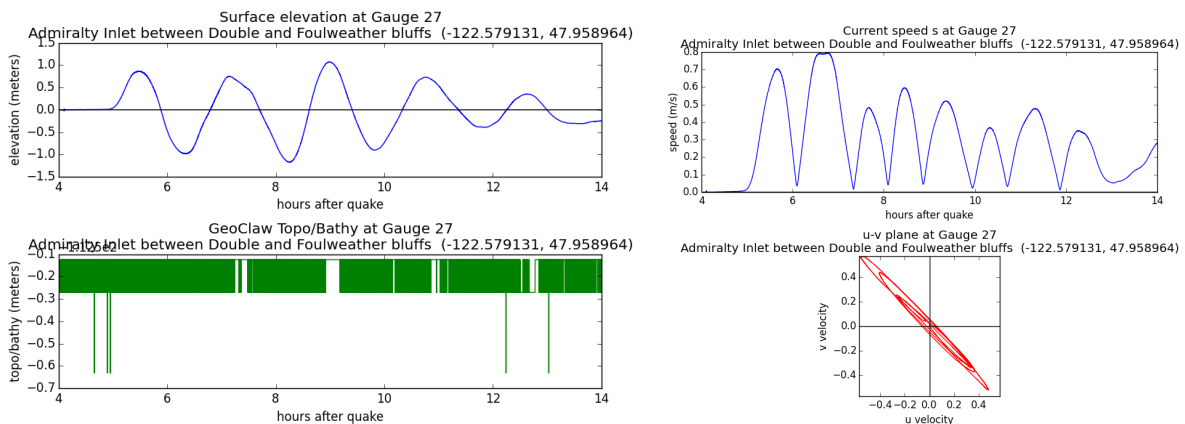
SF-L event:



CSZ L1 event:



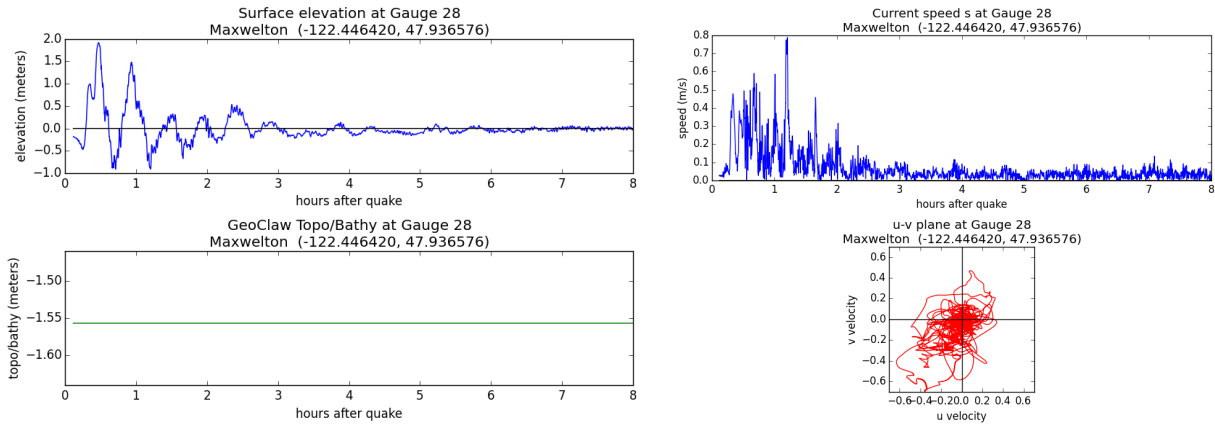
AK event:



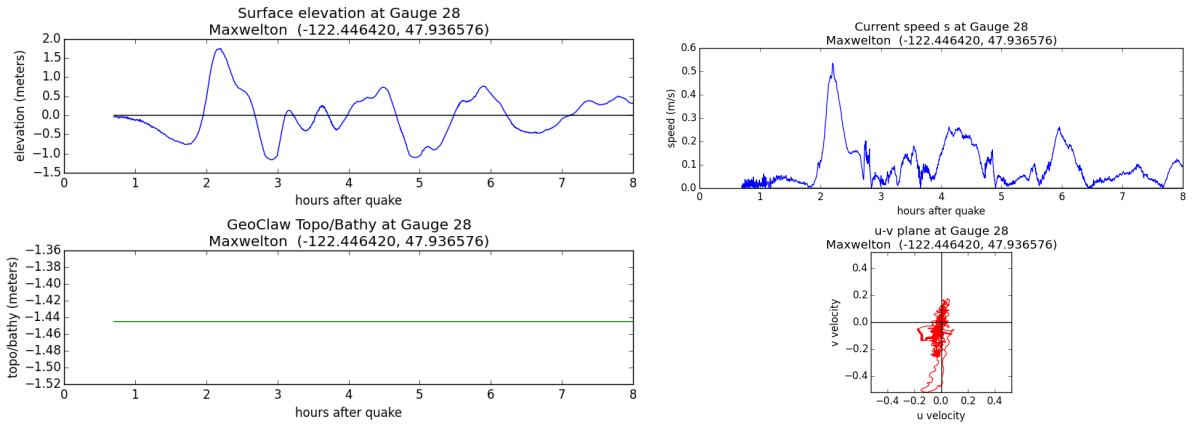
Gauge 28: Maxxelton.

Computed on region SW_Whidbey.

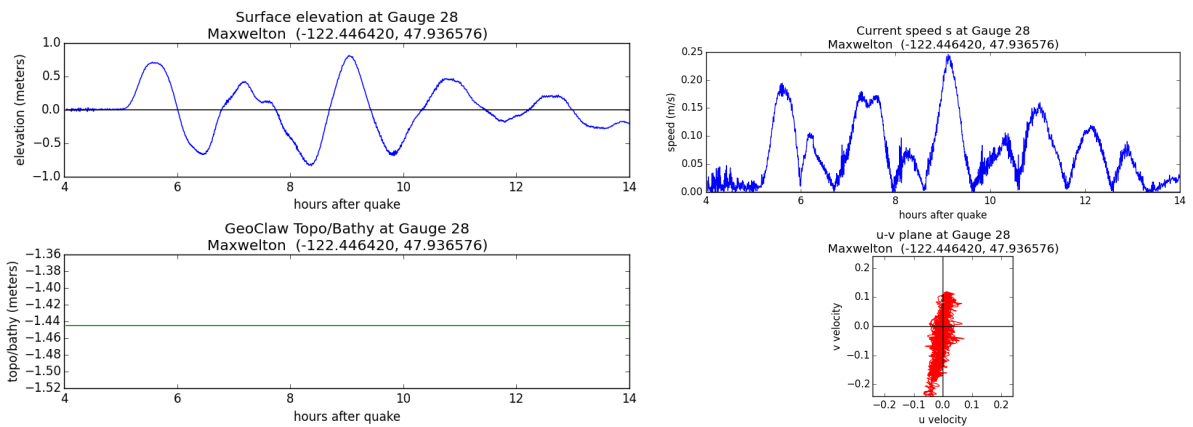
SF-L event:



CSZ L1 event:



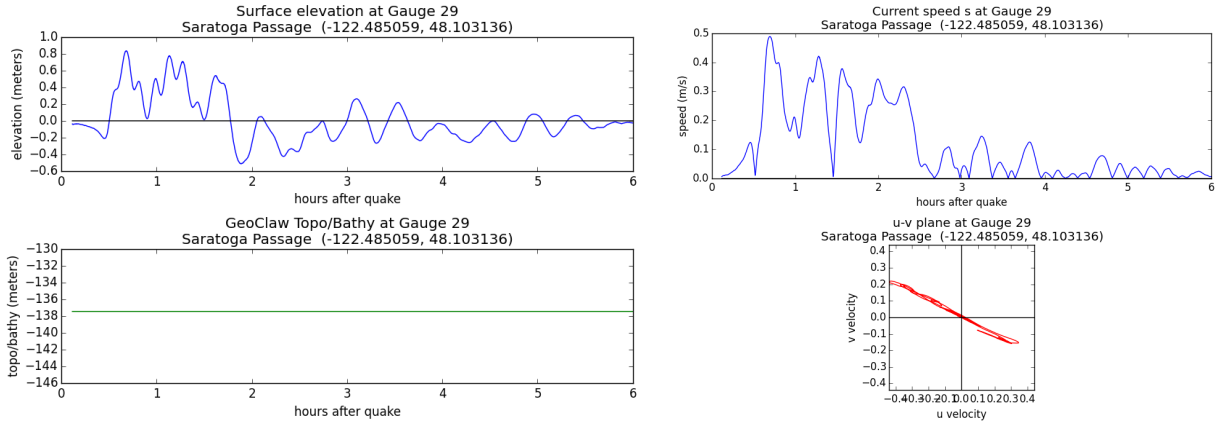
AK event:



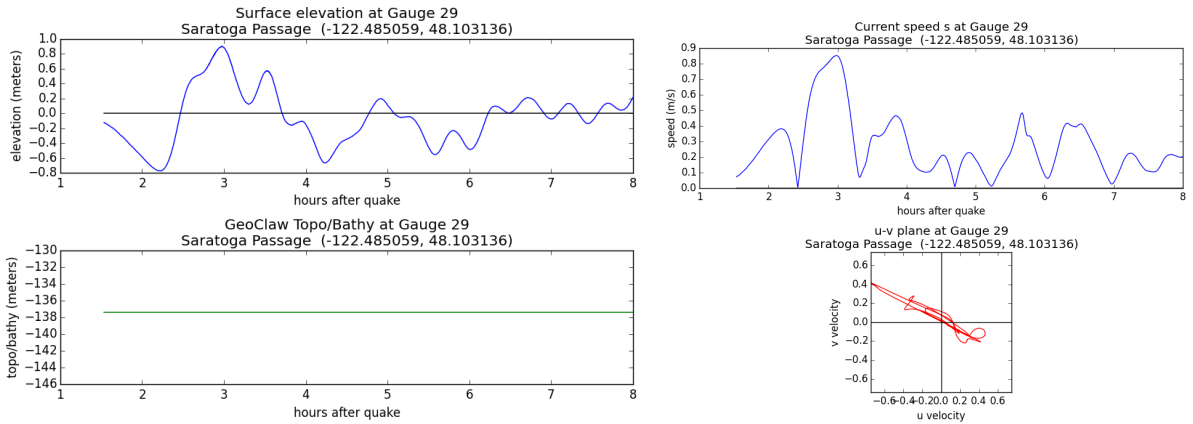
Gauge 29: Saratoga Passage.

Computed on region E.Whidbey.

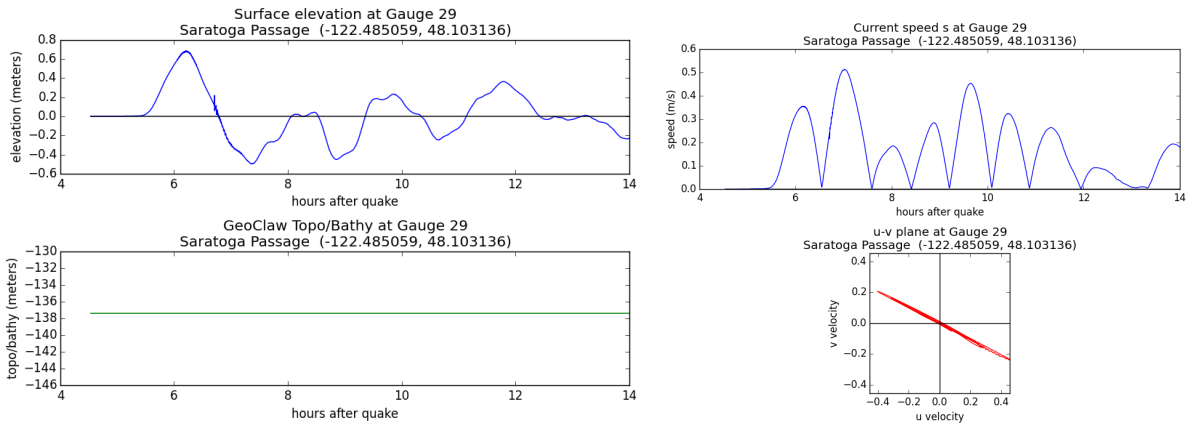
SF-L event:



CSZ L1 event:



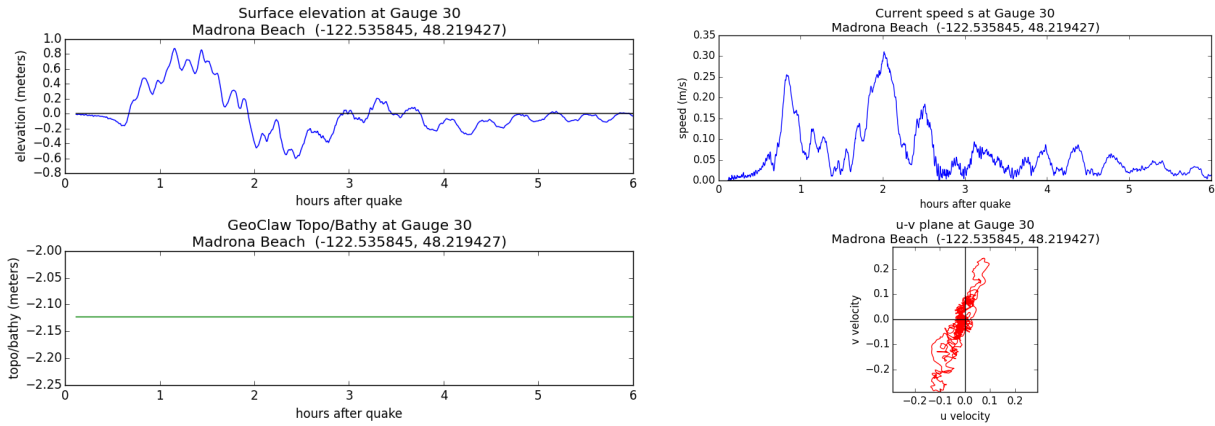
AK event:



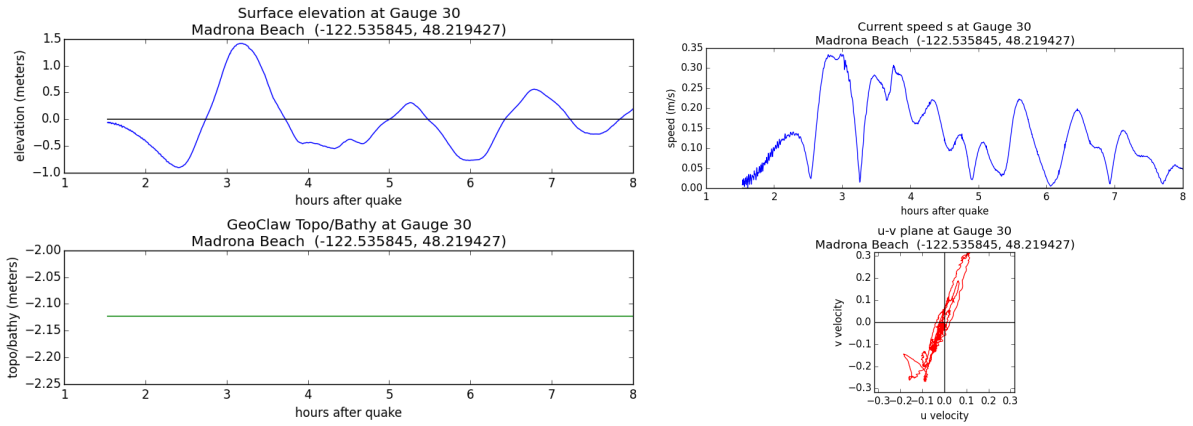
Gauge 30: Madrona Beach.

Computed on region E.Whidbey.

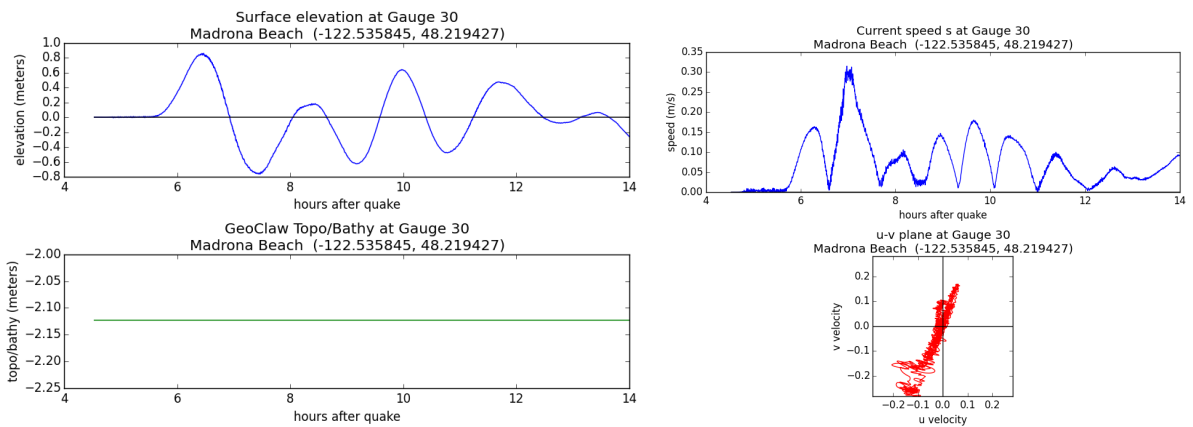
SF-L event:



CSZ L1 event:



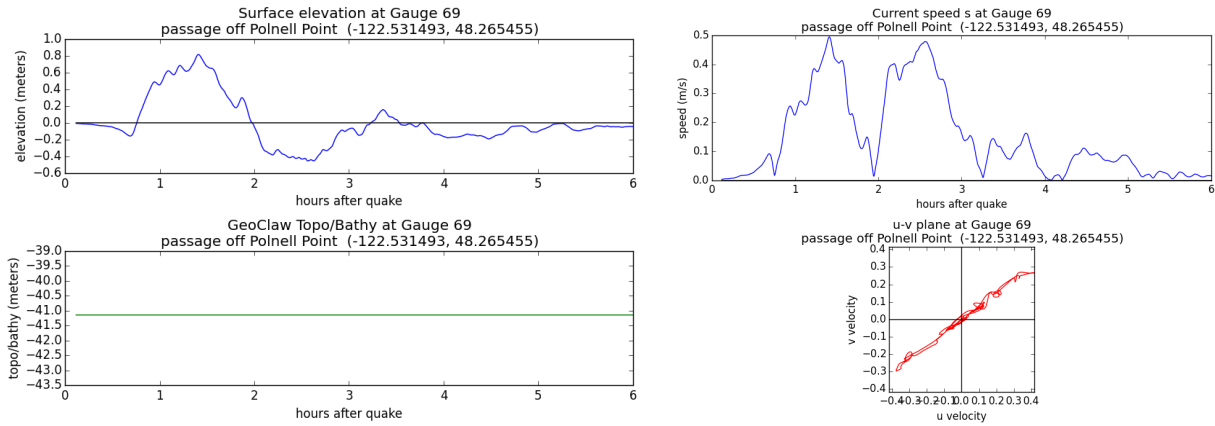
AK event:



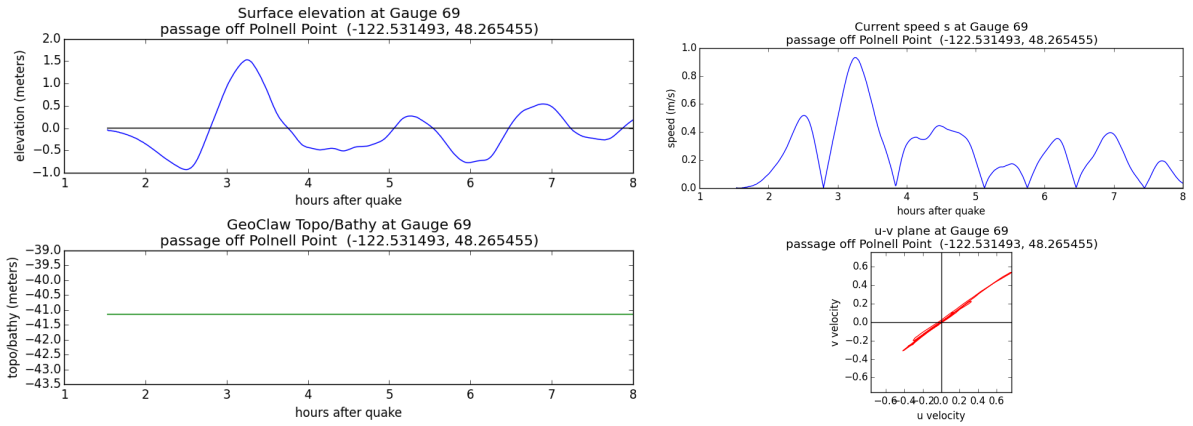
Gauge 69: passage off Polnell Point.

Computed on region E.Whidbey.

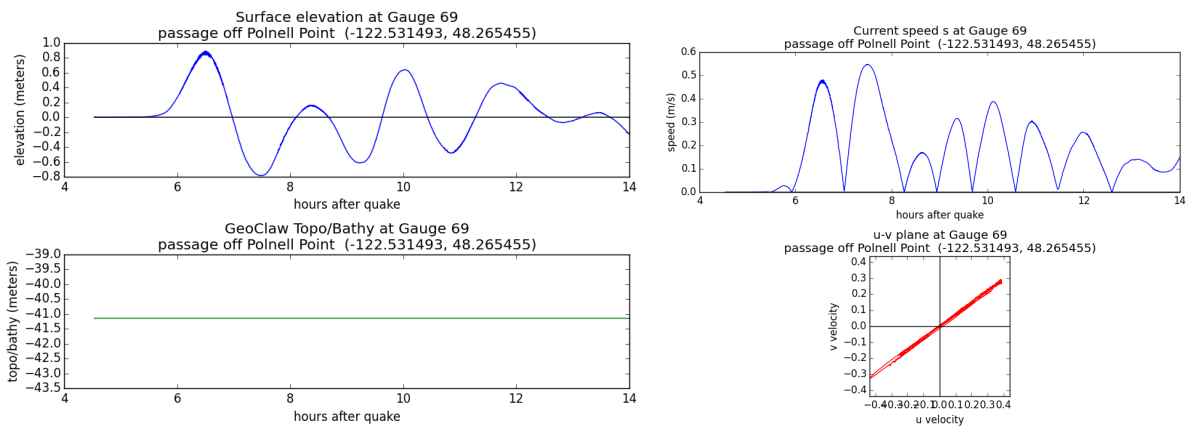
SF-L event:



CSZ L1 event:



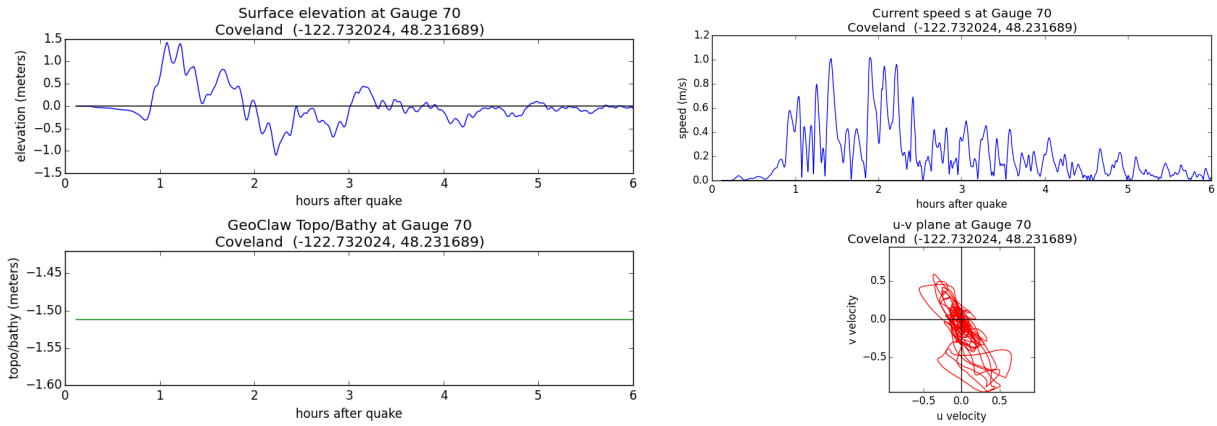
AK event:



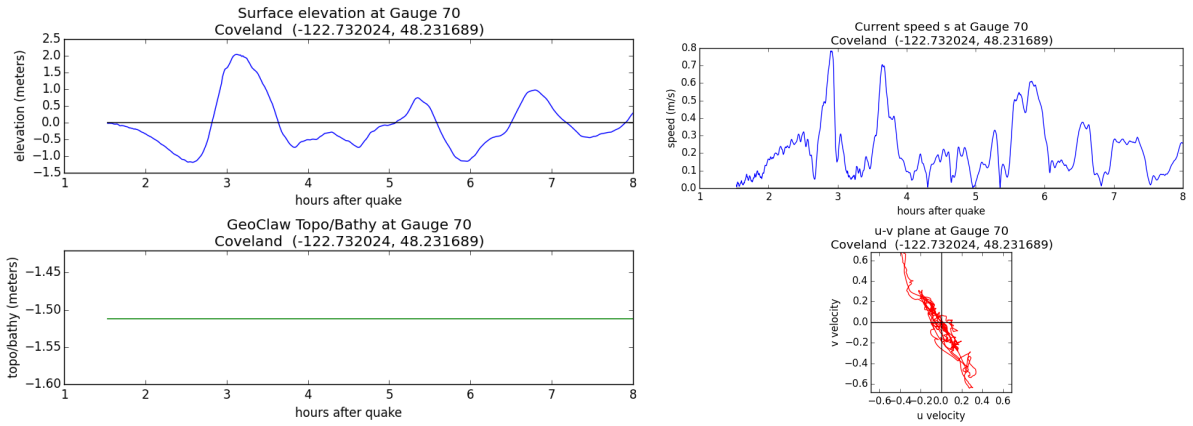
Gauge 70: Coveland.

Computed on region E.Whidbey.

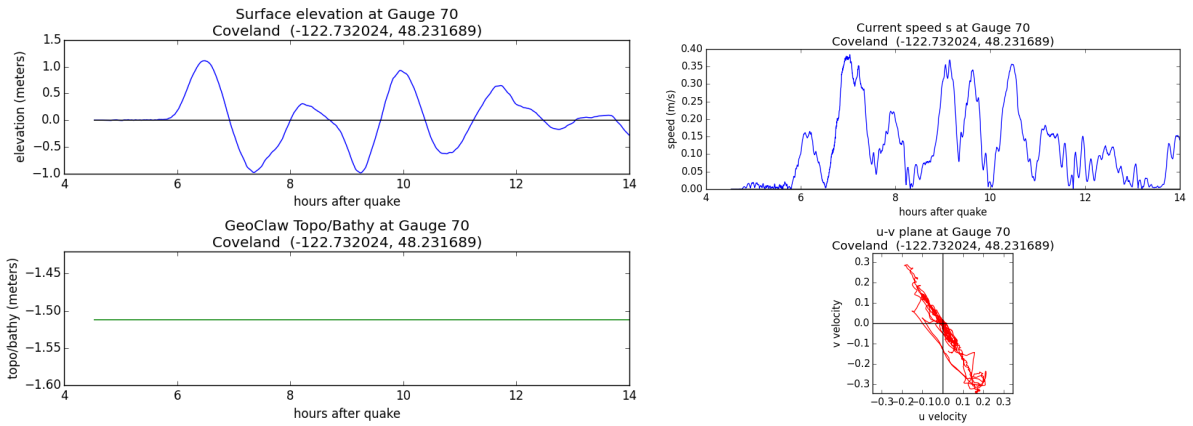
SF-L event:



CSZ L1 event:



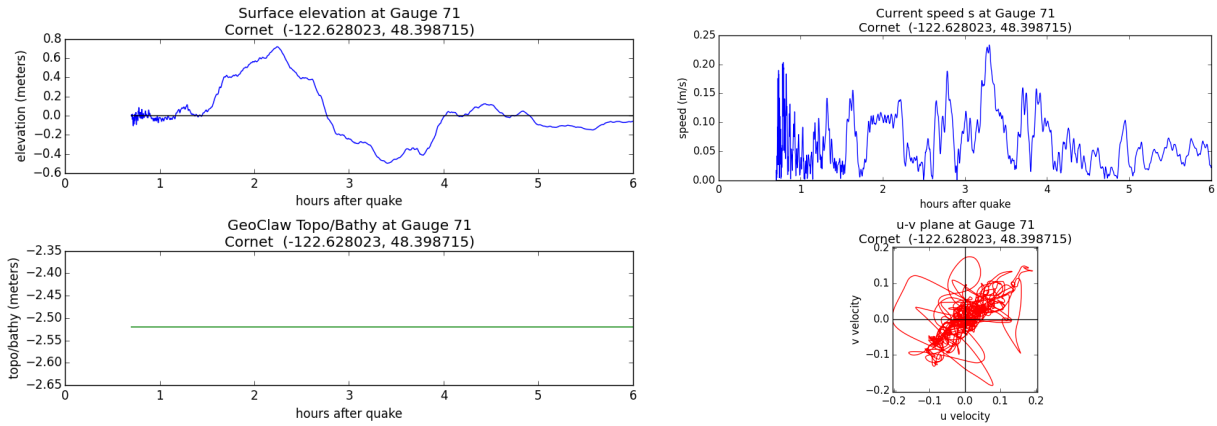
AK event:



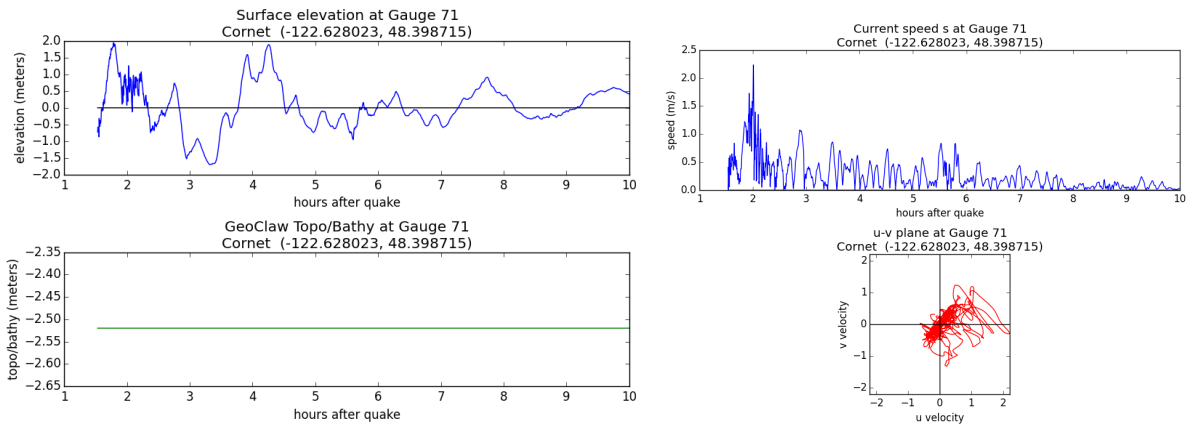
Gauge 71: Cornet.

Computed on region Skagit.

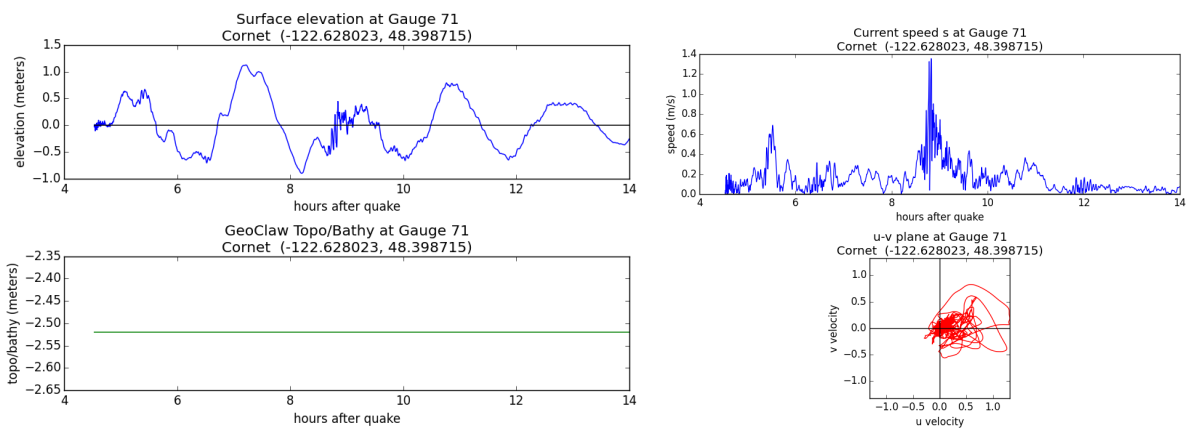
SF-L event:



CSZ L1 event:



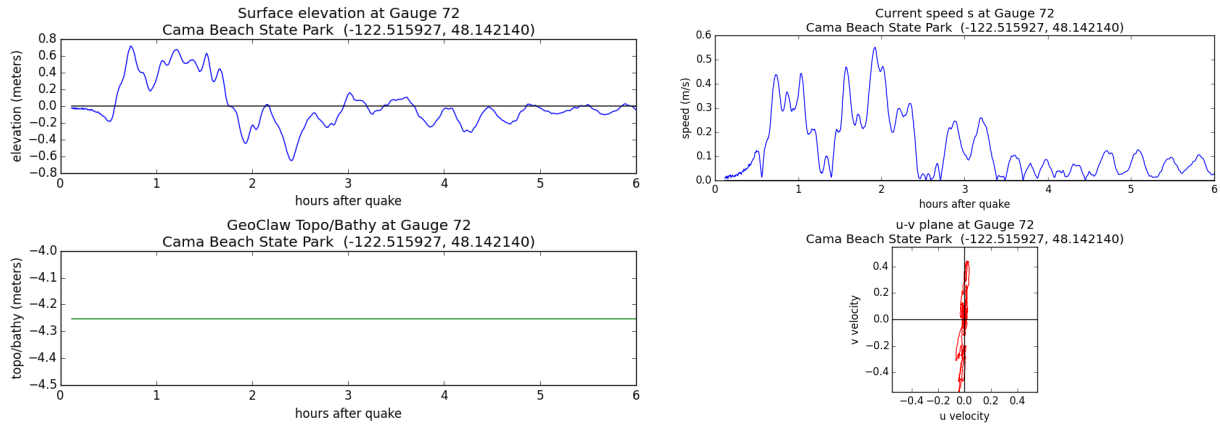
AK event:



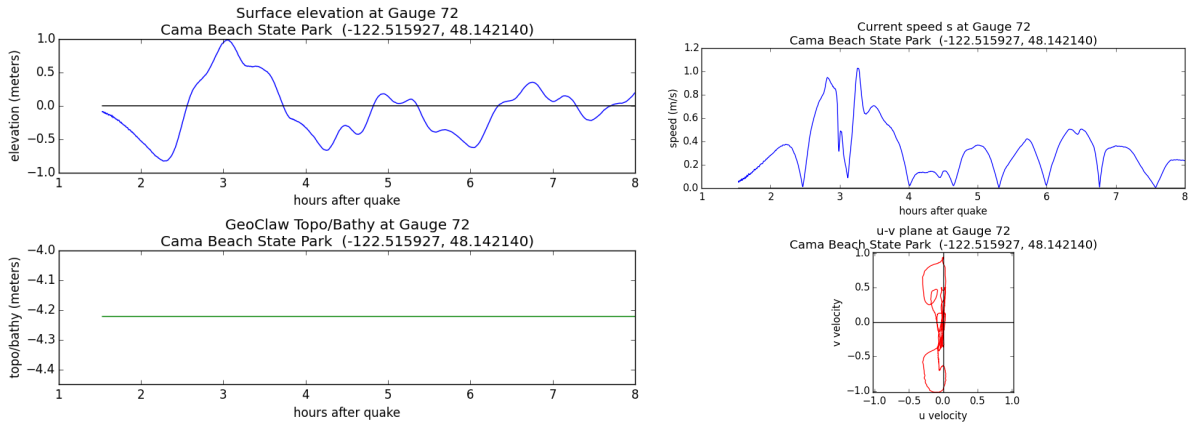
Gauge 72: Cama Beach State Park.

Computed on region E.Whidbey.

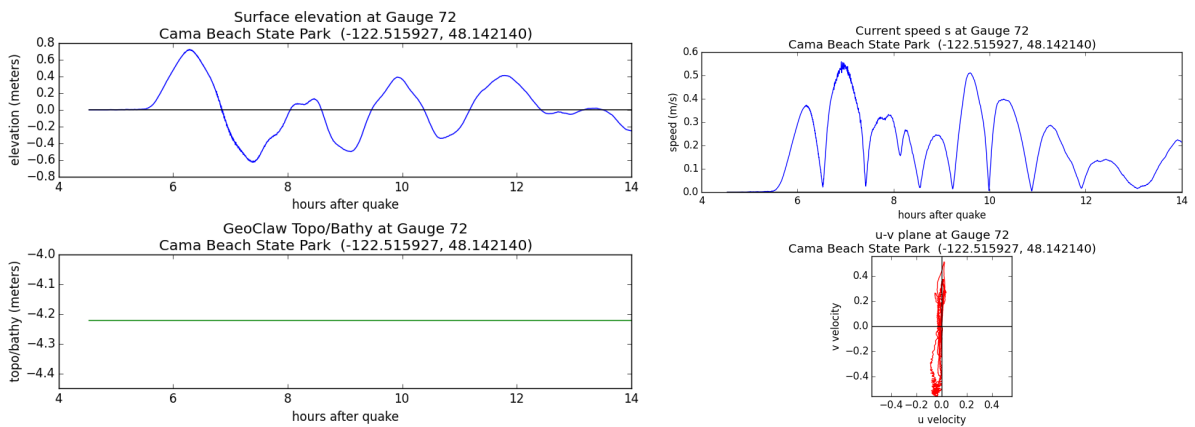
SF-L event:



CSZ L1 event:



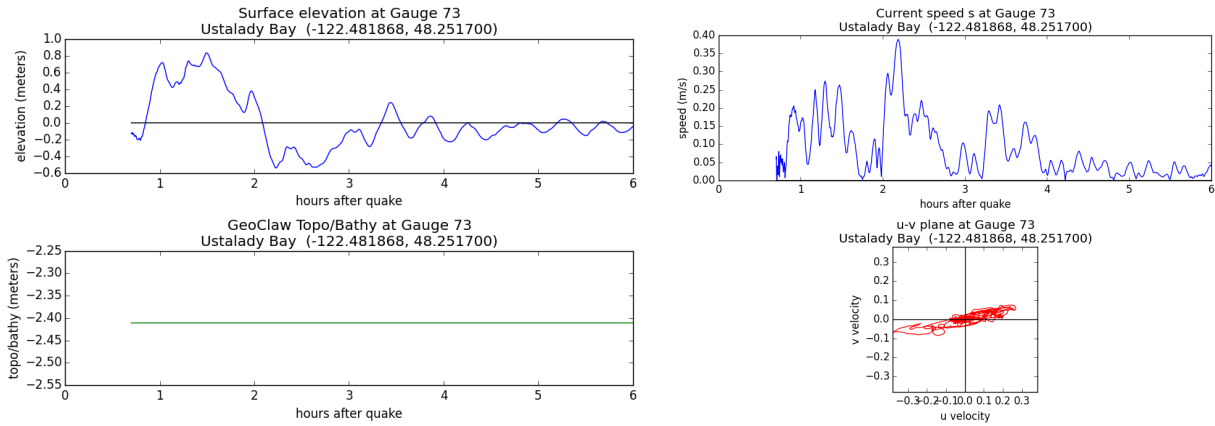
AK event:



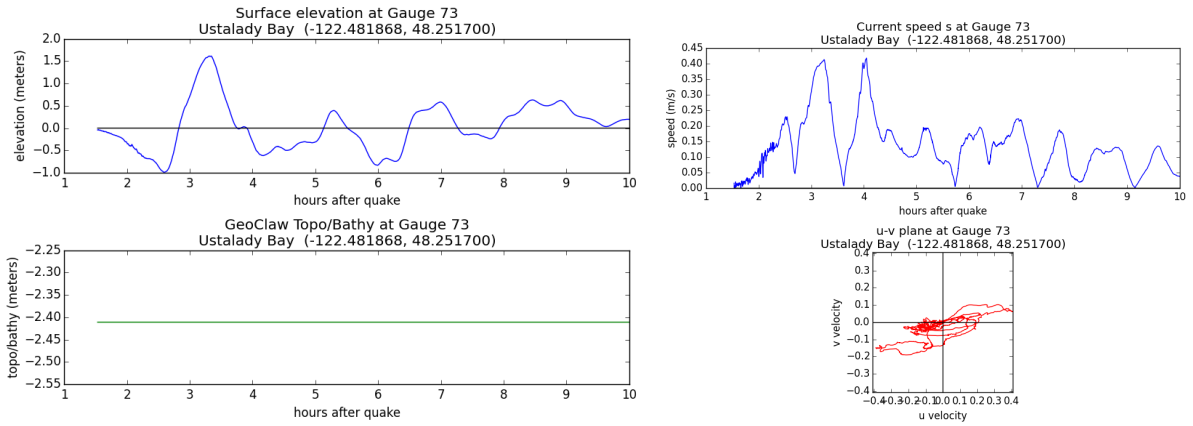
Gauge 73: Ustalady Bay.

Computed on region Skagit.

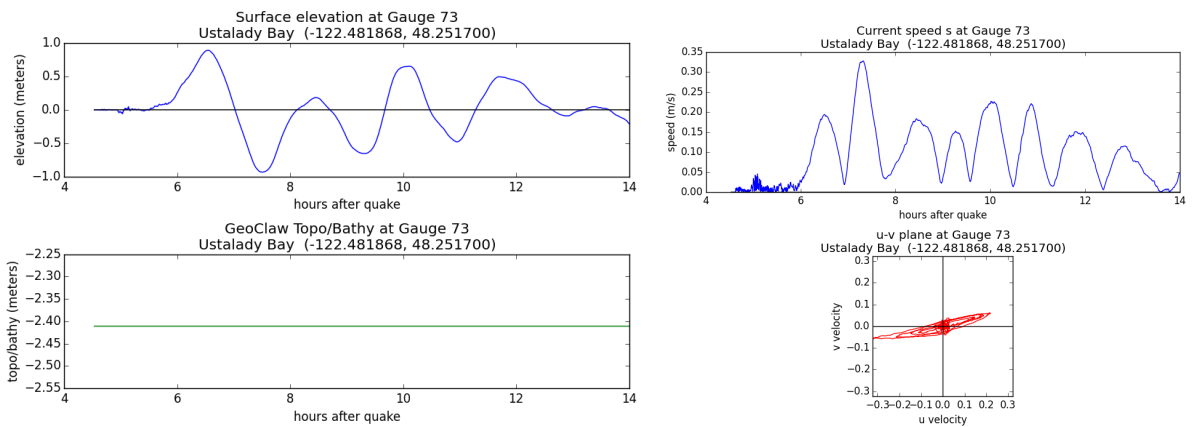
SF-L event:



CSZ L1 event:



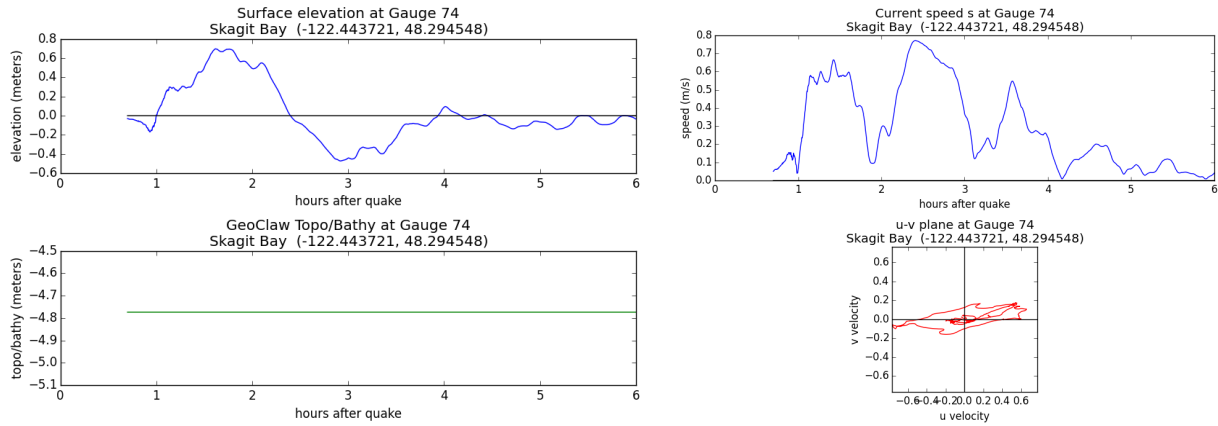
AK event:



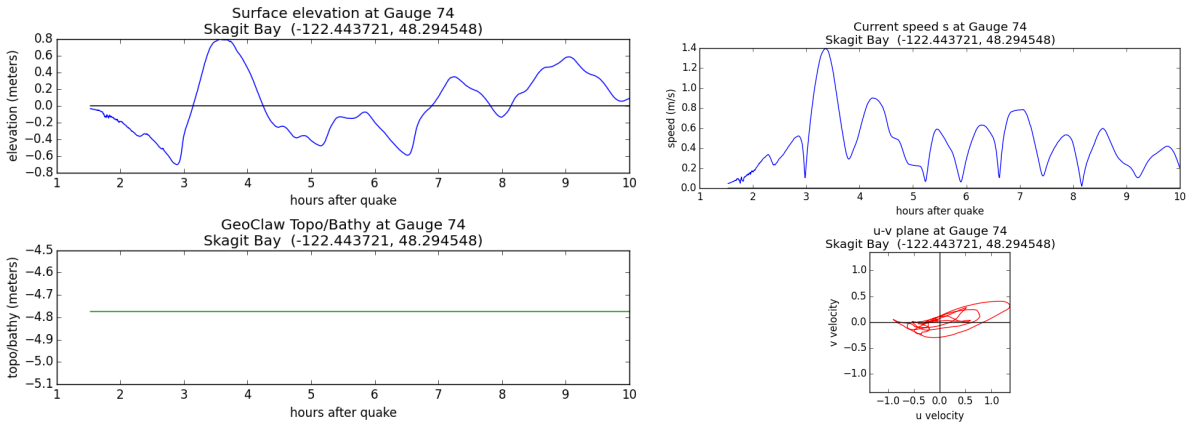
Gauge 74: Skagit Bay.

Computed on region Skagit.

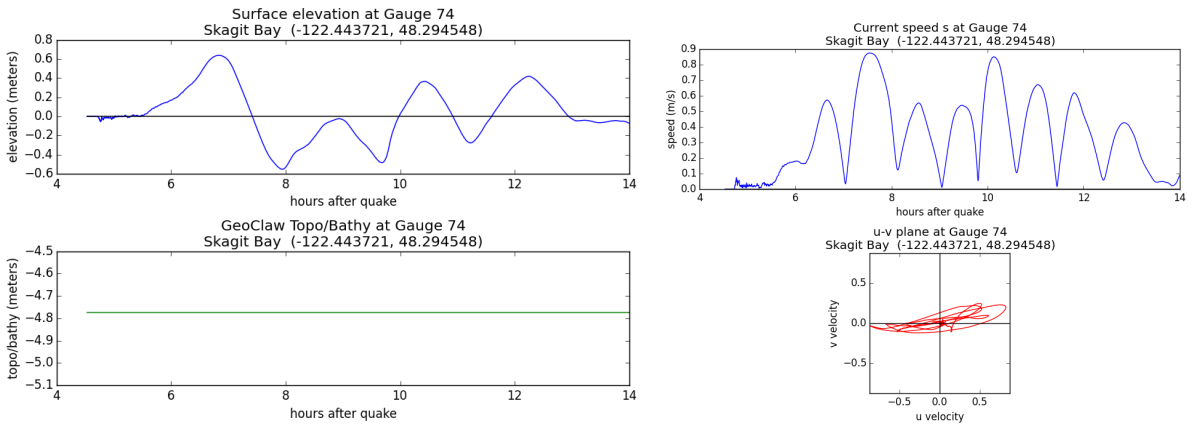
SF-L event:



CSZ L1 event:



AK event:



Appendices

A Data format

The deliverables described here are available on the Supplementary Materials website [13], with a permanently archived version available at [14]. These sites also contain additional materials and the code used to produce input data, run GeoClaw, postprocess output, and produce the plots shown in this paper and on the website.

A.1 fgmax values

For each earthquake source, output data is provided in a set of netCDF files, one for each of the regions associated with the source as listed in Table 2 and shown in Sections 6.1 through 6.6. There are six regions for each of 3 tsunami sources, so a total of 18 netCDF files are provided with results. The netCDF files archived have names of the form REGION_EVENT_results.nc where REGION is replaced by the fgmax region on which it was computed, and EVENT is replaced by the event (one of SFL, CSZ.L1, AKmaxWA).

The netCDF files contain the field variables described below. Some are generated before the GeoClaw run as part of the input, and are independent of the tsunami source event, depending only on the fgmax region. Others are generated after the run from the fgmax output. Note that all variables are stored on two-dimensional uniform grids as defined by the lon and lat arrays. Only the points on this grid where fgmax_point == 1 are used as fgmax points and only at these points is fgmax output available.

Values created as part of the GeoClaw input:

- lon: longitude, x (degrees),
- lat: latitude, y (degrees),
- Z: topography value Z from the DEM, relative to MHW (m),
- fgmax_point: 1 if this point is used as an fgmax point, 0 otherwise,
- allow_wet_init: 1 if this point is initialized as usual, 0 if this point is forced to be dry, regardless of initial topography value.

Values created based on the GeoClaw output:

- dz: Co-seismic surface deformation interpolated to each point (m),
- B: post-seismic topography value B from GeoClaw at gauge location (m),
- h: maximum depth of water over simulation (m),
- s: maximum speed over simulation (m/s),
- hss: maximum momentum flux hs^2 over simulation (m^3/s^2),
- hmin: minimum depth of water over simulation (m),
- arrival_time: apparent arrival time of tsunami (s),

In addition, the netCDF files contain the following metadata values:

- tfinal: Final time of GeoClaw simulation (seconds),
- history: Record of times data was added to file,
- outdir: Location of output directory where data was found,
- run_finished: Date and time run finished,

Recall that the fgmax points are exactly aligned with the 1/3" DEM points. The finest level computational finite volume grid is also aligned so that cell centers are exactly at the fgmax points, and Z in the netCDF file is the value from the DEM at this point. However, the topography value B used in a grid cell in GeoClaw is obtained by integrating a piecewise bilinear function that interpolates the 1/3" DEM, and so B does not exactly equal Z initially. Moreover, B is the value after any co-seismic deformation associated with the event.

A.2 Gauge time series

The gauge time series was captured from each simulation every time step, but was then interpolated to 5 second increments to create the time series stored in the netCDF file for each gauge. The gauges were generally turned on only after the finest level computational grids were introduced around the fgmax region, and so time series do not start at $t = 0$ in general. Most gauges were within some fgmax region and so the finest computational grid around the gauge had a resolution of $1/3''$. The time step then depends on the maximum depth over this region (since GeoClaw requires computing with a time step satisfying the CFL condition), but in general was less than 1 second.

The netCDF files archived have names of the form `REGION_EVENT_gauge00000.nc` where `REGION` is replaced by the fgmax region on which it was computed, `EVENT` is replaced by the event (one of `SFL`, `CSZ.L1`, `AKmaxWA`), and `00000` is replaced by the gauge number.

The netCDF files contain the following field variables:

`times`: time (seconds post-quake),
`zGeo`: post-seismic topography value B from GeoClaw at gauge location (m),
`h`: depth of water at gauge in simulation (m),
`u`: E/W velocity u at gauge (m/s),
`v`: N/S velocity v at gauge (m/s),
`level`: AMR refinement level at gauge at this time.

In addition, the netCDF files contain the following metadata values:

`history`: Record of times data was added to file,
`outdir`: Location of output directory where data was found,
`run_finished`: Date and time run finished,

B Modeling Details and GeoClaw Modifications

A pre-release version of GeoClaw Version 5.6.1 was used for the modeling. This open source software is distributed as part of Clawpack, and is available from [7]. The released version 5.6.0 was used with the addition of some some modifications to be released in 5.6.1 that sped up a part of the code. (Version 5.6.1 was released on October 28, 2019, see http://www.clawpack.org/release_5_6_1.html.)

Some additional modifications were made to the software to deal with issues that arose in this modeling project. These are briefly described in this appendix and archived in the code included at [14], with more documentation. These new features are also described further in a set of Jupyter notebooks available at http://www.clawpack.org/new_features_for_v5.7.0 and will be incorporated into the Version 5.7.0 release of Clawpack. These supplementary materials can also be viewed at [13]. Many of these modifications will be incorporated into the next release of Clawpack (version 5.7.0) for more general use.

Summary of changes to GeoClaw (Fortran code):

- The manner in which fgmax points are updated in GeoClaw was originally developed in a manner that did not scale well to millions of points. The internal algorithms have been sped up substantially, without changing the computational results.
- As part of speeding the code up, a new format for specifying fgmax points was introduced in which an ASCII raster file having a header identical to that used for topography files (`topo_type==3` in GeoClaw) can be provided, with the data values consisting of a 1 at points that are selected and 0 at non-selected points. Previously list of all points was provided. This does not change the capabilities in itself but helps increase the speed (and reduces the file size of input data).
- A boolean parameter `variable_eta_init` was introduced. If true, then the sea level used to initialize grid cells to wet or dry when new levels of grid refinement are introduced is adjusted, if necessary, by the co-seismic surface displacement as defined by interpolating the `dtopo` file to the center of the grid

cell. This is to account for the fact that when the shore subsides the water just offshore subsides as well. Failure to initialize properly can result in artificial flooding onshore. This has no effect for the CSZ or AKmaxWA simulations and little effect for SF-L due to the small amount of subsidence in the study region.

- An array `wet_mask` was introduced, based on the `allow_wet_init` array described in Section 5.1, along with a parameter `t_stays_dry`. When initializing new grids in GeoClaw at times $t < t_stays_dry$, the cell is forced to be dry if `wet_mask == 0`. Otherwise, the cell is initialized as usual in GeoClaw.

Summary of new Python code:

New Python code was developed that can also be found in the archived code [14], and is documented further within the repository. In particular, the repository contains:

- Code to subsample topography DEMs,
- `marching_front.py`, to implement the marching front algorithms described above.
- `region_tools.py` implementing Ruled Rectangles.
- `make_input_files.py` for each fgmax region, to pre-process DEMs and select fgmax points, define Ruled Rectangle flag regions for adaptive refinement around the fgmax points, and determine dry regions below MHW. These scripts were generated from Jupyter notebooks that are also archived and that can be viewed at [13].
- `fgmax_tools.py` contains tools for post-processing results and writing netCDF files, an updated version of the code in GeoClaw to handle the new style of fgmax files.
- `process_fgmax_common.py` uses these tools for post-processing fgmax results and writing netCDF files.
- `process_gauges.py` for post-processing gauge results and writing netCDF files.

C Gauge comparisons

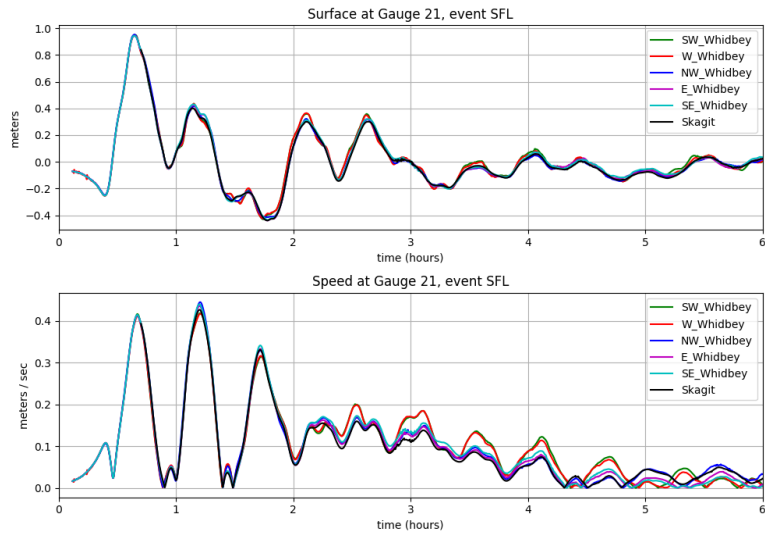
In this appendix we present a few comparisons of time series at key gauges, as a test that the different runs for different fgmax regions are consistent with one another.

C.1 Admiralty Inlet, Gauge 21

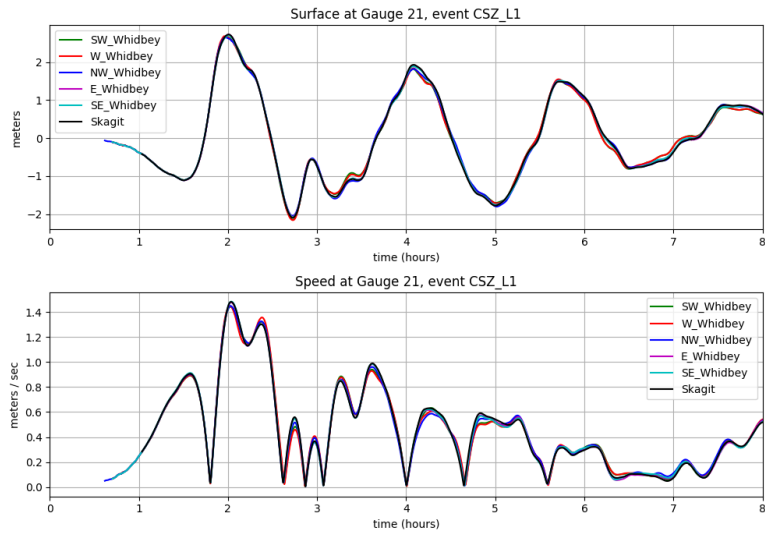
Gauge 21 in Admiralty Inlet was not included in any fgmax region, but this gauge was monitored in every run to check consistency. For the most part this gauge was covered by a 2" grid, although the grid resolution fluctuated a bit in the AKmaxWA simulations, as mentioned in Section 7.

In the figures below, for each of the 3 events, we plot the Gauge 21 output (surface and speed) from each fgmax region simulation together in order to verify that similar results were obtained from each simulation. We do not expect them to be identical since each fgmax region had a different portion of the domain refined to 1/3" and to some extent also to 2". In general they agree very well, particularly for leading largest waves.

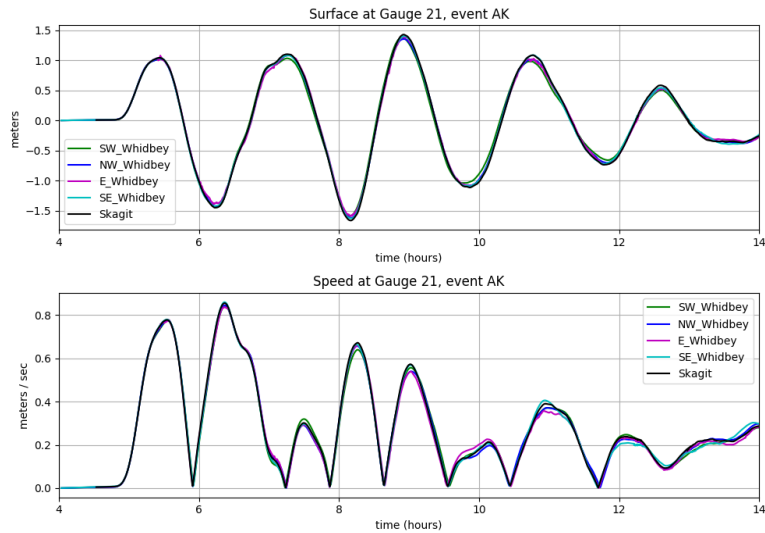
SF-L event:



CSZ L1 event:



AKmaxWA event:



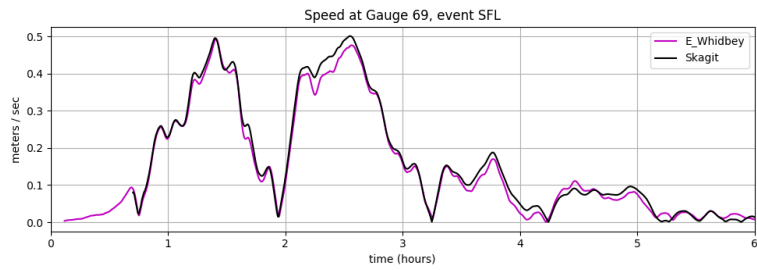
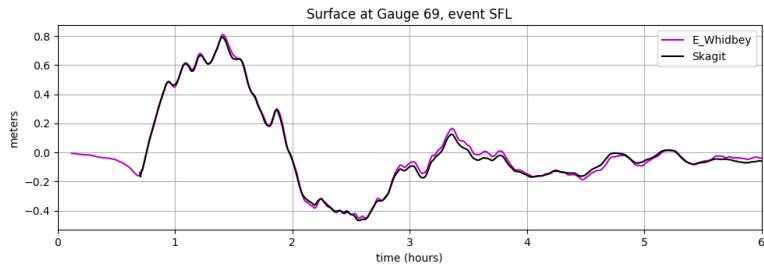
C.2 Polnell Point, Gauge 69

Gauge 69 lies offshore Polnell Point, between eastern Whidbey Island and the north coast of Camano Island. This point is at the boundary between the **E_Whidbey** and **Skagit** fgmax regions, and in the plots below we show the simulation results obtained from these two regions together (for each event).

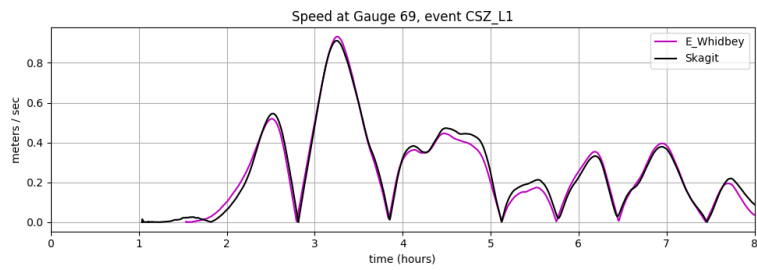
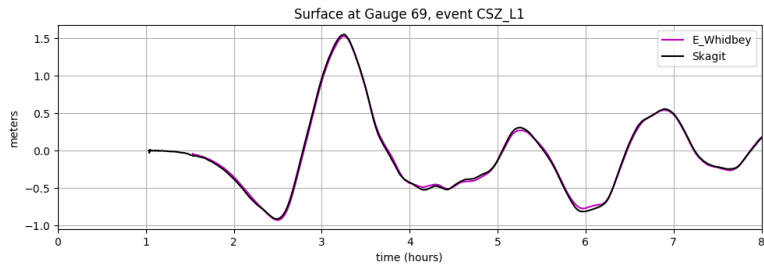
Again we do not expect these results to be identical since 1/3" grid resolution is used on a different side of this point in each simulation. However, as hoped, they do agree quite well, which helps to confirm that splitting the simulations into individual runs is justified.

Moreover, the good agreement at this point also indicates that for all of the events there is little wave energy that reaches the **E_Whidbey** region via Deception Pass. The narrow passage at Deception Pass is one way waves enter the **Skagit** region, and this passage was and the surrounding area was refined to 1/3" resolution in the **Skagit** simulation. It was not, however, refined to 1/3" in the **E_Whidbey** simulation, nor was the coastline and complex dike structure of the Skagit River Delta resolved in the **E_Whidbey** simulation, although it was in the **Skagit** simulation. If waves passing through the **Skagit** region were important in the **E_Whidbey** region, then we would expect more significant differences between the **Skagit** and **E_Whidbey** results at Gauge 69.

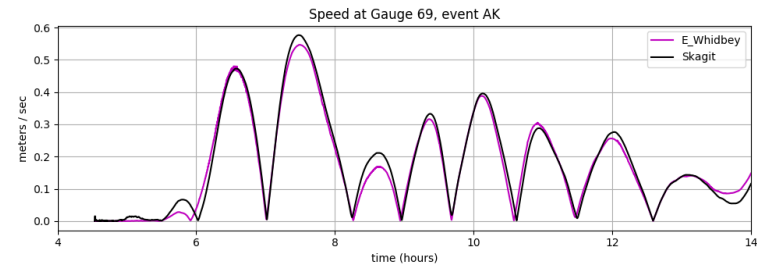
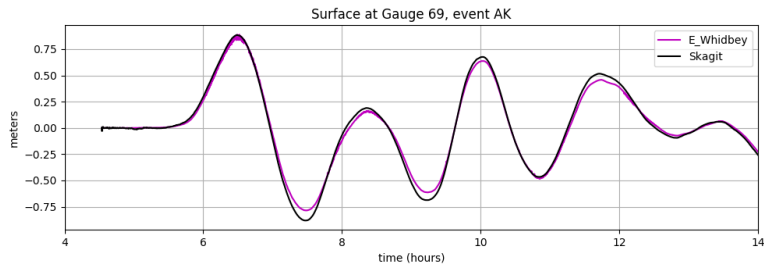
SF-L event:



CSZ L1 event:



AKmaxWA event:



C.3 Deception Pass, Gauge 8

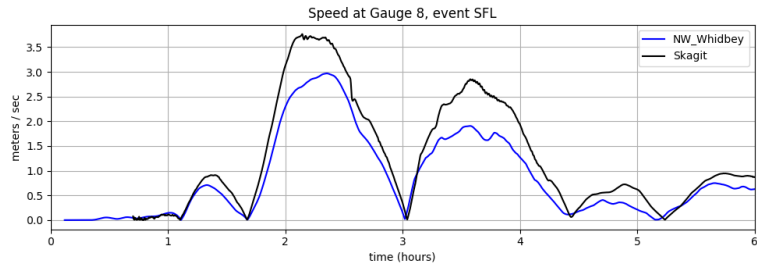
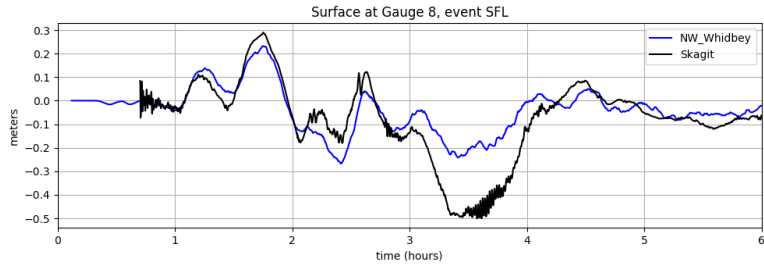
Deception Pass separates the north coast of Whidbey Island from the mainland. This narrow passage experiences very strong tidal currents, as high as 4–5 m/s at times. The tsunami currents are very strong, particularly for the CSZ-L1 and AK events, which show maximum speeds of roughly 7 and 6 m/s respectively.

It is important to note that these tsunami simulations are performed on a background of stationary water, at the level of MHW, and tidal currents are not included in the simulations. If the tsunami arrives during a flood tide, for example, then the current speed through Deception Pass could be much greater.

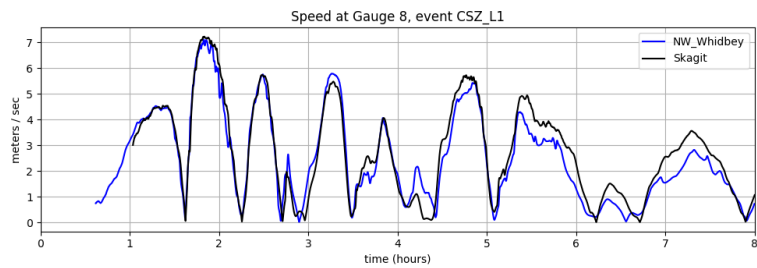
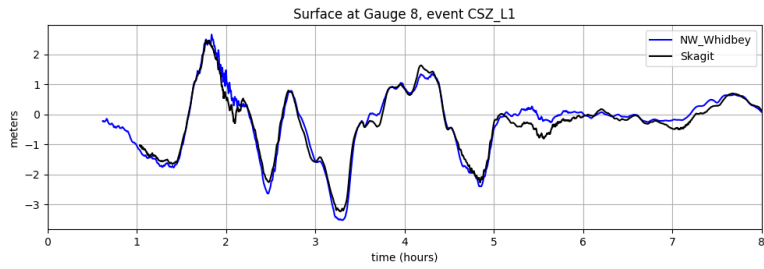
Deception Pass is also at the boundary of the NW.Whidbey and Skagit fgmax regions. The figures below show comparisons of the time series calculated at this gauge from the two fgmax regions. The agreement is not as close as in the last two sections, but still there is good agreement of the peaks, particularly for the CSZ-L1 and AKmaxWA events. Since these tsunamis arrive directly from the Strait of Juan de Fuca and the west side of Whidbey Island, we believe the results obtained from the W.Whidbey simulation are best to use at Gauge 8 for the CSZ-L1 and AKmaxWA events.

The SF-L event is relatively weak, and examining time series elsewhere and frames of the simulation, we concluded that the primary wave observed reaches Deception Pass after propagating up the east side of Whidbey Island and through the fgmax region denoted Skagit. The comparison below also shows that the predicted amplitude and current speed is larger in the gauge results from the Skagit simulation than from the NW.Whidbey simulation, and so we recommend using the Skagit version of Gauge 8 results for the SF-L event.

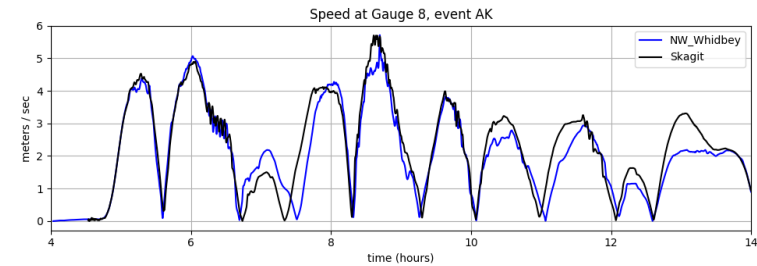
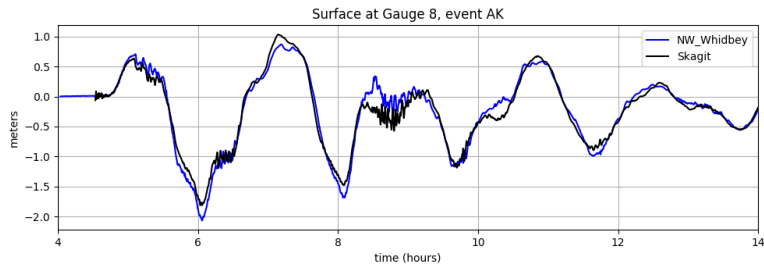
SF-L event:



CSZ L1 event:



AKmaxWA event:



D Skagit River Delta

As noted elsewhere in the report, the topography of the Skagit River Delta presented a challenge because of the extensive network of dikes and levies that protect roughly 150 km² of dry land that is below MHW.

This is illustrated by comparing Figure 20, which shows all points with DEM value $Z < 0$ as blue, and Figure 21, in which the points identified as dry in spite of having $Z < 0$ as pink.

The merged PTPSm-DEM provided by NCEI appears to contain newer data than the 1/3" PT-DEM that also covers this region (see Section 3). Nonetheless, there are remaining issues with the DEM and in order to identify areas below MHW that should be initialized as dry, we set `sea_level_mask = -0.6 m` in the algorithm described in Section 5.1. Figure 24 shows the incorrect results that are obtained with the marching front algorithm using `sea_level_mask = 0`, along with the results obtained by setting `sea_level_mask = -0.6 m` in the region in the red polygon. Outside this region we were able to set `sea_level_mask = 0` and the marching front algorithm allows this flexibility. The code used to produce the input for GeoClaw is archived in the code repository. The code and plots produced by the Jupyter notebook `make_input_files.ipynb` for the Skagit region can also be viewed on the webpage [13].

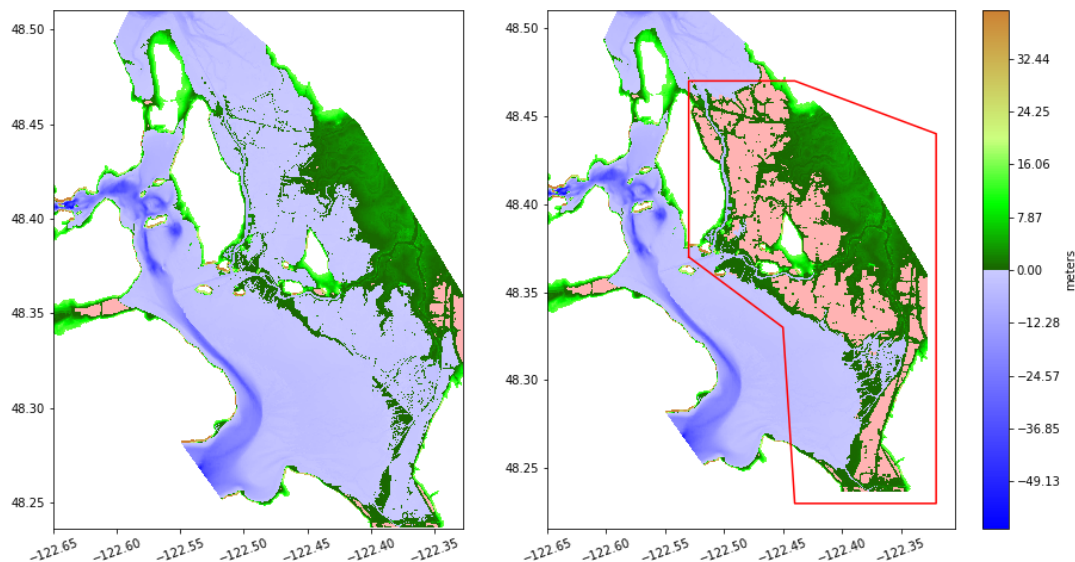


Figure 24: Left: Result of applying the marching front algorithm of Section 5.1 with `sea_level_mask = 0`. Right: Result of first applying the marching front algorithm of Section 5.1 with `sea_level_mask = -0.6` and then freezing the region indicated in the red polygon while applying the algorithm again with `sea_level_mask = 0` over the remainder of the fgmmax region.

Figure 25 shows the northern extent of the Skagit region and extends farther north to illustrate the additional topographic issues around Padilla Bay. The pink regions in this figure were determined to be dry land by the marching front algorithm with `sea_level_mask = -0.6 m`. The region north of latitude 48.52 is not in the Skagit fgmmax region and was not refined to 1/3". So instead of using an `allow_wet_init` array, the GeoClaw code was modified to initialize all cells to be dry if they lie between 48.52N and 48.57N and east of 122.5W. This had the effect of initializing some cells to dry that should have been wet, but over the first few hours of the simulation (before the tsunami arrived at roughly 2.5 hours), the water slowly filled in the areas seaward of dikes. We also ran some simulations without doing anything special in this region north of 48.52N (filling all cells below MHW initially), and found that this had little impact on the results in the Skagit region.

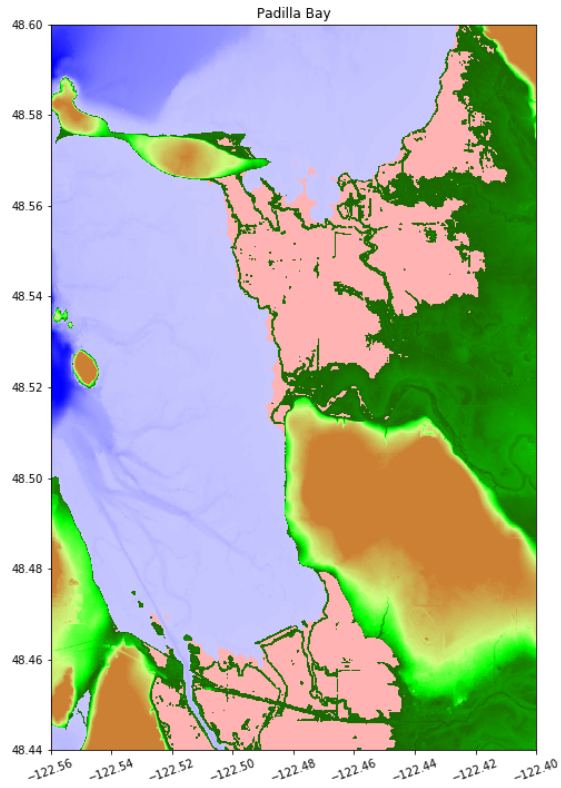


Figure 25: Results of running the marching front algorithm over Padilla Bay with `sea_level_mask = -0.6` m, including the northern extent of the Skagit fgmax region.

Another point to note in the Skagit region is that the tsunami continues to slowly move across this low lying land for many hours after first reaching the shore, reminiscent of the manner in which the 2011 tsunami slowly moved across the Sendai Plain in Japan. For this reason we ran the CSZ-L1 simulation out to 10 hours in this region rather than the 8 hours simulated elsewhere. Figure 26 shows how the maximum flow depth h evolves, as captured 6, 8, 10, and 12 hours post-earthquake. The water is continuing to slowly spread outwards even at 12 hours.

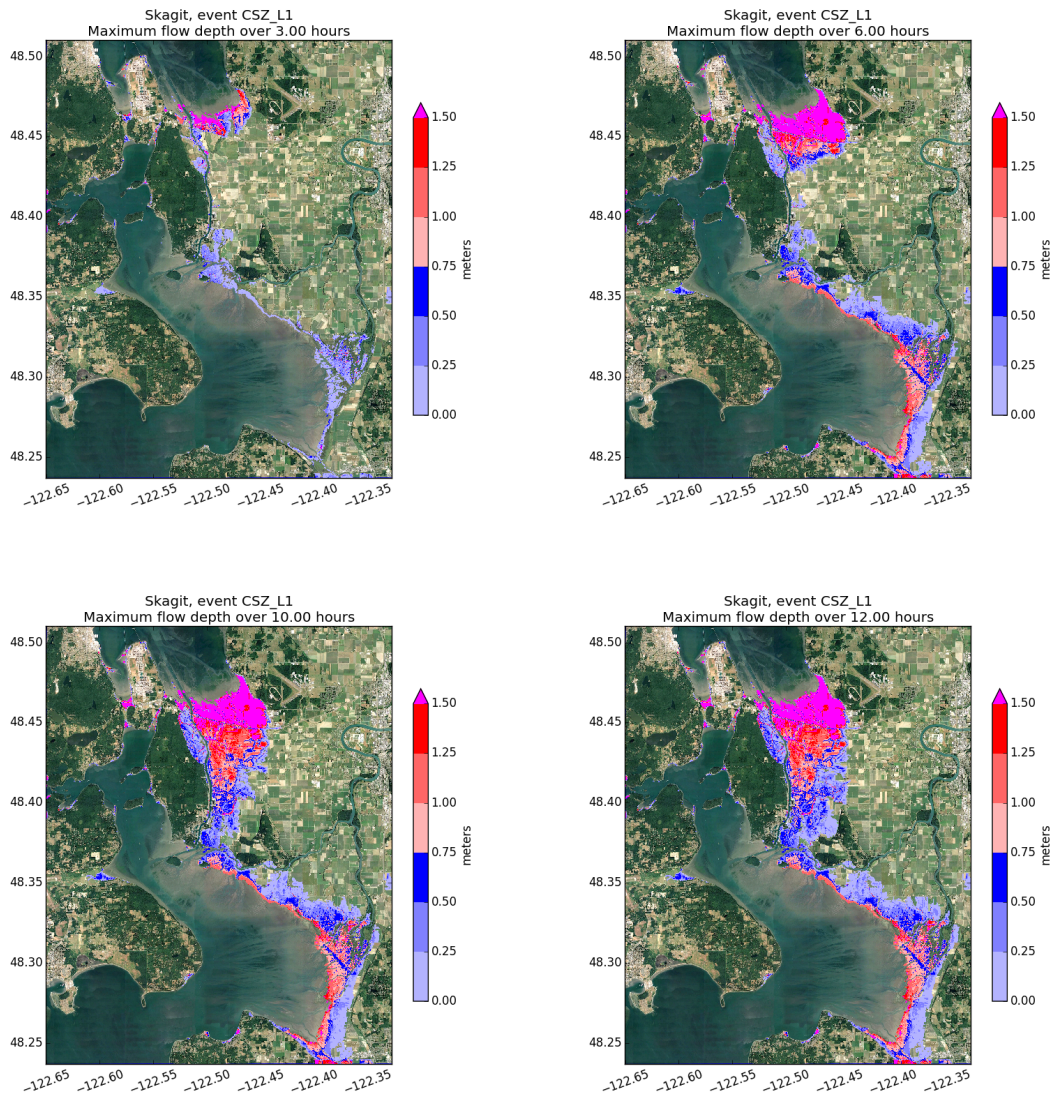


Figure 26: Maximum water depth due to the CSZ-L1 source up to time T for four different choices of the full simulation time T . The top row shows $T = 3$ and 6 hours, the bottom row shows $T = 10$ and 12 hours post-quake.

Acknowledgments

The earthquake deformation files for the CSZ-L1 and SF-L events were provided by the NOAA Center for Tsunami Research (NCTR), PMEL, as were the unit source parameters of Table 1 for the Alaska source. We acknowledge computing time provided by the CU-CSDMS High-Performance Computing Cluster, and by the Applied Mathematics Department at the University of Washington. We thank NCEI for providing the merged 1/3" PTPSm-DEM.

References

- [1] L. ADAMS, F. GONZÁLEZ, AND R. LEVEQUE, *Tsunami Hazard Assessment of Whatcom County, Washington, Project Report – Version 2*, 2019, http://staff.washington.edu/rjl/pubs/THA_Whatcom.
- [2] J. C. ALLAN, J. ZHANG, F. E. O'BRIEN, AND L. L. GABEL, *Columbia River Tsunami Modeling: Toward Improved Maritime Planning Response*. DOGAMI Special Paper 51, State of Oregon, 2018, <https://doi.org/10.13140/RG.2.2.14868.14725>.
- [3] B. ATWATER, M.-R. SATOKO, K. SATAKE, T. YOSHINOBU, U. KAZUE, AND D. YAMAGUCHI. USGS professional paper 1707, 2005.
- [4] M. J. BERGER, D. L. GEORGE, R. J. LEVEQUE, AND K. T. MANDLI, *The geoclaw software for depth-averaged flows with adaptive refinement*. Preprint and simulations: www.clawpack.org/links/papers/awr10, 2010.
- [5] C. CHAMBERLAIN AND D. ARCAS, *Modeling tsunami inundation for hazard mapping at Everett, Washington, from the Seattle Fault*. OAA Technical Memorandum OAR PMEL-147, 2015, <https://doi.org/10.7289/V59Z92V0>, <https://repository.library.noaa.gov/view/noaa/11189>.
- [6] C. D. CHAMBERLAIN, V. V. TITOV, AND D. ARCAS, *Modeling tsunami inundation impact on the Washington coast from distant seismic sources*. PMEL Tech report, 2009, ??
- [7] CLAWPACK DEVELOPMENT TEAM, *Clawpack software*, 2017, <https://doi.org/10.5281/zenodo.820730>, <http://www.clawpack.org>. Version 5.4.1.
- [8] E. GICA AND D. ARCAS, *Tsunami Inundation Modeling of Anacortes and Bellingham, Washington due to a Cascadia Subduction Zone Earthquake*. PMEL Tech report, 2016, ftp://newportftp.pmel.noaa.gov/tsunami/WaEMD/Anacortes_Bellingham/documentation/Anacortes_Bellingham_Washington_Report.pdf.
- [9] E. GICA, M. SPILLANE, V. TITOV, C. CHAMBERLAIN, AND J. NEWMAN, *Development of the forecast propagation database for NOAAs short-term inundation forecast for tsunamis (SIFT)*. NOAA Technical Memorandum OAR PMEL-139, 2008, <https://www.pmel.noaa.gov/pubs/PDF/gica2937/gica2937.pdf>.
- [10] F. GONZÁLEZ, R. LEVEQUE, L. ADAMS, C. GOLDFINGER, G. PRIEST, AND K. WANG, *Probabilistic Tsunami Hazard Assessment (PTHA) for Crescent City, CA Final Report September 11, 2014*. Univ. Washington ResearchWorks Archive: <http://hdl.handle.net/1773/25916>, 2014.
- [11] F. GONZÁLEZ, R. J. LEVEQUE, J. VARKOVITZKY, P. CHAMBERLAIN, B. HIRAI, AND D. L. GEORGE, *GeoClaw Results for the NTHMP Tsunami Benchmark Problems*. <http://depts.washington.edu/clawpack/links/nthmp-benchmarks/geoclaw-results.pdf>, 2011.
- [12] R. LEVEQUE, F. GONZÁLEZ, AND L. ADAMS, *Tsunami Hazard Assessment of Snohomish County, Washington, Project Report – Version 2*, 2018, http://staff.washington.edu/rjl/pubs/THA_Snohomish.
- [13] R. J. LEVEQUE, L. M. ADAMS, AND F. I. GONZÁLEZ, *Tsunami Hazard Assessment of Portions of Island and Skagit Counties, Washington*. (website containing reports and data), 2019, http://depts.washington.edu/ptha/IslandSkagitTHA_2019/.

- [14] R. J. LEVEQUE, L. M. ADAMS, AND F. I. GONZÁLEZ, *Tsunami Hazard Assessment of Portions of Island and Skagit Counties, Washington*. (permanent archive of code and data), 2019, <https://doi.org/??>
- [15] R. J. LEVEQUE, D. L. GEORGE, AND M. J. BERGER, *Tsunami modeling with adaptively refined finite volume methods*, *Acta Numerica*, (2011), pp. 211–289.
- [16] NOAA, *Sift propagation database metadata file*. PMEL Tech report, ?, http://sift.pmel.noaa.gov/ComMIT/compressed/info_sz.dat.
- [17] NOAA NCEI, *Port Townsend 1/3 Arc-second MHW Coastal Digital Elevation Model*. <https://www.ngdc.noaa.gov/metaview/page?xml=NOAA/NESDIS/NGDC/MGG/DEM/iso/xml/366.xml&view=getDataView&header=none>, Accessed 2017.
- [18] NOAA NCEI, *Puget Sound 1/3 Arc-second MHW Coastal Digital Elevation Model*. <https://www.ngdc.noaa.gov/metaview/page?xml=NOAA/NESDIS/NGDC/MGG/DEM/iso/xml/5164.xml&view=getDataView&header=none>, Accessed 2017.
- [19] NOAA NCEI, *Strait of Juan de Fuca 1/3 arc-second NAVD 88 Coastal Digital Elevation Model*. <https://www.ngdc.noaa.gov/metaview/page?xml=NOAA/NESDIS/NGDC/MGG/DEM/iso/xml/11514.xml&view=getDataView&header=none>, Accessed 2017.
- [20] M. D. PETERSEN, C. H. CRAMER, AND A. D. FRANKEL, *Simulations of Seismic Hazard for the Pacific Northwest of the United States from Earthquakes Associated with the Cascadia Subduction Zone*, *Pure Appl. Geophys.*, 159 (2002), pp. 2147–2168.
- [21] K. SATAKE, K. WANG, AND B. F. ATWATER, *Fault slip and seismic moment of the 1700 Cascadia earthquake inferred from Japanese tsunami descriptions*, *J. Geophys. Res.*, 108(B11) (2003), p. 2535, <https://doi.org/10.1029/2003JB002521>.
- [22] V. TITOV, D. ARCAS, C. MOORE, R. LEVEQUE, L. ADAMS, AND F. GONZÁLEZ, *Tsunami Hazard Assessment of Bainbridge Island, Washington, Project Report*, 2018, http://staff.washington.edu/rjl/pubs/THA_Bainbridge.
- [23] R. C. WITTER, Y. ZHANG, K. WANG, G. PRIEST, C. GOLDFINGER, L. STIMELY, J. ENGLISH, AND P. FERRO, *Simulating tsunami inundation for a range of Cascadia megathrust earthquake scenarios at Bandon, Oregon USA*, *Geosphere*, 9 (2013), pp. 1783–1803.